

Wilfrid Laurier University

## Scholars Commons @ Laurier

---

Theses and Dissertations (Comprehensive)

---

2012

# Synthesis and Investigation of the Liquid Crystalline Properties of Polycyclic Aromatic Hydrocarbons

Joseph A. Paquette

Wilfrid Laurier University, paqu4000@mylaurier.ca

Follow this and additional works at: <https://scholars.wlu.ca/etd>



Part of the [Materials Chemistry Commons](#), [Organic Chemistry Commons](#), and the [Physical Chemistry Commons](#)

---

### Recommended Citation

Paquette, Joseph A., "Synthesis and Investigation of the Liquid Crystalline Properties of Polycyclic Aromatic Hydrocarbons" (2012). *Theses and Dissertations (Comprehensive)*. 1610.  
<https://scholars.wlu.ca/etd/1610>

This Thesis is brought to you for free and open access by Scholars Commons @ Laurier. It has been accepted for inclusion in Theses and Dissertations (Comprehensive) by an authorized administrator of Scholars Commons @ Laurier. For more information, please contact [scholarscommons@wlu.ca](mailto:scholarscommons@wlu.ca).

# **Synthesis and Investigation of the Liquid Crystalline Properties of Polycyclic Aromatic Hydrocarbons**

**Joseph A. Paquette**

**Honours Bachelor of Science in Biological Chemistry, University of Guelph, 2010**

**THESIS**

**Submitted to the Department of Chemistry**

**Faculty of Science**

**in partial fulfilment of the requirements for**

**Master of Science in Chemistry**

**Wilfrid Laurier University**

**Joseph A. Paquette 2012©**

## Abstract

In this thesis, the synthesis and liquid crystalline properties of a series of novel substituted dibenz[a,c]anthracenes is reported. Specifically, a series of hexaalkoxydibenz[a,c]anthracenes were prepared and found not to exhibit a mesophase. In contrast, when substituents are introduced on the aromatic core, columnar mesophases are observed over broad temperature ranges. A series substituted derivatives was prepared and their mesomorphic properties compared. In general, electron-withdrawing substituents promote broad mesophase temperature ranges, as do larger substituents. The liquid crystalline phase is a result of the electronic effects, size and shape of the substituents in the 10 and 13 positions.

We also synthesized a series of discotic compounds based on substituted dibenzo[a,c]tetracenedione, dibenzo[a,c]pentacenedione and tetrabenzo[a,c,d,f]pentacenedione, with 4, 4 and 8 aliphatic side chains, respectively, using similar methodologies to that of the dibenz[a,c]anthracene compound. These compounds were also found to exhibit columnar mesophases. The mesophase temperature range suggests that the larger aromatic core stabilizes both the crystalline and liquid crystalline phases. The dione functional groups also give a synthetic handle for further synthetic modifications to probe the structure-property relationships of these PAHs.

## **Acknowledgements**

I would firstly like to thank my supervisor Ken Maly for graciously taking me on as his M.Sc. student. You have been an instrumental part of my thesis and I will always appreciate your advice, knowledge, kindness and friendship. I would also like to thank my committee members Dr. Vladimir Kitaev and Dr. Stephen MacNeil as well as my external examiner Dr. Michael Chong for their input on my thesis.

Everyone in the Science building and in Science Research who have made my experience at Wilfrid Laurier University a very enjoyable one that I will not forget. I would like to thank all the members past and present of the Maly lab with whom I have had the pleasure of working and those who have contributed to my project: Phil, Colin, Melissa, Katie, Kyle, Linsey, Josh, Michelle, Rebecca and Laiya.

I also want to thank my Mom and Dad for their support and encouragement throughout my Master's degree. You are amazing parents and I don't think I could have done it without you. I can't forget my sisters, Michelle, Peekie and Renee who are so very awesome.

I would like to thank all the organizations who have contributed funding for this project: Wilfrid Laurier University, NSERC, CFI, ACS Petroleum Research Fund and MRI Early Researcher Award. I would also like to acknowledge the help of Dr. Vance Williams and Oliver Calderon at SFU for their help with XRD data collection and analysis.

## Table of Contents

Abstract .....	i
Acknowledgements.....	ii
Table of Contents .....	iii
List of Figures .....	v
List of Schemes.....	viii
List of Tables.....	ix
Abbreviations .....	x
Chapter 1 Introduction.....	1
1.1 Self-Organization of Materials .....	1
1.2 Introduction to Liquid Crystals.....	2
1.3 Phases of Discotic Mesogens .....	5
1.3.1 Nematic Phases of Discotic Mesogens.....	6
1.3.2 Smectic Phases of Discotic Mesogens.....	6
1.3.3 Columnar Phases.....	7
1.3.4 Cubic Phase .....	8
1.4 Mesophase Characterization .....	8
1.4.1 Polarized Optical Microscopy.....	8
1.4.2 Differential Scanning Calorimetry.....	10
1.4.3 X-Ray Powder Diffraction .....	11
1.5 Structures of Discotic Mesogens.....	12
1.6 Applications of Columnar Liquid Crystals.....	16
1.7 Research Objectives .....	22
Chapter 2 Dibenz[a,c]anthracene .....	24
2.1 Introduction .....	24
2.2 Synthesis of hexaalkoxydibenz[a,c]anthracene .....	25
2.3 - Post-synthetic modification of dibenz[a,c]anthracene.....	27

2.3.1 Bromination of dibenz[a,c]anthracene .....	27
2.3.2 Further modification of dibenz[a,c]anthracene .....	28
2.3.3 NO <sub>2</sub> and NH <sub>2</sub> dibenz[a,c]anthracene .....	31
2.4 Mesophase Characterization .....	32
2.5 Discussion .....	36
2.6 Summary .....	43
Chapter 3 Dibenzo -tetra/pentacene and Tetrabenzopentacene -diones .....	44
3.1 Introduction .....	44
3.2 Synthesis of dibenzo -tetra/pentacene and tetrabenzopentacene -diones .....	45
3.3 Mesophase Characterization .....	49
3.4 Discussion .....	51
3.5 Summary .....	53
Chapter 4 Conclusions and Future Work .....	54
Chapter 5 Experimental .....	57
5.1 General .....	57
5.1.1 NMR Spectroscopy .....	57
5.1.2 Mesophase Characterization .....	57
5.1.3 Chemicals and Solvents .....	58
5.2 Synthesis .....	59
References .....	87

## List of Figures

Figure 1-1: A calamitic and a discotic mesogen and their effective molecular shape of rods and disks, respectively. ....	4
Figure 1-2: Representation of liquid crystals phases for calamitic. ....	4
Figure 1-3: Typical transitions for discotic liquid crystals. From left to right we see the crystal state, the liquid crystal state (in this case a columnar phase) and the isotropic liquid state.....	5
Figure 1-4: Structures of nematic phases. a) discotic nematic, b) chiral nematic and c) columnar nematic. ....	6
Figure 1-5: o-terphenyl crown ether which possesses a smectic discotic phase. ....	6
Figure 1-6: Packing arrangements of discotic molecules in the liquid crystal phase. Shown are the hexagonal, rectangular and oblique conformations, respectively. ....	7
Figure 1-7: a) Phthalocyanine derivative exhibiting a cubic phase and b) a graphical representation of a cubic phase.....	8
Figure 1-8: Representation of polarized optical microscopy. ....	9
Figure 1-9: Polarized optical micrograph of a) compound 15 at 80 °C, b) compound 20 at 240 °C and c) 19 at 191 °C. The micrographs are viewed at 100x magnification. ....	10
Figure 1-10: Representative DSC of a mesogenic compound showing transitions from solid to liquid crystal and liquid crystal to isotropic liquid. ....	11
Figure 1-11: Planes observed within hexagonal 2D lattice. ....	12
Figure 1-12: Esterbenzene discotic molecules.....	12
Figure 1-13: Triphenylene discotic mesogens.....	14
Figure 1-14: Large polyaromatic hydrocarbons and heterocycle. ....	16
Figure 1-15: Representative DSC of a mesogenic compound 12 showing the transitions from solid to liquid crystal and liquid crystal to isotropic liquid. ....	18

Figure 1-16: Formation of electronic band from single molecule to column. ....	18
Figure 1-17: Discotic Mesogens and their charge-carrier mobilities. ....	21
Figure 1-18: Diagram of a photovoltaic cell using a discotic liquid crystal as the hole-transporting layer.....	22
Figure 1-19: Dibenz[a,c]anthracene and acenedione derivatives. ....	23
Figure 2-1: Discotic triphenylenes and extended analogues. ....	25
Figure 2-2: Polarized optical micrographs ....	33
Figure 2-3: Representative molecules for table 2-1, 2-2 and 2-3. ....	33
Figure 2-4: Liquid crystal ranges of di-Bromo substituted hexaalkoxydibenz[a,c]anthracenes. ....	34
Figure 2-5: Summary of mesomorphic ranges of hexadecyloxydibenz[a,c]anthracene derivatives (13-20, 23, 24 and 3 <sup>79</sup> ) taken on heating at 5 °C·min <sup>-1</sup> .....	35
Figure 2-6: Representative diffractogram of compound 20. ....	36
Figure 2-7: Hammett plot of the clearing temperatures taken on heating compared to the Hammett-sigma values of mono and disubstituted compounds.....	38
Figure 2-8: Comparison of the clearing temperatures taken on heating of the mono-halogenated, compounds and di-halogenated compounds .....	39
Figure 2-9: Representative moiety of 23 that illustrates lowest energy conformation (106°) of nitro group ortho to an alkoxy side chain.....	40
Figure 2-10: Phase behaviour of hexaalkoxytriphenylene (2) and the substituted compounds 25a, <sup>97</sup> b, <sup>98</sup> c, d and 26. ....	41
Figure 2-11: Comparison of clearing temperature of compound 17a-d with respect to their Hammett $\sigma_m$ values. <sup>90</sup> .....	42
Figure 3-1: Triphenylene dione derivative. ....	44



Figure 3-2: Micrographs of compounds 31, 36 and 45 showing textures typical of a columnar hexagonal phase. ....	50
Figure 3-3: Graphical representation of phase behaviour of 28, <sup>101</sup> 31, 36 and 45 on heating.....	51
Figure 3-4: Derivatives of discotic triphenylene molecules. ....	52
Figure 4-1: Future target compounds. ....	55
Figure 4-2: Future target discotic molecules. ....	56

## List of Schemes

Scheme 2-1: Synthesis of hexaalkoxydibenz[a,c]anthracene. <sup>81, 83</sup> .....	26
Scheme 2-2: Synthesis of the monobrominated hexadecyloxydibenz[a,c]anthracene and the dibrominated series of hexaalkoxydibenz[a,c]anthracene. ....	28
Scheme 2-3: Synthesis of mono and dichlorinated DBA.....	29
Scheme 2-4: Synthesis of diiodo substituted DBA. ....	30
Scheme 2-5: Synthesis of nitrile (18) and iodo (16) substituted DBA from monobromosubstituted DBA, 12.....	30
Scheme 2-6: Synthesis of dicyano hexadecyloxydibenzanthracene (19) from 13a.....	31
Scheme 2-7: Synthetic approach to the synthesis of nitro and amino substituted dibenz[a,c]anthracene. ....	32
Scheme 3-1: General synthetic scheme demonstrating the suzuki coupling and ring closing reaction .....	45
Scheme 3-2: Synthesis of dibenzotetracenedione 31.....	46
Scheme 3-3: Synthesis of dibenzopentacenedione 36. ....	46
Scheme 3-4: Synthetic attempts toward the synthesis of tetrabenzopentacene. ....	48
Scheme 3-5: Synthesis of tetrabenzopentacenedione. ....	49

## List of Tables

Table 1-1: Phase transition temperatures of esterbenzene columnar mesogens.....	13
Table 1-2: Thermal behaviour of triphenylene discotic mesogens.....	14
Table 1-3: Phase transition temperatures of large polyaromatic hydrocarbon/heterocycle.....	16
Table 2-1: Phase behaviour of compounds 14a-i.....	33
Table 2-2: Phase behaviour of compounds 13, 14a, 15-20, 23 and 24.....	34
Table 2-3: Diffractogram data of 13, 19, 14a, 20. ....	35
Table 3-1: Phase behaviour of compounds 31, 36 and 45 as determined by DSC on heating .....	50

## Abbreviations

2D	2-dimensional
AcOH	Glacial acetic acid
AEB	Acetylated triesterbenzene
CHCl <sub>3</sub>	Chloroform
COD	1,5-Cyclooctadiene
Col	Columnar phase
Col <sub>h</sub>	Hexagonal columnar
Col <sub>o</sub>	Oblique columnar
Col <sub>r</sub>	Rectangular columnar
Cr	Crystalline solid
Cr1	First crystalline phase
Cr2	Second crystalline phase
DBA	Dibenz[ <i>a,c</i> ]anthracene
DC	Trialkyldecacyclene
DCM	Dichloromethane
DDQ	2,3-Dichloro-5,6-dicyano-1,4-benzoquinone
DLC	Discotic liquid crystal
DMF	Dimethylformamide
DMSO	Dimethyl sulfoxide
DSC	Differential scanning calorimetry
EtOAc	Ethyl acetate
EtOH	Ethanol
eq.	Equivalents
FET	Field effect transistor
g	Grams

H	Proton
HAT	Hexaalkoxytriphenylene
HBC	Hexabenzocoronene
HEB	Hexaesterbenzene
HET	Hexaestertriphenylene
hex	Hexanes
HOMO	Highest occupied molecular orbital
HRMS	High resolution mass spectrometry
Hz	Hertz
I	Isotropic liquid
<i>J</i>	J coupling constant
LC	Liquid crystal
LCD	Liquid crystal display
LED	Light emitting diode
LUMO	Lowest unoccupied molecular orbital
MALDI	Matrix-assisted laser desorption/ionization
Me	Methyl
MeOH	Methanol
mg	milligrams
MHAT	Mono-functionalized hexaalkoxytriphenylene
MHz	Megahertz
mL	milliliters
mmol	millimole
mol	mole
<i>n</i> -BuLi	<i>n</i> -Butyllithium
NCS	N-chlorosuccinimide
NMR	Nuclear magnetic resonance
OLED	Organic light emitting diode

PC	Phthalocyanine
POM	Polarized optical microscopy
PV	Photo-voltaics
T <sub>c</sub>	Clearing temperature
TEB	Tetraesterbenzene
TFAA	Trifluoro acetic anhydride
THF	Tetrahydrofuran
TLC	Thin layer chromatography
T <sub>m</sub>	Melting temperature
XRD	X-Ray diffraction
δ	Chemical shift

## Chapter 1 Introduction

### 1.1 Self-Organization of Materials

Molecular self-assembly and self-organization are Nature's methods for the creation of dynamic and complex materials necessary for life on earth. The building blocks of life, i.e. DNA, proteins and enzymes are a hierarchical organization of discrete molecules that utilize non-covalent intramolecular interactions for their formation.<sup>1</sup> These non-covalent interactions include hydrogen bonding,  $\pi$ -stacking, polar-nonpolar interactions, metal coordination, ionic interactions, etc.<sup>2</sup> The interesting part of self-assembly of soft materials is that it is spontaneous.<sup>3</sup> These interactions, while on their own are small, when they are compounded, prove stable enough to resist environmental changes. The stability of the building blocks is based on the number and concentration of the different interactions.<sup>4</sup> One particularly interesting example of a self-assembled material is a liquid crystalline phase.<sup>5, 6</sup> The interactions that are crucial for the formation of liquid crystals are very similar to those of biologically relevant interactions: van der Waals forces,  $\pi$ -stacking, dipolar interactions, charge transfer interactions and hydrogen bonding.<sup>2</sup> These forces in effect control the properties of liquid crystals. Since these interactions are weak, it allows for partial dissociation to repair disordered units and obtain a uniform and more stable system; this is also known as self-healing. A better understanding of how the structure and morphology of a molecule will affect the self-assembly of supramolecular materials will allow for an efficient and effective design of these building blocks so that their properties can be utilized.

## 1.2 Introduction to Liquid Crystals

Liquid crystalline phases are now considered a fourth state of matter along with solid, liquid and gas. They possess both order and mobility and are considered an intermediate phase of matter, hence the term mesophase. Crystalline solids are characterized by the order which is positional and orientational; the molecules are set to occupy a specific site in the lattice and also to point their molecular axes in a specific direction. A liquid contains molecules that are diffuse and free flowing with unrestricted molecular motion and no orientational or positional order about them. Liquid crystal phases possess the orientational order of a solid while being diffuse and free flowing like a liquid. The liquid crystallinity arises from the microsegregation of two constituents: the crystalline character is a result of the interactions between aromatic conjugated cores and the liquid character comes from the flexible saturated alkyl chains.<sup>7</sup> Compounds of this type are referred to as mesogens because they can exhibit a mesophase (see figure 1.1 for examples).

Liquid crystals were first discovered at the end of the 19<sup>th</sup> century by Friedrich Reinitzer, Otto Lehman and others as they described a new state of matter.<sup>8, 9</sup> When Reinitzer was determining the melting point of cholesteryl benzoate, he noticed a melt at 145.5 °C to a cloudy liquid and then another melting point at 178.5 °C to a clear transparent liquid.<sup>8</sup> Reinitzer then sent a sample to Otto Lehmann, a physicist known to study the crystallization of compounds under a microscope. He explained this behaviour as “double melting”.<sup>9</sup> He later coined the term “soft crystals” followed by “crystalline fluids” but as he became more convinced that this was a homogenous phase of matter sharing the properties of both liquids and solids, he began to call them “liquid crystals”. The term liquid crystal was eventually accepted worldwide by the scientific community. Reinitzer is generally accredited with being the discoverer of the liquid crystal.<sup>10</sup> The properties and shape required of a molecule to form this class of matter is not



obvious. In 1907 Daniel Vorländer reported that the liquid crystal state arises from a molecular structure that is as straight as possible,<sup>11</sup> and this linear rod-like shape of mesogenic molecules was generally accepted over the next 70 years. These are known today as calamitic liquid crystals.

There are two main types of liquid crystals: lyotropic and thermotropic. The former depends on the concentration of molecules and the temperature of the system for the formation of liquid crystals.<sup>12, 13</sup> The latter, the more commonly seen liquid crystal, depends solely on temperature of the system. Calamitic mesogens have a tendency to align along their long molecular axis and show free rotation about this axis in the LC state. Consequently, they are often represented as elongated ellipsoids or cylinders.<sup>14</sup>

Subsequently, a different type of mesogen was hinted at, with some experimental evidence and some theoretical predictions<sup>15-18</sup> that consisted of a single component disc-like molecule that forms thermotropic mesogens. In 1977, the first evidence for liquid crystals of disc-like molecules were reported by Chandrasekhar et al.<sup>19</sup>, which opened into a whole new field of liquid crystal research. This evidence was then corroborated by the French research groups of Dubois and Levelut who were also able to show that discotic molecules formed a liquid crystal phase.<sup>20, 21</sup> However, discotic liquid crystals opened a different direction for research in molecular electronics and organic photovoltaics.<sup>22-24</sup> As a result, discotic liquid crystals have received significant attention in recent years. Discotic mesogens, such as the triphenylene, contain a rigid core with normally six to eight flexible side chains that are laterally attached to the core. These molecules are represented by a flat disk shape. The principal axis is normal to the plane of the disk in the discotic mesogens (refer to figure 1-1).

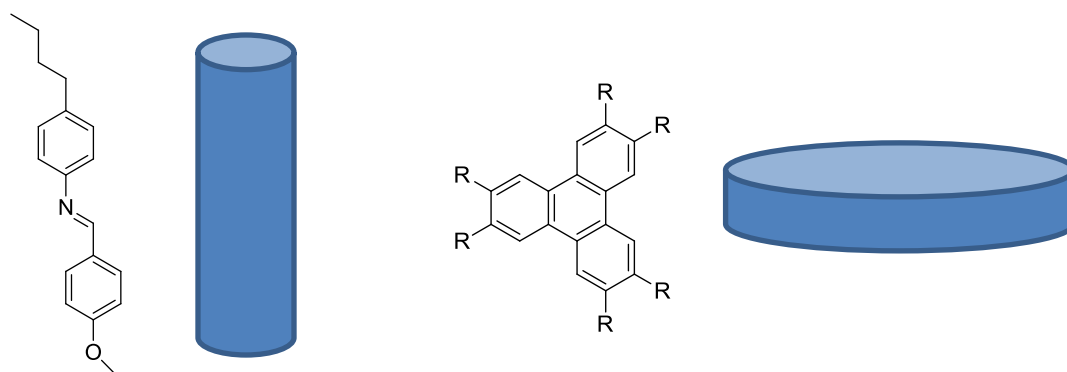


**Figure 1-1: A calamitic and a discotic mesogen and their effective molecular shape of rods and disks, respectively.**

A calamitic mesogen, when in the liquid crystal state, can exhibit different phases; a smectic phase (which includes smectic C and smectic A) and a nematic phase. The nematic phase is the most common and contains the least order of the phases. The molecules have no positional order but can self-align to possess long range directional order usually parallel to their main axes. The smectic phase forms well defined layers that are arranged one over the other allowing mobility between layers. In the smectic A phase the molecules are oriented along the mesogen normal while the smectic C phase possesses a tilt away from the normal, figure 1-2.

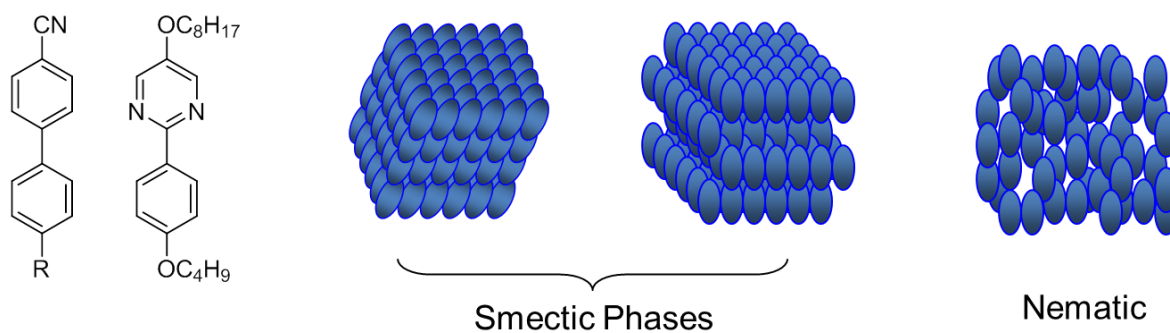


**Figure 1-2: Representation of liquid crystals phases for calamitic mesogens.**

My thesis will focus on discotic liquid crystals. To gain a better understanding of discotic liquid crystals explanation of the different types of phases seen among these compounds will be discussed.

### 1.3 Phases of Discotic Mesogens

Depending on the shape and symmetry of a discotic molecule, there are a variety of packing arrangements discotic mesogens can adopt in the liquid crystal phase. There are four types of phases seen with discotic mesogens: nematic, smectic, columnar and cubic. The columnar phase is however by far the most prevalent phase. The other phases are rarely observed, and few discotic mesogens are known to exhibit more than one mesophase.<sup>25, 26</sup> Two important transitions occur in a liquid crystal: the melting temperature ( $T_m$ ) is when mesogen melts from a crystal or solid to a liquid crystal and the clearing temperature ( $T_c$ ) is when the liquid crystal melts to an isotropic liquid (figure 1-3). When thermodynamically stable mesophases are obtained on heating and cooling the phases are called enantiotropic; if the phase is obtained only on cooling the phase is called monotropic and is a metastable phase since the transition occurs below the melting point.

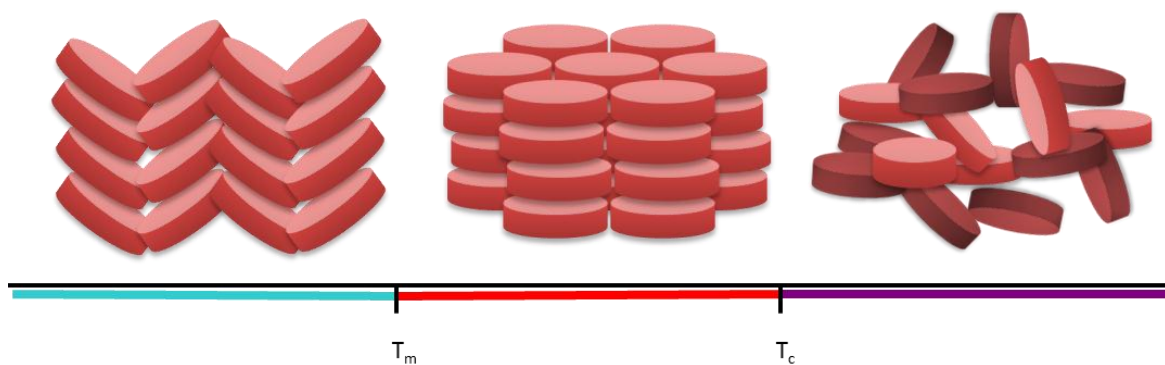


Figure 1-3: Typical transitions for discotic liquid crystals. From left to right we see the crystal state, the liquid crystal state (in this case a columnar phase) and the isotropic liquid state.

### 1.3.1 Nematic Phases of Discotic Mesogens

The nematic phase of disk-like molecules can be further divided into 3 categories: discotic nematic, chiral nematic and columnar nematic (figure 1-4). The discotic nematic phase is the least ordered and more symmetrical phase compared to the others.<sup>27</sup> In this phase the molecules have translational and rotational movement around their axis, although they tend to orient themselves in a preferential direction, along their director. The chiral nematic phase also known as a cholesteric phase, displays a helical arrangement where alignment between stacks is rotated from one to another to produce a long range chirality of the stacks.<sup>28</sup> Columnar nematic phase possess the 1D stacking to form columns, but do not have a 2D ordering of the stacks.

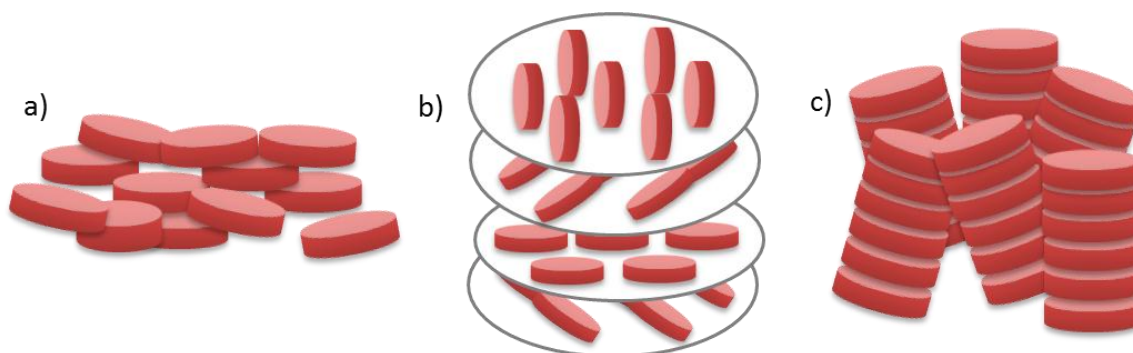


Figure 1-4: Structures of nematic phases; a) discotic nematic, b) chiral nematic and c) columnar nematic.

### 1.3.2 Smectic Phases of Discotic Mesogens

A smectic phase will occur when there are a reduced or uneven number of peripheral chains. The discs are arranged in layers separated by the peripheral chains.<sup>29</sup> The packing does not produce any columnar aggregates and is considered a rare phase for discotic liquid crystals. An example can be seen with an *ortho*-

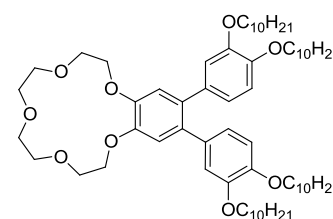


Figure 1-5: *o*-terphenyl crown ether which possesses a smectic discotic phase.

terphenyl crown ether<sup>30</sup> (figure 1-5). These phases may also be called a lamellar phase and are similar to the calamitic mesogens in the smectic phase.

### 1.3.3 Columnar Phases

In these phases molecules self-assemble into columns which will then organize into a 2-dimensional lattice. Depending of the amount of order in the column and the orientation of the molecules in the column, there has been evidence of up to 7 different classes of columnar phases. Three of the more common arrangements include: hexagonal ( $\text{Col}_h$ ), rectangular ( $\text{Col}_r$ ) and oblique ( $\text{Col}_{ob}$ ).

A hexagonal mesophase is denoted that because of the hexagonal packing arrangement that the columns adopt (figure 1-6). A rectangular phase is when the stacking of columns in a rectangular packing arrangement, usually due to the core being surrounded by disordered aliphatic side chains. An oblique mesophase arises from the stacking of molecules into a column with a tilted orientation.<sup>31</sup>

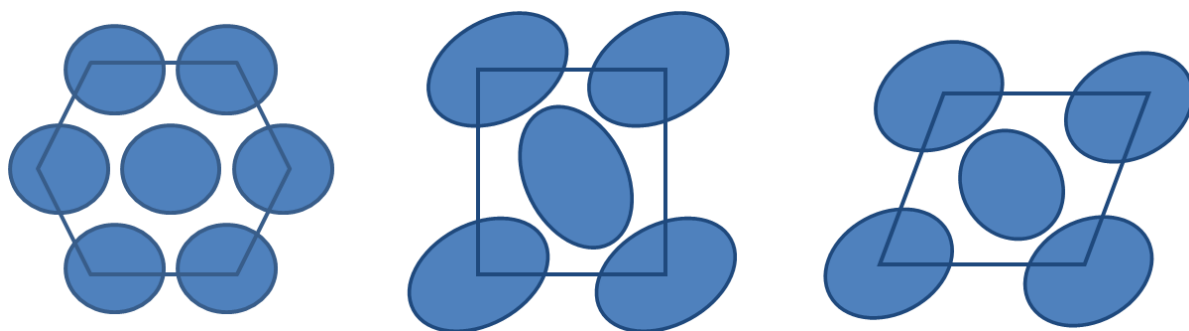


**Figure 1-6: Packing arrangements of discotic molecules in the liquid crystal phase. Shown are the hexagonal, rectangular and oblique phases, respectively.**

### 1.3.4 Cubic Phase

A cubic phase is more prevalent in a lyotropic liquid crystal system, however there are examples of discotic liquid crystals displaying this phase, such as phthalocyanine derivatives.<sup>32</sup>

This phase consists of columns that are branched and form a network of columns (figure 1-7).

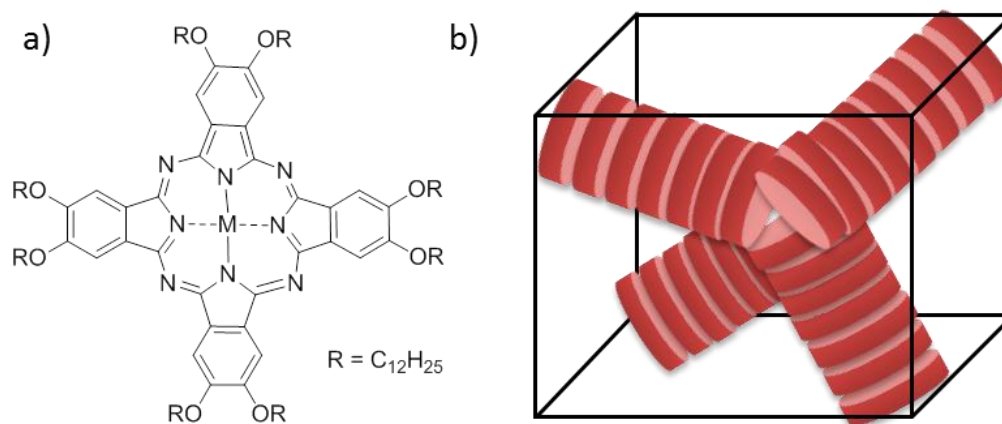


Figure 1-7: a) Phthalocyanine derivative exhibiting a cubic phase and b) a graphical representation of a cubic phase.

## 1.4 Mesophase Characterization

There are several techniques that are utilized to identify and characterize liquid crystal phases. Among them are polarized optical microscopy, differential scanning calorimetry and X-ray diffraction. A discussion of the basic theory of these techniques and how they are used will be presented.

### 1.4.1 Polarized Optical Microscopy

Initial characterization of a liquid crystal requires polarized optical microscopy (POM). Ordered phases such as crystalline solids and liquid crystals are optically anisotropic: their optical properties depend on orientation. This property is known as birefringence: the materials have a different refractive index depending on the orientation of the sample. With POM, a sample is placed between two linear polarizing filters orthogonal to each other; light will only be transmitted if anisotropy occurs. The birefringence of liquid crystals causes the plane-polarized

light to be rotated as it passes through a sample, leading to transmission of light through the cross-polarizers. The sample is mounted on a heating stage which is used to heat and cool the sample so that measurements can be performed to detect the presence of a liquid crystal phase, and if applicable the transition temperatures of the liquid crystal, (figure 1-8).

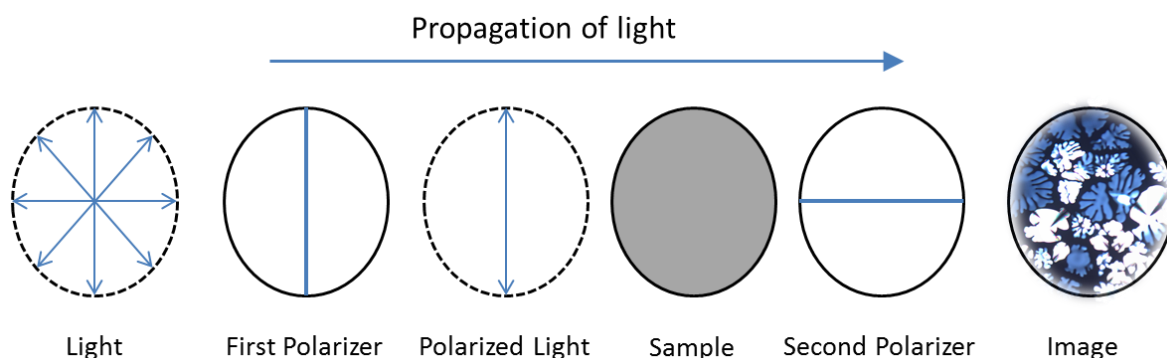


**Figure 1-8: Representation of polarized optical microscopy.**

A typical polarized optical micrograph can be seen in figure 1-9. The textures that are seen with a polarized optical micrograph can give insight into the type of phase. The textures shown in figure 1-8 and 1-9 are consistent with that of a columnar hexagonal phase.<sup>33</sup> These micrographs however are varied in texture and only allows for empirical assignment of the phases; therefore further characterization is required to identify the mesophase.

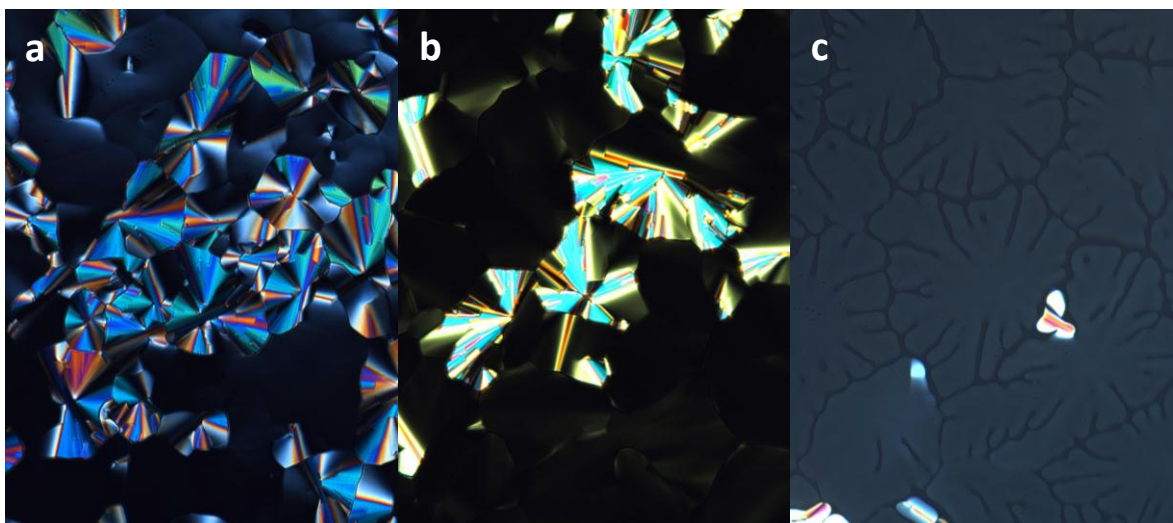
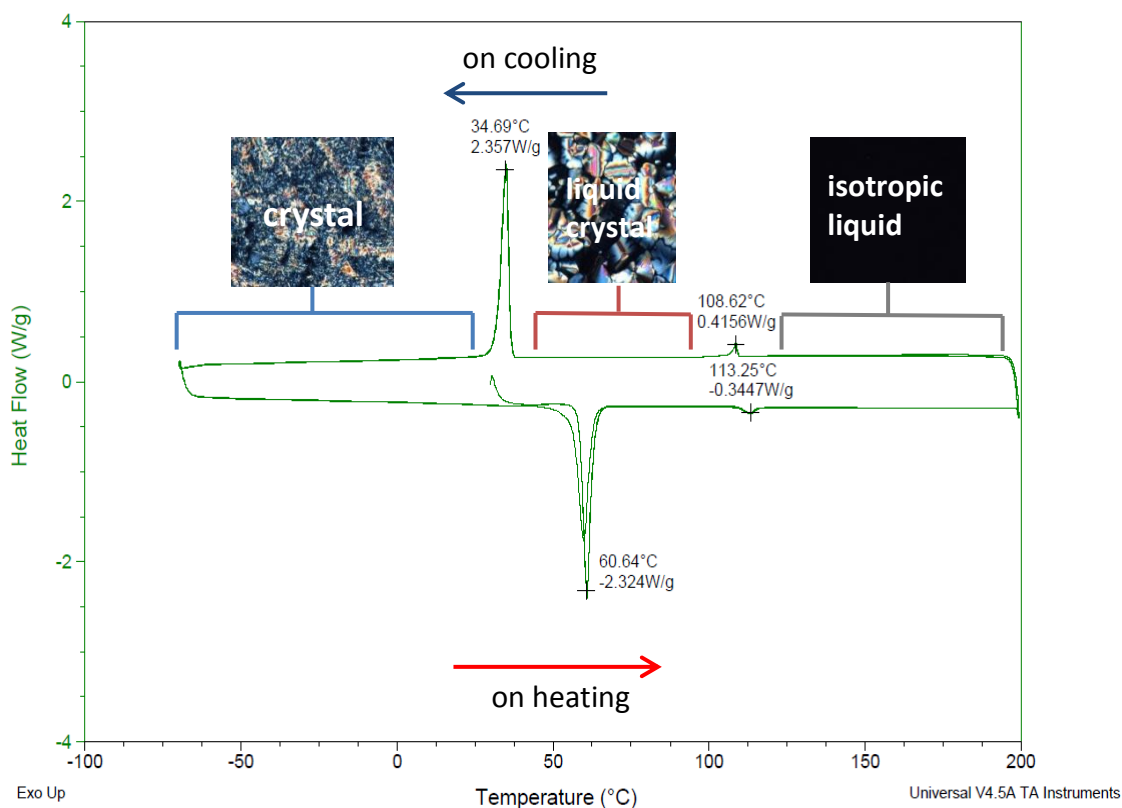


Figure 1-9: Polarized optical micrograph of a) compound 15 at 80 °C, b) compound 20 at 240 °C and c) 19 at 191 °C. The micrographs were taken at 100x magnification.

#### 1.4.2 Differential Scanning Calorimetry

Differential Scanning Calorimetry (DSC) is a thermoanalytical technique that is used for the precise measurements of the temperatures of transition of a liquid crystal. The principle underlying the technique is that when a sample undergoes a phase transition, more or less heat will be required to maintain a constant temperature between the sample and the reference.<sup>34</sup> Whether more or less heat is required will depend on whether the transition is exothermic or endothermic. If a liquid sample transitions into a liquid crystal, an exothermic process, it will absorb heat and require less heat to maintain a constant temperature between the sample and the reference. Likewise, if a sample melts from a solid to a liquid crystal, an endothermic phase transition, it will require more heat for the transition. The difference between the sample and the reference will give the enthalpies of transition while revealing precise temperatures or transition. A typical DSC can be seen in figure 1-10. The peaks correspond to the phase transition temperatures, and the enthalpies of transition can be obtained by integration of the area under the peak.





**Figure 1-10: Representative DSC of a mesogenic compound showing transitions from solid to liquid crystal and liquid crystal to isotropic liquid.**

This method is applied for the analysis of mesogenic molecules. DSC can give insight into the phases particular mesogens will have. Data acquired from a DSC of a mesogen will normally give 2 transitions: solid to liquid crystal and liquid crystal to liquid and can be used to corroborate results from POM. Some however, also display a transition from liquid crystal to glassy or a transition from a columnar phase to another distinct columnar phase. These transitions may or may not be visible by microscopy or by calorimetry.

### 1.4.3 X-Ray Powder Diffraction

X-ray powder diffraction is a technique using X-ray on powder samples for the structural characterization of materials.<sup>35</sup> An X-ray is passed through a sample in the liquid crystal state where it is scattered in three-dimensions. It can then be collected by a 2D detector, averaged,

and projected onto a single dimension. Rotational averaging of the scattered radiation is collected and leads to smooth diffraction rings around the beam axis. The angle between the beam and the ring is called the scattering angle and is denoted  $2\theta$ . In accordance in Bragg's law each ring corresponds to a particular reciprocal lattice vector in the sample, where  $n$  is an integer,  $\lambda$  is the wavelength and  $d$  is the interplanar distance.

$$2d \sin \theta = n\lambda$$

X-ray diffraction can give the long range intercolumnar spacing and the symmetry of packing. Based on this information it can be used to identify the phase. The 100 and 110 reflections are measurements used to calculate the distance between two columns based on their trigonometric relationship. Figure 1-11 shows the planes typically seen with a hexagonal array in the liquid crystalline phase.

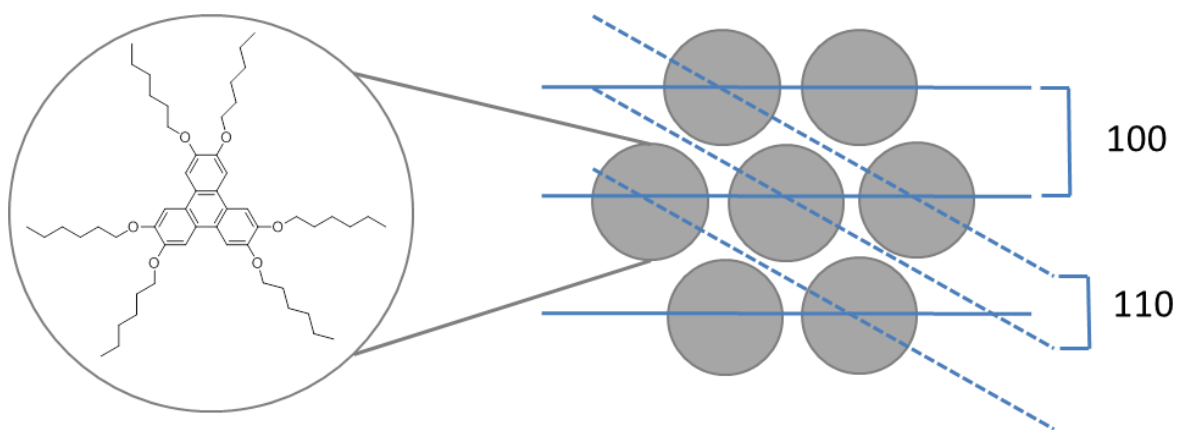
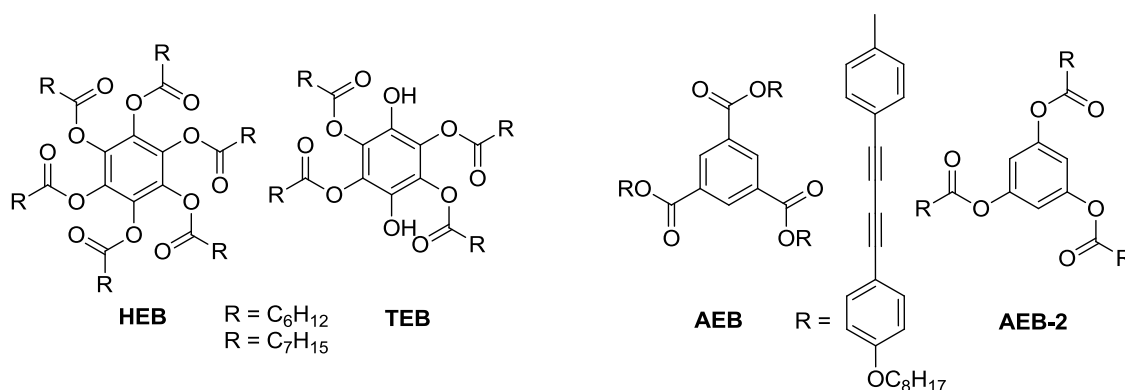


Figure 1-11: Planes observed within hexagonal 2D lattice.

### 1.5 Structures of Discotic Mesogens

One of the most basic discotic molecules shown to exhibit mesomorphic behaviour contains a benzene ring core. The benzene molecule made its appearance into material science when it was discovered, by Chandrasekhar, that the hexaesterbenzene (**HEB**) derivatives showed a columnar phase, figure 1-12.<sup>19, 36</sup> **HEB** compounds have been studied, with a focus on tailoring

their physical properties to understand the molecular interactions involved in stabilizing discotic columnar phases.<sup>37-39</sup> With the **HEB** we see an increase in the breadth of the liquid crystal phase when the alkyl chains are increased in size.<sup>19</sup> Similarly with the tetraesterbenzene (**TEB**), there is an increase in the breadth of the LC phase with a lengthening of the side chains.<sup>40</sup> Another discogen with benzene as a core is acetylated triestersbenzenes (**AEB**). We see a drastic increase in the temperature of the liquid crystal range, whereas the phloroglucinol analogue (**AEB-2**) does not exhibit mesomorphism,<sup>41</sup> demonstrating how important the linkage to the core can be. This also highlights the effect of a small change to the discotic core to the mesophase.



**Figure 1-12: Esterbenzene discotic molecules.**

**Table 1-1: Phase transition temperatures of esterbenzene columnar mesogens.**

Structure	Phase Transition Temperatures (°C)	Reference
<b>HEB-6</b>	Cr 86 Col <sub>h</sub> 86 I	19
<b>HEB-7</b>	Cr 80 Col <sub>h</sub> 84 I	19
<b>TEB-6</b>	Cr 55 Col <sub>h</sub> 57 I	36
<b>TEB-7</b>	Cr 68 Col <sub>h</sub> 70 I	36
<b>AEB</b>	Cr 137 Col <sub>h</sub> 146 I	41
<b>AEB2</b>	NON LC	41

The most studied cores in the field of discotic liquid crystals are triphenylene molecules. There are over 500 examples of triphenylene based DLCs. The symmetrical triphenylene molecule, hexaalkoxytriphenylene (**HAT**) can give insight into the effect of changing the alkyl chain length and the functional groups on the core to the mesophase behaviour (figure 1-13). An

increase in the size of the aliphatic chain causes a decrease in the size of the liquid crystal range<sup>42</sup> (table 1-2). When the connector is modified to an ester linkage, hexaestertriphenylene (**HET**), there is a significant change on mesophase even though the core and aliphatic chain length remain constant.<sup>42</sup> Considerable effort has also been given to the creation of unsymmetrical compounds. The mono-functionalized hexaalkoxytriphenylene (**MHAT**) molecule is one example that shows the effects of unsymmetrical aliphatic side chains.<sup>43</sup> As a single aliphatic chain of the HAT6 molecule is changed to a n-octyl chain, a depression of the liquid to liquid crystal transition of over 10°C (M(8)HAT6) is seen. This again demonstrates the sensitivity of the mesophase behaviour with respect to the structure of the mesogen.

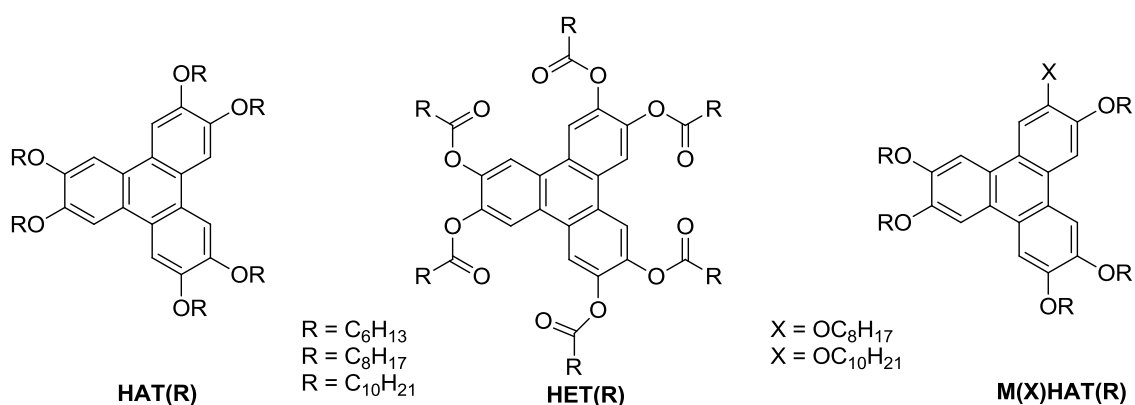
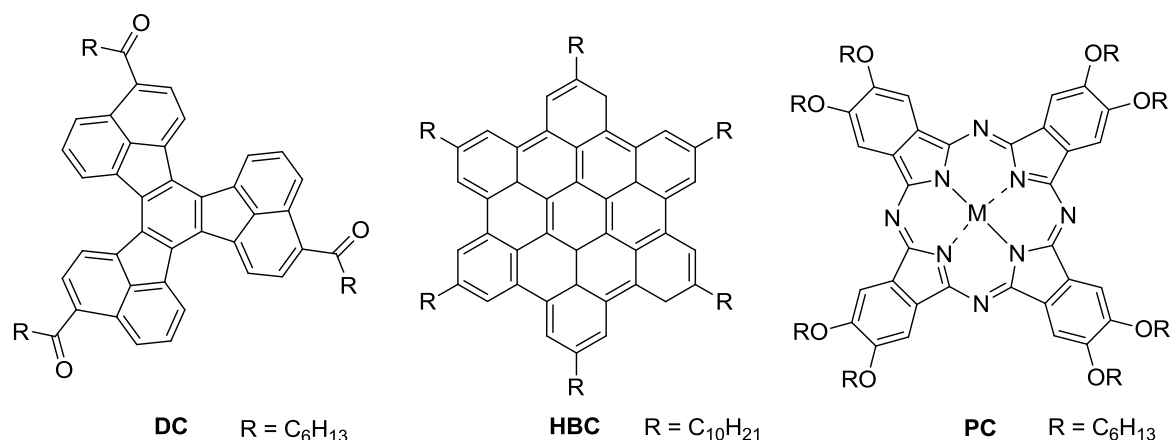


Figure 1-13: Triphenylene discotic mesogens.

Table 1-2: Thermal behaviour of triphenylene discotic mesogens.

Structure	Phase Transition Temperature (°C)	Reference
<b>HAT6</b>	Cr 68 Col <sub>h</sub> 97 I	42
<b>HAT8</b>	Cr 66.8 Col <sub>h</sub> 85.6 I	42
<b>HAT10</b>	Cr 58 Col <sub>h</sub> 69 I	42
<b>HET6</b>	Cr 108 Col <sub>h</sub> 120 I	42
<b>HET8</b>	Cr 62 Col <sub>h</sub> 125 I	42
<b>HET10</b>	Cr 67 Col <sub>r</sub> 108 Col <sub>h</sub> 121.5 I	42
<b>M8HAT6</b>	Cr 54.8 Col <sub>h</sub> 91.3 I	43
<b>M10HAT6</b>	Cr 45 Col <sub>h</sub> 71.8 I	43

Large aromatic molecules are known to possess broad mesophase temperature ranges. It was theorized that increasing the size of the core while maintaining minimal constraint around the core would avoid crystallization and would achieve liquid crystallinity.<sup>44</sup> A trialkyldecacyclene (**DC**) discotic mesogen (figure 1-14) has many interesting properties that include multiple redox states<sup>45</sup> and has been used as a dopant to improve the lifetime of electroluminescent devices.<sup>46</sup> These discogens, despite their attractive properties, do not exhibit a broad mesophase range, while the deoxygenated versions do not exhibit mesomorphism. A hexabenzocoronene (**HBC**) is a very large, symmetrical, all benzene polycyclic aromatic hydrocarbon. This molecule shows good potential for the proposed applications of liquid crystals.<sup>47</sup> This core shows an extremely broad columnar phase range over 300 °C for some derivatives. In fact, some of the **HBC** derivatives will decompose before any evidence of the isotropic liquid phase. Phthalocyanine (**PC**) is a symmetrical aromatic heterocycle with a cavity to accommodate various metal ions as it is considered to be a tetradentate ligand. These **PC** derivatives have attracted significant attention due to their potential utility in organic electronics. This molecule allows for the tailoring of properties such as electronics, optics and improved processability, partly due to its ability to incorporate around 70 different metals in the tetradentate cavity. The octaalkoxy substituted **PC** boasts an impressive columnar range of over 300 °C.<sup>48, 49</sup>



**Figure 1-14: Large polyaromatic hydrocarbons and heterocycle.**

**Table 1-3: Phase transition temperatures of large polyaromatic hydrocarbon/heterocycle.** <sup>a</sup>The transition from LC to I are not reported because the molecule decompose before reaching the isotropic phase.

Structure	Phase Transition Temperature (°C)	Reference
DC	Cr 93 Col 115 Col <sub>r</sub> 262 I	44
HBC	Cr 124 Col <sub>h</sub> >400 I	47
PC (M = 2H) <sup>a</sup>	Cr 119 Col <sub>h</sub>	48
PC (M = Cu) <sup>a</sup>	Cr 120 Col <sub>h</sub>	48
PC (M = Co) <sup>a</sup>	Cr 126 Col <sub>h</sub>	49

## 1.6 Applications of Columnar Liquid Crystals

Unlike their calamitic counterparts, discotic liquid crystals cannot be utilized as switching units in electronic displays, mainly due to a lack of dipole moment and increased viscosity in the liquid crystal state. Nonetheless they have attractive properties useful for many practical applications as optical compensation films in liquid crystal displays (LCD), organic semiconductors, discotic solar cells, organic light emitting diodes (OLED), and field effect transistors.<sup>50</sup>

A product derived from discotic liquid crystal that has reached the market place is optical compensation films for wide viewing angle displays. Although calamitic liquid crystals have a breadth of potential application they are known for their presence in electro-optical devices such as calculators, mobile phones, tablets,<sup>51</sup> etc., these devices are composed of twisted nematic and

superstretched nematic display devices.<sup>52</sup> This technology was limited due to two major flaws: narrow viewing angle and slow response time. A method of correcting these problems was a negative birefringence optical compensation film that would widen the viewing angle to increase the contrast ratio due to high light transmittance and cost effective production of twisted nematic modes.<sup>53</sup> The compensation film is made from discotic liquid crystals that are polymerized by a photoreaction. The poor viewing angle of the LCDs are due to optical anisotropy, light leakage from the cross polarizers and light scattering at the surface of the polarizers and colour filters. The twisted nematic phase orients itself horizontal when no voltage is applied and vertical when the voltage is applied, therefore it should not transmit light when on and transmit light when the voltage is off. The LCs at the surface of the orientation film stay almost horizontal and change their incline. This causes elliptically polarized light which cannot be entirely extinguished by a linear polarizer. Therefore a positive optical anisotropy of the calamitic liquid crystals is compensated by the negative optical anisotropy of discotic liquid crystals. The light should not suffer any distortion and no longer be dependent on the angle thus resulting in a greater viewing angle<sup>54</sup>.

When the discotic aromatic molecules assemble, they form columnar stacks with typical distance between the core of about 3.5 Å. This distance between the molecules should allow an overlap between the HOMO (highest occupied molecular orbital) and the LUMO (lowest unoccupied molecular orbital) of neighbouring molecules. As a result, the innate ability for charge transport along the columns can be exploited for use in optoelectronic devices.

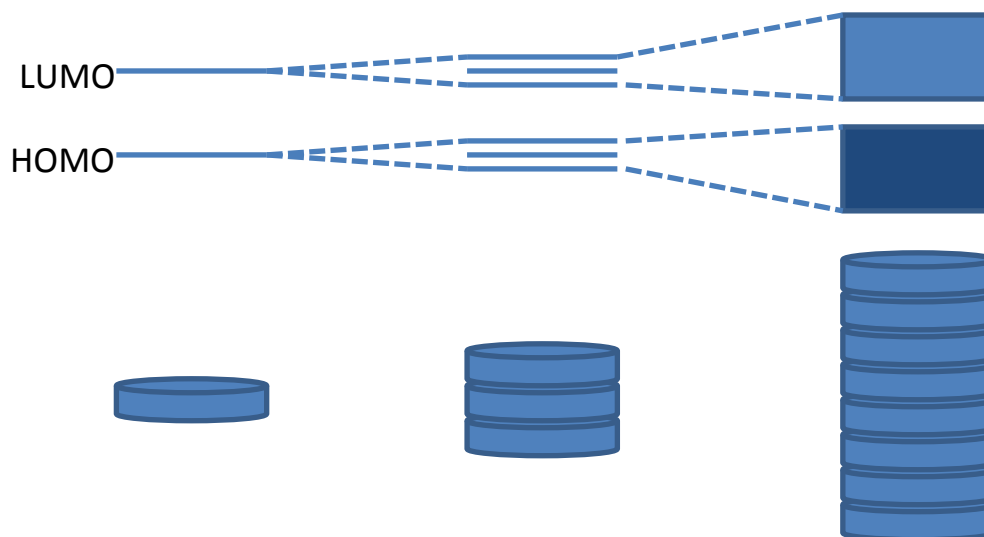


**Figure 1-16: Formation of electronic band from single molecule to column.**

An immense field of scientific research is the development of organic molecules suitable for use in electronic devices such as light-emitting diodes (LEDs), field effect transistors (FET), and photovoltaic (PV) solar cells. The development of this industry requires a basic understanding of the structure-property relationships that are a result of the physics and chemistry of these compounds. A front runner in this field is discotic mesogens. The reasons these molecules garner so much interest is their ability to self-assemble into supramolecular systems that possess order yet maintain a degree of fluidity. The properties are similar to that of a single crystal yet the mobility allows for processing and the self-healing of defects.<sup>55-59</sup>

The conductive properties of discotic liquid crystals were initially studied using triphenylene derivatives, which do not possess intrinsic charges.<sup>60</sup> A doping of this material was utilized to test to conductivity of the mesogens, it was found that the conduction along the columns was significantly higher than that perpendicular to the columns. Therefore, the conduction can be considered uni-directional along the columnar axis.<sup>61</sup> These columns can be thought of as molecular wires with conductive channels, these are the aromatic rigid cores, surrounded by the insulating alkyl chains,<sup>62-64</sup> or more precisely they can be considered a



molecular cable. The long aliphatic chains around the core, ranging from 3 to 8 carbons, cause an intercolumnar distance of around 20-40 Å, depending on the number and length of the chains. Therefore the interactions within the same column are much greater than the interactions between the columnar stacks. Discotic liquid crystals will act as an insulator without any external stimuli due to the large energy gap and low charge concentration. However, they can be made conducting by an electro or photochemical doping, where the columnar stacks gives a path for the generated charges. As the molecules are spatially close, the charges can migrate easily by hopping from one molecule to another.

To measure the charge transport of these mesogens, a time of flight (TOF) technique is utilized, which measures the amount of time it takes a charged particle to pass through a sample once a charge has been applied by light irradiation. The discotic liquid crystals are sandwiched in a cell and depending on the polarity of the applied electric field, either holes or electrons will move across the sample, from the time it takes a mobility  $\mu$  can be deduced. The mobility depends on the voltage  $V$  and the transit time  $t_t$ , where  $v$  is the drift velocity,  $d$  is the film thickness and  $E$  is the applied electric field.<sup>65</sup>

$$\mu = \frac{v}{E} = \frac{d^2}{Vt_t}$$

Many of the electrical properties of materials are attributed to the electronic band structure of the component. When a material is combined to form a macroscopic structure, the band is considered to be continuous as opposed to discrete energy levels of single atoms. The semiconductive property of a material is a result of the band gap between the lower and upper band. The bandgap is what determines how much energy is necessary for the electrons to jump into the excited state. A metal is a material that does not have a band gap and the electrons will

be able to jump from rest (from the valence band) to the excited state without an energy barrier. A semiconductor will have a band gap that will require an external stimulus to excite the electron into the conduction band, this bandgap will be approximately 2 eV ( $10^{-2}$  to  $10^4$  S·cm<sup>-1</sup>). An insulator has a relatively large band gap, anything larger than that of a semiconductor, so that very few electrons will jump the bandgap. The energy gap between the bands can be fine-tuned to meet the standards of the desired device. Discotic liquid crystals are ideal materials for use as semiconductors.

Discotic liquid crystals that show good charge mobility may be found suitable for organic electronics. A way to improve the charge transport is to maximize the degree of order within the column. A discogen with a large core is one method to improve the conductivity. Some prevalent examples in the literature are **HBC** derivatives.<sup>66</sup>

There is an increase in demand for sustainable energy sources; more people are turning to solar cells to meet this demand. The current technology uses inorganic materials such as Si, GaAs, CdS, etc, due to their high charge-carrier mobility and stability; however these inorganic materials are expensive, difficult and have a high energy demand for processing. Recently, organic semiconductors have attracted attention for use in photovoltaics due to their relatively low cost, flexibility and easy processing ideal for large area applications.<sup>67, 68</sup> The power conversion efficiencies are relatively low at around 5 % compared to their inorganic competitors that are >40%, or up to 11 % in dye-sensitized hybrid organic/inorganic cells. For discotic liquid crystals to compete, they must improve efficiency by around a factor of 2.<sup>7</sup> Current examples of discotic liquid crystals at the forefront for practical applications in organic electronics are **HAT**, **HBC** and **PC**, that have been found to possess carrier mobilities of 0.1, 0.28 and  $0.15 \times 10^{-4}$  m<sup>2</sup>V<sup>-1</sup>s<sup>-1</sup>, respectively (figure 1-17).<sup>66</sup>

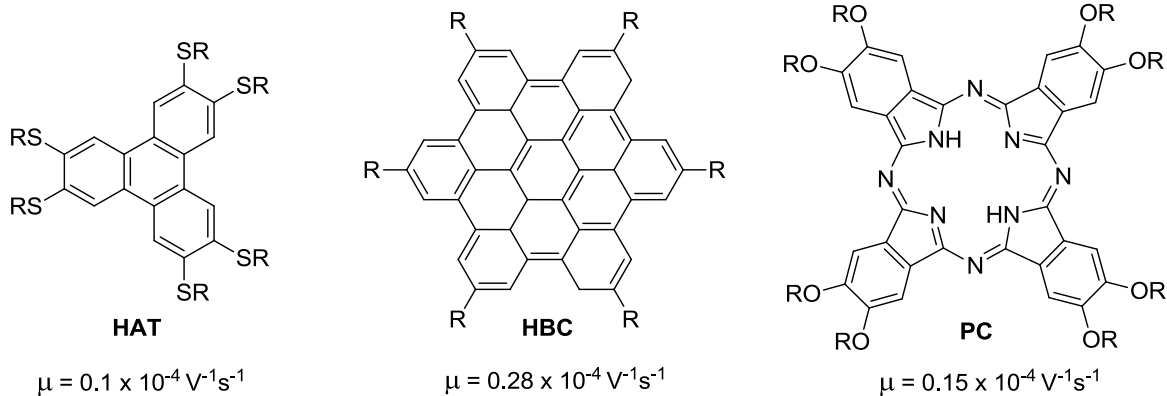


**Figure 1-17: Discotic Mesogens and their charge-carrier mobilities.**<sup>66</sup>

Solar cells work by the photoexcitation of the organic material to produce excitons. The excitons must separate to make charged species in order to diffuse through the organic layer to the electrode. When they recombine too quickly they are unable to cross the material to the electrode and do not produce photocurrent. These devices show better efficiencies when they use donor-acceptor heterojunctions.<sup>69</sup> This material requires an electron-rich and an electron-poor organic semiconductor. With this method the excitons have a much greater chance to separate at the donor-acceptor interface. The greatest challenge to using organic semiconductors is perfecting the film morphology which is essential to the charge transport ability.<sup>70, 71</sup> Discotic liquid crystals have ease of processability and can create a highly ordered system; they simply require a better charge transport ability to compete with the current technologies. Müllen et al.<sup>23</sup> have constructed a p/n type solar cell using a discotic liquid crystalline hexabenzocoronene (HBC), as the hole transporting layer (*p*-type) and electron poor perylene as the electron-transporting layer (*n*-type). This photovoltaic cell exhibited quantum efficiencies of 34 % and power efficiencies of 2 %.<sup>23</sup> A schematic of this photovoltaic cell is shown in figure 1-18.

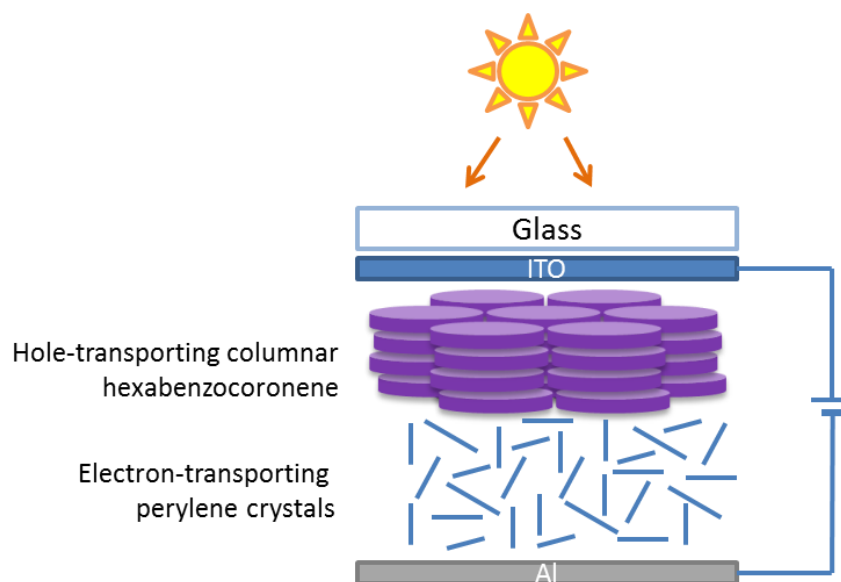


**Figure 1-18: Diagram of a photovoltaic cell using a discotic liquid crystal as the hole-transporting layer.**<sup>23</sup>

Discotic liquid crystals can also be used in organic light emitting diodes (OLEDs) as both the *n*-type or *p*-type layer. Triphenylene discotic liquid crystals are typically used as the hole transporting layer because they possess high charge-carrier mobility.<sup>72</sup> Perylene and its derivatives are used as the electron transporting layer because they also have high charge-carrier mobility and great luminescent properties.<sup>73</sup> As an electric field is applied, holes and electrons move in their respective layer until they combine at the interface to produce light. There has also been the production of a single layer cell where the discotic liquid crystal is both the electron and hole-transporting layer. This was achieved using a bridged triphenylene derivative.<sup>74</sup>

## 1.7 Research Objectives

The objective of this research is to synthesize a new class of discotic liquid crystals in order to better understand the link between the chemical structures and physical properties of these materials. Specifically, the goal of the research is to prepare a series of hexaalkoxydibenz[a,c]anthracenes (figure 1-19) and explore their liquid crystal properties using

POM, DSC and XRD. By introducing substituents onto the aromatic core, we can probe the effects of substituents on the mesophase temperature range.

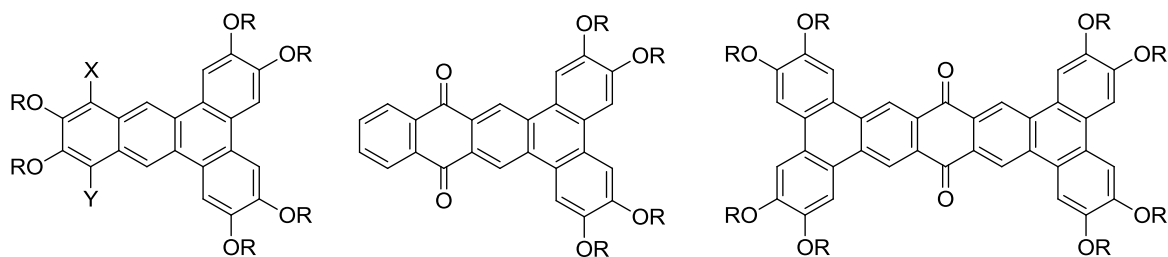


**Figure 1-19: dibenz[a,c]anthracene and acenedione derivatives.**

A second research objective is the synthesis of a series of discotic derivatives of acenediones (figure 1-19) while extending the size of the aromatic core, i.e. from anthracene to tetracene and pentacene. These molecules possess an electron withdrawing carbonyl group in order to probe the ramifications of electronics on the propensity of discotic molecules to form liquid crystal phases. These compounds may also be useful for their potential application as *n*-type semiconductors.

## Chapter 2 Synthesis and mesomorphic properties of hexaalkoxydibenz[a,c]anthracenes

### 2.1 Introduction

Hexaalkoxytriphenylenes (**2**), are one of the most extensively studied compounds that exhibit a columnar mesophase.<sup>72, 75-78</sup> These compounds, however, exhibit a rather narrow range above room temperature.<sup>50</sup> Some studies suggest that increasing the aromatic core in size will effectively increase the temperature range of the liquid crystal phase,<sup>79</sup> and some studies show that it may lead to increased charge transport properties.<sup>80</sup> A similar structure, 10,13-dimethyl-2,3,6,7,11,12-hexakis(hexyloxy)dibenz[a,c]anthracene (**3**), shows one benzene ring elongation of **2** with methyl substituents at the 10 and 13 positions. This compound exhibits a columnar phase above room temperature from 35-88 °C.<sup>79</sup> Extending this idea further a hexaalkoxytrinaphthylene molecule, **4**, was synthesized by our group,<sup>81</sup> expecting this molecule to show a mesophase over a broader temperature range and possibly exhibit such behaviour at ambient temperature. Compound **4**, however, did not exhibit any mesomorphic behaviour. In contrast, heterocyclic analogue of compound **4**, synthesized by Ong *et al.*,<sup>82</sup> hexakis-(decyloxy)diquinoxazino[2,3-a:2',3'-c]phenazines (**6**), displayed a broad mesophase from 86 to 215 °C. The only structural difference between the two discotic molecules is that the latter contains electron poor nitrogen atoms. Similarly to compound **6**, the Williams group was able to synthesize hexaalkoxydibenzo[a,c]phenazine (**5**) which also formed a liquid crystal phase.<sup>33</sup> Compounds **3** and **5** have a dibenz[a,c]anthracene core; compound **3** contains two electron rich methyl groups, while compound **5** contains electron poor nitrogen atoms in the core system. This would lead us to believe that our target molecule, 2,3,6,7,11,12-hexakis(hexyloxy)dibenz[a,c]anthracene, **1**, should in fact display mesomorphic behaviour.

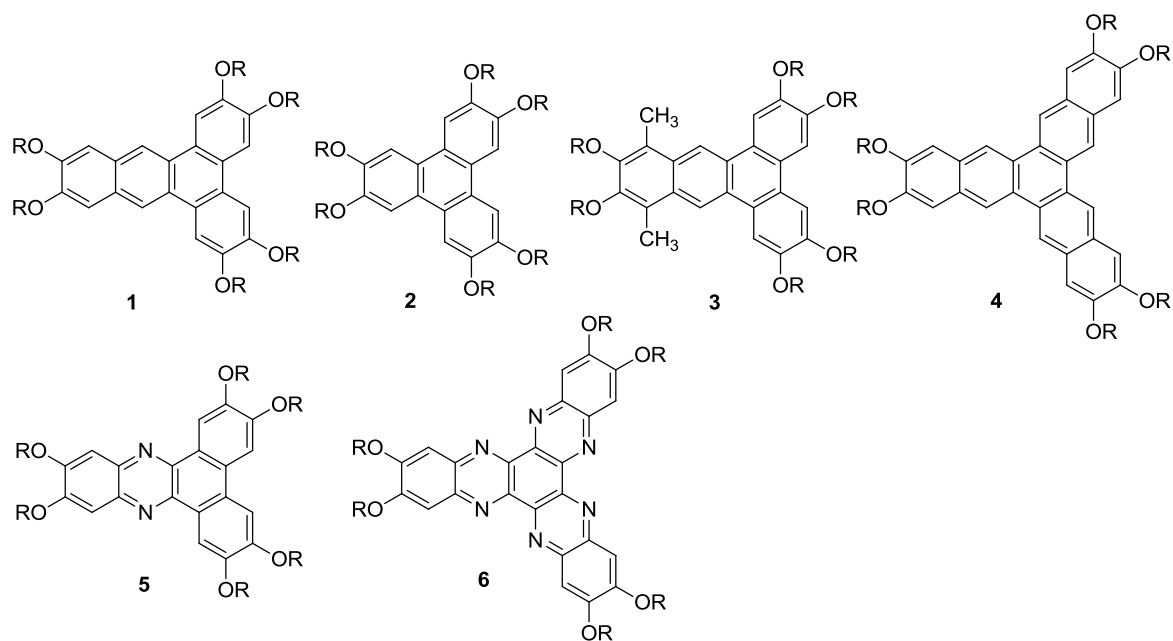
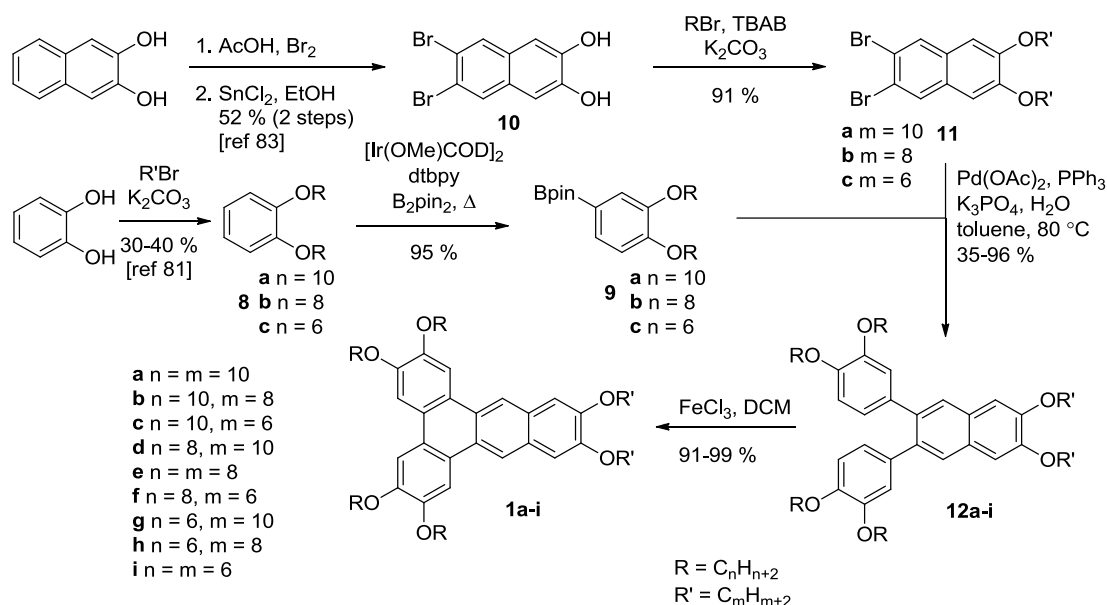


**Figure 2-1: Discotic triphenylenes and extended analogues.**

## 2.2 Synthesis of hexaalkoxydibenz[a,c]anthracene

To access the hexaalkoxydibenz[a,c]anthracene (**1**), a modular approach was taken (Scheme 2-1) that involved a Suzuki cross-coupling of a substituted aryl boronate (**9**) with a dibromonaphthalene (**11**), followed by an oxidative ring closing.

**Scheme 2-1: Synthesis of hexaalkoxydibenz[a,c]anthracenes 1a-i.**



The aryl boronate necessary for cross-coupling was prepared in two steps from commercially available catechol. Alkylation of catechol to produce 1,2-dialkoxybenzene (**8a-c**) with a 40-90 % yield. A procedure using an iridium-catalyzed direct borylation was accomplished on this intermediate molecule using  $[\text{Ir}(\text{OMe})\text{COD}]_2$  and bis(pinacolato)diboron in the presence of 4-4'-di-*tert*-butyl-2,2'-dipyridyl in cyclohexane to give 1-pinacoloboron-3,4-bis(alkoxy)benzene (**9a-c**) with yields of 50-95 %. Tetrabromination of 2,3-dihydroxynaphthalene was done to give 1,4,6,7-tetrabromo-2,3-dihydroxynaphthalene,<sup>84</sup> with a yield of 68 %. To obtain the desired substituted naphthalene with bromo substituents in the 6 and 7 positions, a reduction was performed with  $\text{SnCl}_2 \cdot 2\text{H}_2\text{O}$ , which selectively debrominated at the 1 and 4 positions to give 6,7-dibromo-2,3-dihydroxynaphthalene (**10**), yield of 76 %.<sup>84</sup> An alkylation was done with the desired bromoalkane, tetrabutylammonium bromide and potassium carbonate base to give 6,7-dibromo-2,3-dialkoxynaphthalene (**11a-c**) in 50-90 % yields. Compounds **8** and **11** underwent Suzuki-Miyaura cross coupling using  $\text{Pd}(\text{OAc})_2$ , triphenylphosphine in toluene and 2 M potassium phosphate at 80 °C to give compounds **12a-i**, in



yield of 45-95%. Once the adduct **12** was purified, an oxidative ring closing was performed in dichloromethane with 6 equivalents of iron (III) chloride ( $\text{FeCl}_3$ ) for 30 minutes to afford hexaalkoxydibenz[a,c]anthracene (**1a-i**) in nearly quantitative yields. If the reaction was left longer, decomposition of the product was observed.

This methodology was applied to the formation of the hexaalkoxydibenz[a,c]anthracene with three separate alkyl chain lengths (hexyl, octyl and decyl). This made a total of nine combinations of dibenz[a,c]anthracene derivatives (**1a-i**), which can be seen in scheme 2-1. Unfortunately none of compound **1a-i** exhibited mesomorphic behaviour contrary to our expectations based on similar mesogens (**3** and **5**). Both polarized optical microscopy and DSC showed a single phase transition from crystalline solid to isotropic liquid.

This discovery was surprising considering the similarity to the 10,13-dimethyldibenz[a,c]anthracene derivative (**3**), and substituted dibenzophenazine (**5**).<sup>33</sup> Clearly, the mesomorphic properties of these compounds are sensitive to subtle structural variation of the core.

## 2.3 - Post-synthetic modification of dibenz[a,c]anthracene

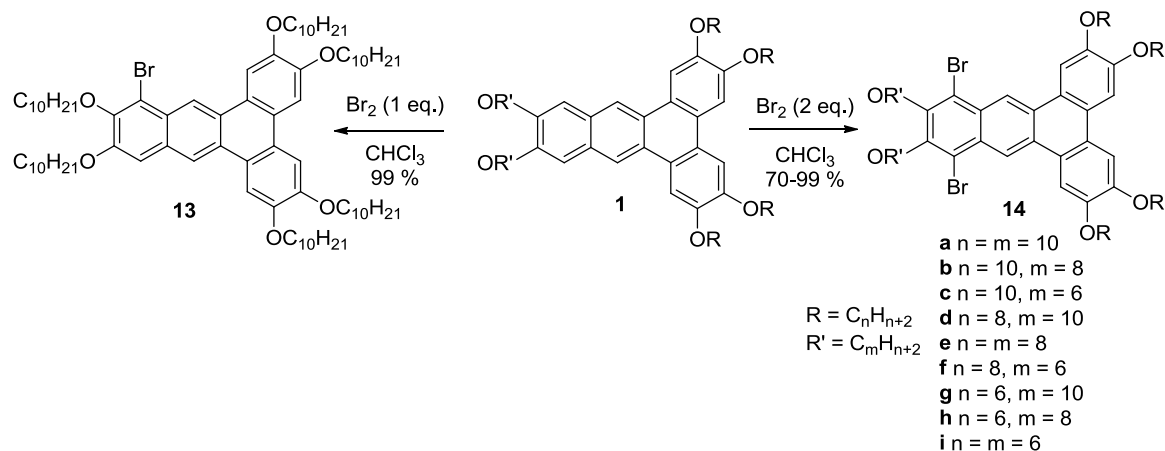
### 2.3.1 Bromination of dibenz[a,c]anthracene

Bromination of the hexaalkoxydibenz[a,c]anthracene series (**1a-i**) was carried out in  $\text{CHCl}_3$  at room temperature with 2 equivalents of bromine for 30 minutes. The resulting products were 10,13-dibromo dibenz[a,c]anthracenes (**14a-i**), obtained in yields of 70-99 % (scheme 2-2).

Compounds **14a-i** were then studied via polarized optical microscopy and differential scanning calorimetry (figure 2-2 and table 2-1). As a stark contrast to the precursor, the

brominated compounds all exhibited broad liquid crystalline phases, with some ranges exceeding 100 °C.

**Scheme 2-2: Synthesis of the monobrominated hexadecyloxydibenz[a,c]anthracene and the dibrominated series of hexaalkoxydibenz[a,c]anthracene.**



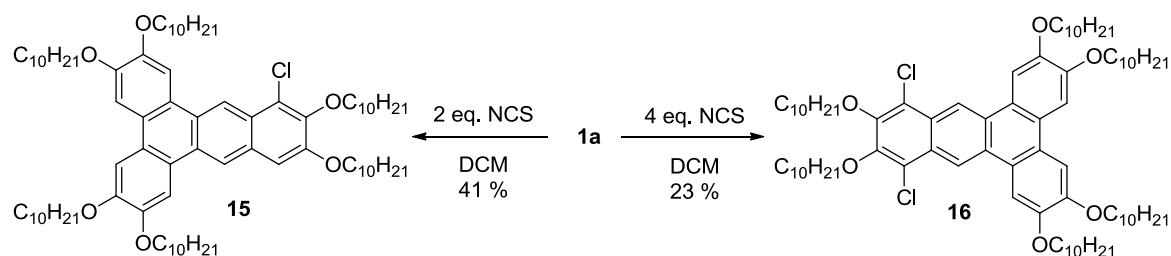
A mono-bromination of dibenz[a,c]anthracene **1a** was performed, by adjusting the equivalents of bromine used (1eq) during the reaction, in chloroform for 30 minutes. The product was obtained in a quantitative yield (**13**). Compound **13** also exhibited a columnar mesophase.

### 2.3.2 Further modification of dibenz[a,c]anthracene

To develop a further understanding of the effects of substituents on the liquid crystal properties of these compounds, we sought to prepare a series of dibenzanthracenes with a variety of functional groups in the 10 and 13 positions in order to probe a structure-property relationships in this class of compounds (scheme 2-3 to 2-6). By varying the electronics and size of the substituents on the dibenz[a,c]anthracene core we should be able to view the dependence of varying factors on liquid crystal temperature range.

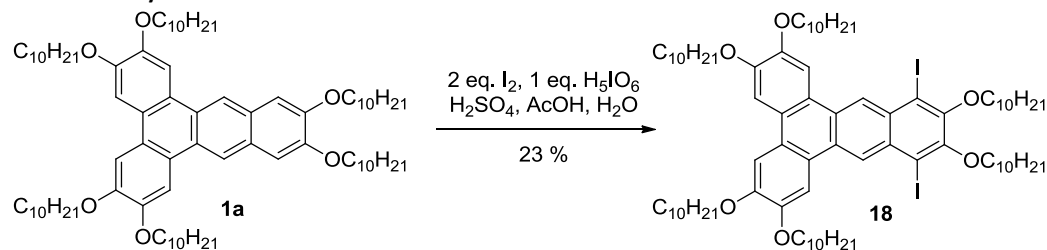
From compound **1a**, a myriad of compounds were accessible via electrophilic aromatic substitutions. To expand the halogen series a chlorination of **1a**, which was adapted from a procedure by Kalyani et al.<sup>85</sup> was performed. This reaction utilized 2 equivalents of N-chlorosuccinimide in dichloromethane. The reaction was carried out at 100 °C in a pressure tube with a Teflon cap for 12 hours. The dichlorination was carried out under the similar reaction conditions, with 4 equivalents of N-chlorosuccinimide and was reacted for 48 hours. These reactions yielded mono (**15**) in 41 % and dichlorinated (**16**) in 23 % yield, respectively.

**Scheme 2-3: Synthesis of mono and dichlorinated DBA**



The mono-iodination of **1a** was attempted with typical iodination conditions with 1 equivalent of  $\text{I}_2$ , periodic acid, glacial acetic acid and concentrated sulfuric acid, the solution was heated and left to stir for 2.5 hours. This reaction, however, did not yield mono-iodinated product (**17**), although by NMR, it was thought to be the correct product as there was seven equivalent aromatic peaks and integrations of the alkyl peaks suggested the correct ratio. Once a more thorough purification was performed, the product was shown to contain a 1:1 mixture of starting material (**1a**) and di-iodinated product (**18**). The chemical shifts of the aromatic peaks present on the core molecule shift according to the concentration in solution, due to aggregation in solution.<sup>86</sup> Consequently, the chemical shift values were difficult to compare because they were not the same from one spectrum to the next. However, this method could be utilized for the formation derivative **18** by a two fold increase of the equivalents of the reagents.

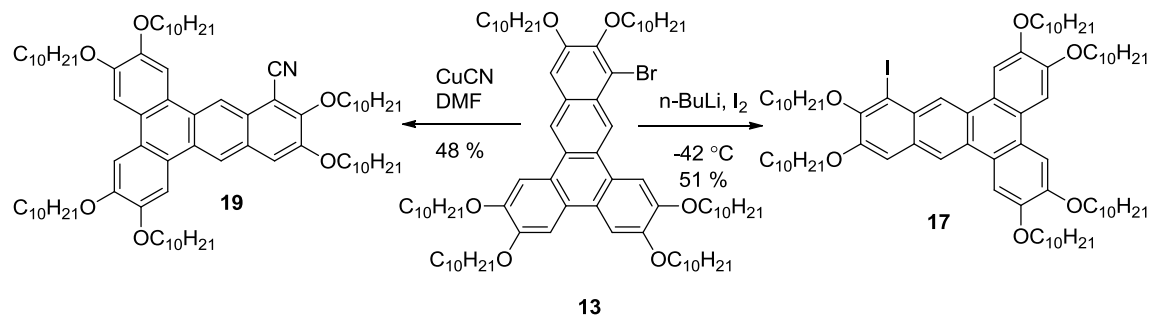
**Scheme 2-4: Synthesis of diiodo substituted DBA.**



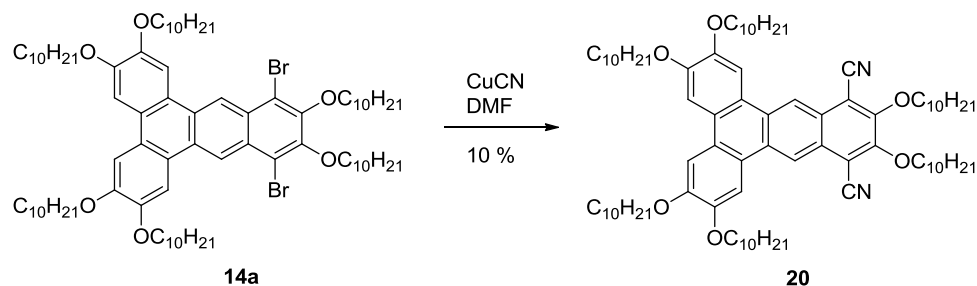
Since it proved difficult to prepare **17** by direct iodination it was instead prepared by a lithium halogen exchange on **13** in the presence of *n*-BuLi and I<sub>2</sub> in dry THF at -42 °C (scheme 2-5). This pathway was successful in creating the desired product (**17**) with a modest yield of 51 %.

A nitrile group is a desirable functional group in this series as they are known to produce stable mesophases over broad temperature ranges.<sup>50</sup> The cyanation of **13** and **14a** were achieved from a modified procedure,<sup>87</sup> where the starting material was dissolved in dry DMF and 1.25 and 2.5 equivalents of CuCN were added. The reaction was heated at reflux for 24 hours under an N<sub>2</sub> atmosphere. The reaction mixture was treated with ethylenediamine followed by an extraction and purification via column chromatography to yield compound **19** and **20** in 48 and 10 % yields respectively (scheme 2-5 and 2-6).

**Scheme 2-5: Synthesis of nitrile (**18**) and iodo (**16**) substituted DBA from monobromosubstituted DBA, **12**.**



**Scheme 2-6: Synthesis of dicyano hexadecyloxydibenzanthracene (19) from 13a.**

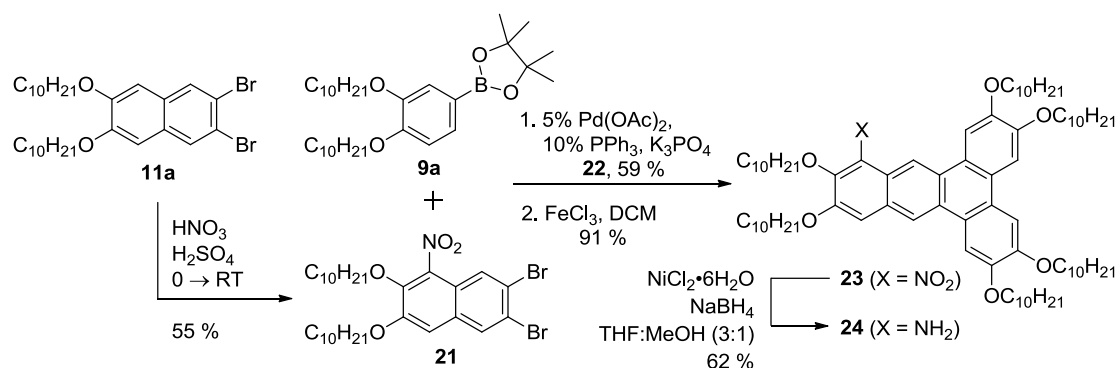


### 2.3.3 NO<sub>2</sub> and NH<sub>2</sub> dibenz[a,c]anthracene

To prepare nitro and amino derivatives **23** and **24**, the functional group was introduced prior to Suzuki coupling because the solubility of compound **1a** was not well suited for the reaction conditions required for nitrations. Specifically, the nitration was performed on 6,7-dibromo-2,3-dihydroxynaphthalene (**11a**) using 60 % HNO<sub>3</sub> and concentrated sulfuric acid. The desired 1-nitro-6,7-dibromo-2,3-dihydroxynaphthalene (**21**) was obtained in a modest yield of 55 %. Compound **21** was treated with the standard Suzuki-Miyaura cross-coupling reaction with Pd(OAc)<sub>2</sub> and PPh<sub>3</sub> in toluene and 2M K<sub>3</sub>PO<sub>4</sub>, in the presence of the **9a**. The product was heated to 80 °C until the disappearance of starting materials was seen as monitored by TLC, to give compound **22** in 59 % yield. Subsequent ring closing with FeCl<sub>3</sub> in dichloromethane yielded 10-nitro-dibenze[a,c]anthracene (**23**) in 91 % yield.

A convenient method to produce the amino substituted DBA (**24**) would be the reduction of the nitro group. Typical reductive techniques were performed on compound **21**. A reduction procedure modified from Kumar et al.<sup>88</sup> was done on compound **23** using NiCl<sub>2</sub>•6H<sub>2</sub>O and NaBH<sub>4</sub> in THF:MeOH (3:1). This method yielded the reduced product **24** in a 62 % yield (scheme 2-7).

**Scheme 2-7: Synthetic approach to the synthesis of nitro and amino substituted dibenz[a,c]anthracene.**



## 2.4 Mesophase Characterization

The liquid crystalline properties of compounds **13-20**, **23**, **24** were studied by polarized optical microscopy and differential scanning calorimetry.

All of the substituted derivatives of compound **1a** possessed a mesophase. The micrographs in figure 2-2 show the liquid crystal phases of compounds **13-20**, **23**, **24** as seen by polarized optical microscopy. The textures seen in the micrographs are consistent of a columnar hexagonal phase.<sup>33</sup>

Differential Scanning Calorimetry (DSC) was used to acquire precise measurements of the temperatures of transition that are seen in this class of liquid crystals. DSC for the mesogens was performed at a constant temperature change of 5 or 10  $^{\circ}\text{C} \cdot \text{min}^{-1}$ , and the transition temperatures are reported on heating. The phase behaviour of compounds **14a-i** are summarized in table 2-1 and compounds **1a**, **13**, **14a**, **15-20**, **23**, **24** are summarized in table 2-2.

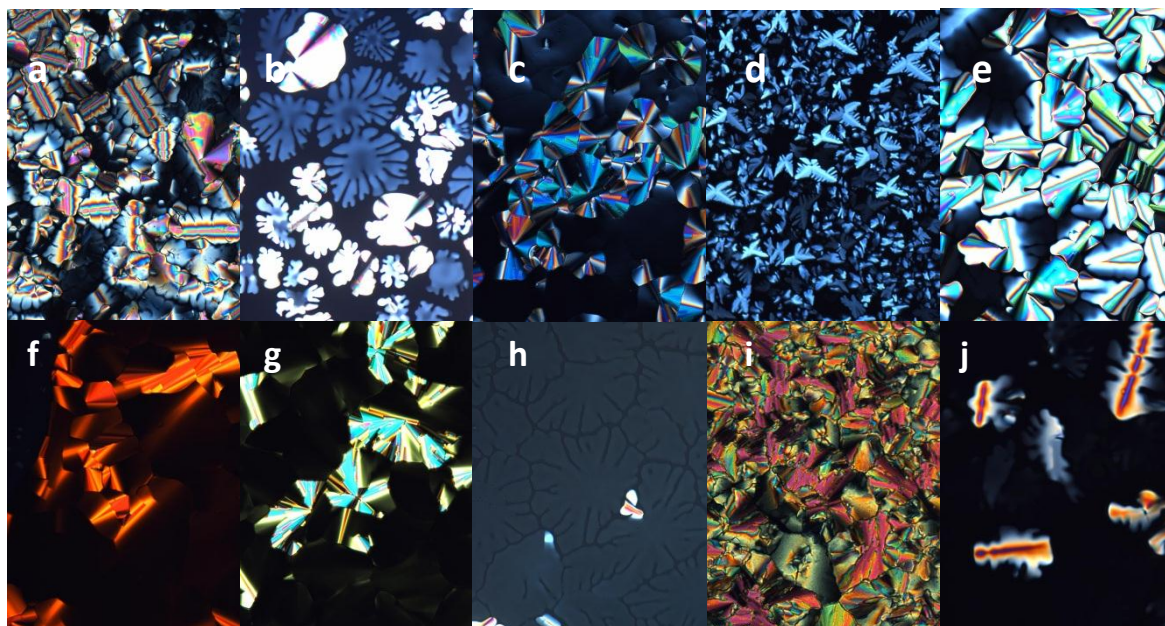


Figure 2-2: Polarized optical micrographs of a) mono-Br (13) at 100 °C, b) di-Br (14a) at 125 °C, c) mono-Cl (15) at 40 °C, d) di-Cl (16) at 41 °C, e) mono-I (17) at 107, f) di-I (18) at 130 °C, g) mono-CN (19) at 193 °C, h) di-CN (20) at 191 °C, i) mono-NO<sub>2</sub> (23) at 54 °C and j) mono-NH<sub>2</sub> (24) at 55 °C. All micrographs were taken on cooling at a rate of 5 °C·min<sup>-1</sup> and were taken at 200x magnification.

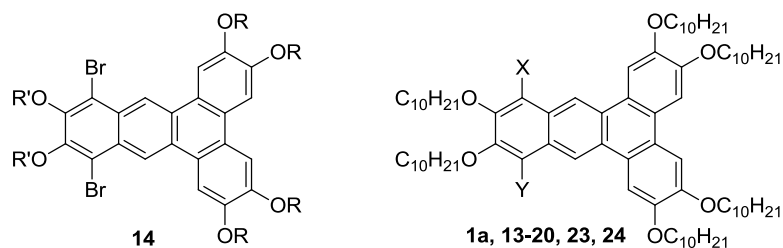


Figure 2-3: Representative molecules for table 2-1, 2-2 and 2-3.

Table 2-1: Phase behaviour of compounds 14a-i based on DSC with scan rate of 10 °C·min<sup>-1</sup> on heating.

Compound	R, R'	Phase Transition				
		Transition Temperature °C (enthalpies of transition J·g <sup>-1</sup> )				
<b>14a</b>	R = C <sub>10</sub> H <sub>21</sub> , R' = C <sub>10</sub> H <sub>21</sub>	Glass	30.6	Col <sub>h</sub>	142.2 (2.9)	I
<b>14b</b>	R = C <sub>10</sub> H <sub>21</sub> , R' = C <sub>8</sub> H <sub>17</sub>	Glass	51.6	Col <sub>h</sub>	141.8 (2.6)	I
<b>14c</b>	R = C <sub>10</sub> H <sub>21</sub> , R' = C <sub>6</sub> H <sub>13</sub>	Glass	41.6	Col <sub>h</sub>	147.7 (3.0)	I
<b>14d</b>	R = C <sub>8</sub> H <sub>17</sub> , R' = C <sub>10</sub> H <sub>21</sub>	Glass	38.1	Col <sub>h</sub>	142.1 (4.6)	I
<b>14e</b>	R = C <sub>8</sub> H <sub>17</sub> , R' = C <sub>8</sub> H <sub>17</sub>	Glass	60.1	Col <sub>h</sub>	157.4 (5.3)	I
<b>14f</b>	R = C <sub>8</sub> H <sub>17</sub> , R' = C <sub>6</sub> H <sub>13</sub>	Glass	71.2	Col <sub>h</sub>	169.3 (6.0)	I
<b>14g</b>	R = C <sub>6</sub> H <sub>13</sub> , R' = C <sub>10</sub> H <sub>21</sub>	Glass	36.2	Col <sub>h</sub>	125.1 (5.5)	I
<b>14h</b>	R = C <sub>6</sub> H <sub>13</sub> , R' = C <sub>8</sub> H <sub>17</sub>	Glass	59.6	Col <sub>h</sub>	155.7 (5.0)	I
<b>14i</b>	R = C <sub>6</sub> H <sub>13</sub> , R' = C <sub>6</sub> H <sub>13</sub>	Glass	47.2	Col <sub>h</sub>	179.0 (7.5)	I

Table 2-2: Phase behaviour of compounds **13**, **14a**, **15-20**, **23** and **24**. The enthalpies of transition are taken on heating at 5 °C·min<sup>-1</sup>.

Compound	X, Y	Phase Transition				
		Transition Temperature °C (enthalpies of transition J·g <sup>-1</sup> )				
<b>15</b>	X = Cl, Y = H	Cr	34.2 (3.6)	Col	47.7 (1.5)	I
<b>16</b>	X = Y = Cl	Cr	36.3 (0.8)	Col	53.9 (4.3)	I
<b>13</b>	X = Br, Y = H	Cr	60.6 (39.6)	Col	113.3 (1.7)	I
<b>14a</b>	X = Y = Br	Glass	30.6	Col	142.1 (3.2)	I
<b>17</b>	X = I, Y = H	Cr	61.6 (40.0)	Col	109.5 (0.8)	I
<b>18</b>	X = Y = I	Cr	48.2 (51.4)	Col	162.9 (3.0)	I
<b>19</b>	X = CN, Y = H	Cr	56.7 (41.0)	Col	193.2 (4.1)	I
<b>20</b>	X = Y = CN	Glass	25.1	Col	242.7 (7.2)	I
<b>23</b>	X = NO <sub>2</sub> , Y = H	Glass	20.5	Col	61.9 (2.9)	I
<b>24</b>	X = NH <sub>2</sub> , Y = H	Cr	34.0 (2.8)	Col	50.0 (10.4)	I

Furthermore, the phase behaviour of compounds **13-20**, **23** and **24** have been summarized graphically, figures 2-4 and 2-5, for visual comparison of phase behaviour with respect to substituent present at the 10 or 10 and 13 positions.

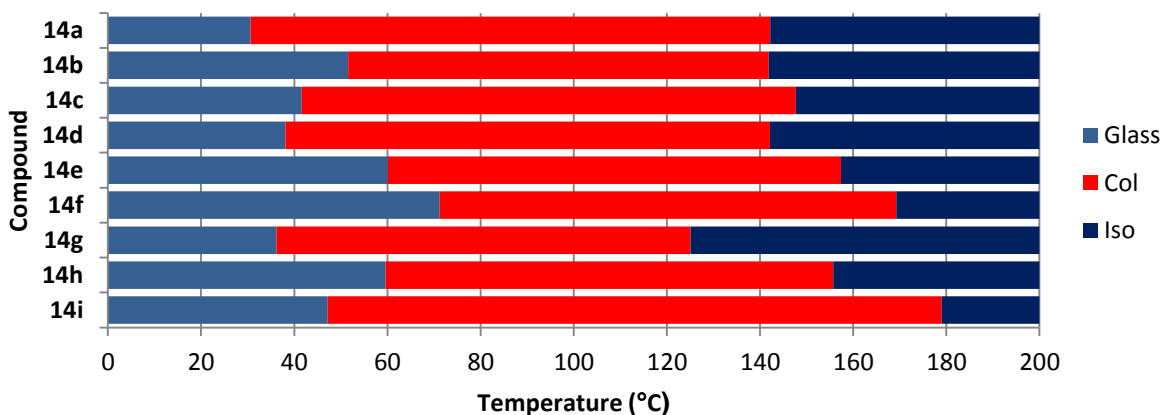


Figure 2-4: Liquid crystal ranges of di-bromo substituted hexaalkoxydibenz[a,c]anthracenes (**14a-i**). The transitions acquired by DSC are reported on heating at 10 °C·min<sup>-1</sup>. I is an isotropic liquid, Col is a columnar phase and glass indicates a glassy solid phase.



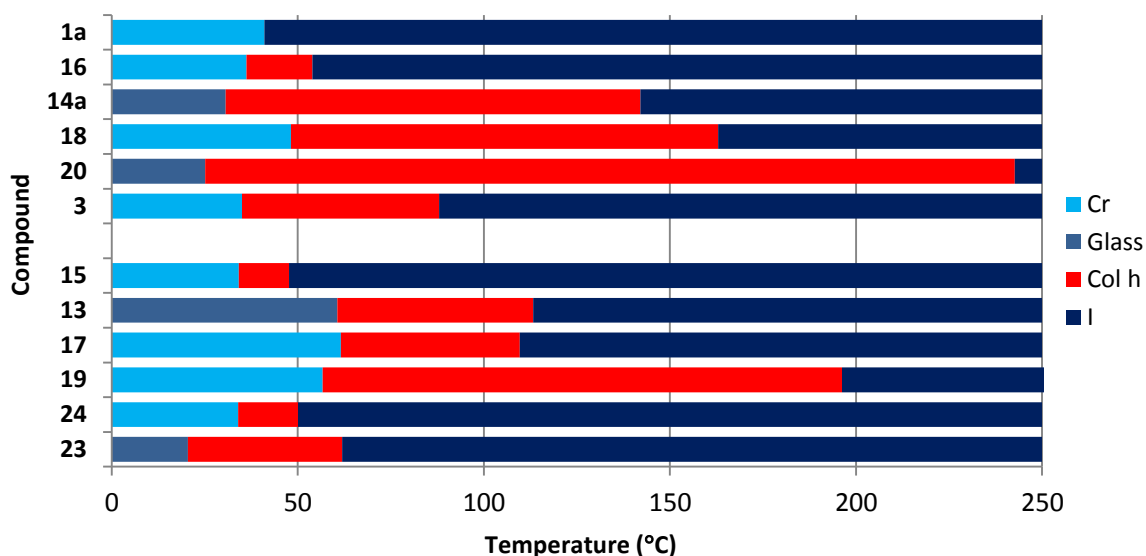
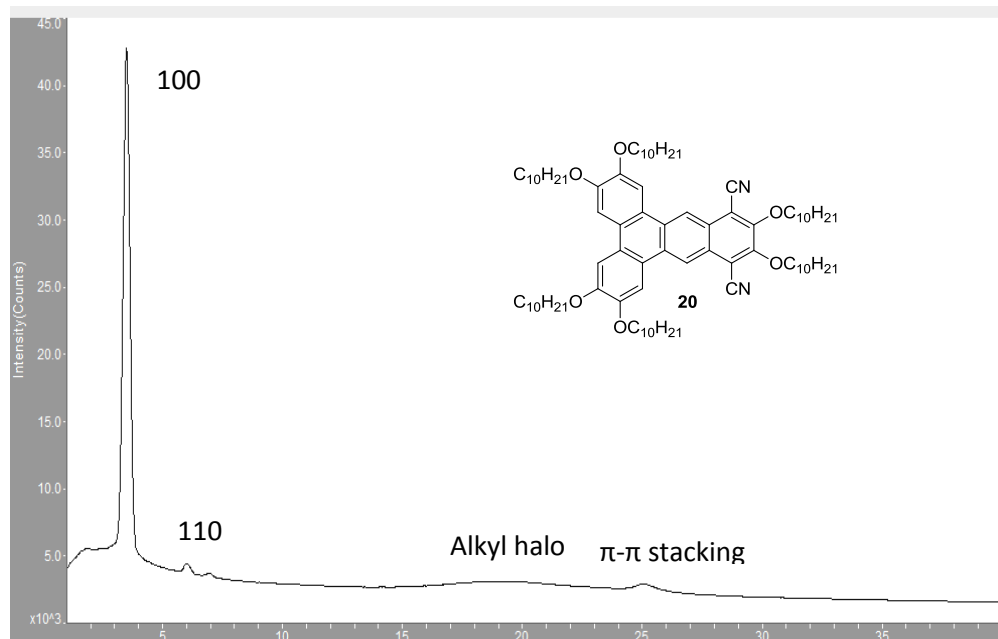


Figure 2-5: Summary of mesomorphic ranges of hexadecyloxydibenz[a,c]anthracene derivatives (**13-20**, **23**, **24** and **3<sup>79</sup>**) taken on heating at 5 °C·min<sup>-1</sup>. Cr indicates a crystal phase, Glass a glassy phase, Col h a columnar hexagonal phase and I an isotropic liquid phase.

Representative compounds **13**, **14a**, **19** and **20**, that exhibited a liquid crystal phase were analyzed using X-ray diffraction by Oliver Calderon and Professor Vance Williams at Simon Fraser University and the data are summarized in table 2-2. A representative diffractogram is presented in figure 2-6 for compound **20**.

Table 2-3: Diffractogram data of **13**, **19**, **14a**, **20**.

Compound	X, Y	Temp (°C)	d-spacing (Å)	Intensity (%)	Miller index ( <i>hkl</i> )	Phase
<b>13</b>	X = Br, Y = H	73	23.0	100	(100)	Col <sub>h</sub> (a = 26.5Å)
			4.6	0	<i>alkyl halo</i>	
			3.9	0	<i>π-π</i>	
<b>19</b>	X = CN, Y = H	75	23.6	100	(100)	Col <sub>h</sub> (a = 27.3Å)
			4.3	0.1	<i>alkyl halo</i>	
			2.8	0.1	<i>π-π</i>	
<b>14a</b>	X = Y = Br	67	23.2	100	(100)	Col <sub>h</sub> (a = 26.8Å)
			4.5	0.8	<i>alkyl halo</i>	
			3.5	3.9	<i>π-π</i>	
<b>20</b>	X = Y = CN	31	24.9	100	(100)	Col <sub>h</sub> (a = 28.7Å)
			14.5	2.9	(110)	
			4.4	1.3	<i>alkyl halo</i>	
			3.4	6.1	<i>π-π</i>	



**Figure 2-6: Representative X-Ray diffractogram of compound 20.**

The values that are obtained from the 100 and 110 reflections are used to calculate the distance between the columns. The trigonometric relationship for a hexagonal columnar phase is  $a = \frac{2}{\sqrt{3}}d$  while the (100) and (110) spacings should have a ratio of  $\sqrt{3} : 1$ . This representative data does in fact meet this relationship, which indicates that compounds **13**, **14a**, **19** and **20** are in a hexagonal columnar mesophase. These results are consistent with the information that was acquired by POM and DSC.

## 2.5 Discussion

The trends in phase behaviour that can be seen in figures 2-2 and 2-3 show that even a small change to the dibenz[*a,c*]anthracene (**1**) core can make an immense impact on the molecule

and even allow the formation of a liquid crystal phase. This is made evident by compounds **1a-i** that did not exhibit a liquid crystal phase as would be expected; instead they melted directly from the solid state to an isotropic liquid. This behaviour is a contrast to what was expected when looking at molecules with similar structures (**3** and **5**).<sup>33, 89</sup> These compounds display a relatively broad columnar phase. Compound **3** has methyl substituents at the 10 and 13 positions. The presence of a substituent in these positions must be necessary for a mesophase to occur. The evident difference between the structures **1** and **5** is that compound **5** contains an aromatic core with nitrogen atoms that make the aromatic system electron deficient. This may suggest that a decrease in electron density of the core will increase the propensity of these discotic compounds to produce a liquid crystal phase. A similar trend is found when hexaalkoxytrinaphthylenes<sup>81</sup> (**4**) and hexaazatrinaphthylenes<sup>82</sup> (**6**) are compared. In these two systems we see the formation of a liquid crystal phase solely when the core contains a nitrogen atom. This supports the argument that an electron withdrawing substituent promotes the formation of the liquid crystal phase, which reduces the electrostatic repulsion between the molecules in the stack, which in turn, favours  $\pi$ -stacking.<sup>90-92</sup> In contrast  $\pi$ -stacking is disfavoured for electron rich compounds **1a-i**.

An attempt to explain the trends that are seen with compounds **1**, and **13-20**, **23**, **24**, is done by comparing the clearing temperatures from a liquid crystal to a liquid on heating, to their Hammett sigma values.<sup>93</sup> Hammett sigma values are derived from the  $pK_a$ s of substituted benzoic acids and are an indication of whether a substituent is electron donating or withdrawing. When the data is compared a clear trend is visible: as the electron withdrawing power of the substituent increases so do the clearing temperature values, which is in agreement with the work of Bushby et al.<sup>75, 94, 95</sup> Compounds **13-20**, **23**, **24** (Figure 2-7) show a significant linear correlation ( $R^2 = 0.46$ ). Compounds **15**, **16** and **23** are obvious outliers and if they are removed from the series a much more significant linear fit is seen ( $R^2 = 0.94$ ). The broad mesophase ranges may be due to a more

favourable stacking of the electron deficient aromatic core. It is important to note that the 10 and 13 substituted compounds, **16**, **14a**, **18** and **20** have a much higher clearing temperature than their mono-substituted counterparts **15**, **13**, **17** and **19**. It is possible that dipole-dipole interactions and increased dispersion interactions may be contributing to the stability of the liquid crystal phase. Noteworthy exceptions include **1a** and **23**. Compound **1a** would be expected to show a clearing point somewhere in between the methyl (**3**) and bromo (**14a**) compounds, but it does not exhibit a liquid crystal phase. This suggests that the presence of a substituent in the 10 or 10 and 13 position is important for mesophase formation.

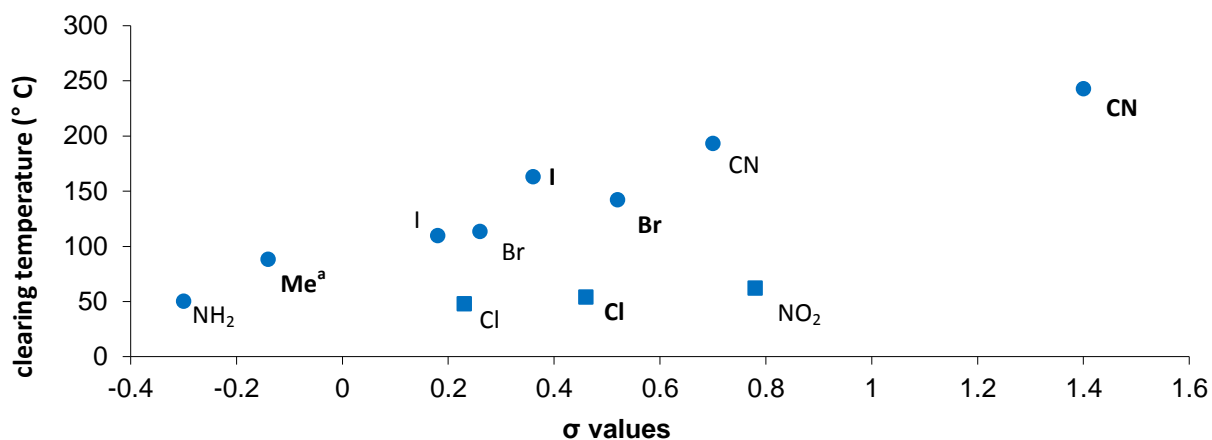


Figure 2-7: Hammett plot of the clearing temperatures taken on heating compared to the Hammett-sigma values of mono and disubstituted compounds. The disubstituted compounds are represented by the sum of their sigma values.  
<sup>a</sup>Compound **3** is taken from Lau et al.<sup>79</sup>

If the transition temperatures of the mono-halogenated series are compared, compounds **15**, **13** and **17**, we can see a steady increase in the transitions from crystal to liquid crystal at 34.2, 60.6 and 61.6 °C, and from liquid crystal to isotropic liquid at 47.7, 113.25 and 109.7 °C, respectively. A method of quantifying the properties of these substituents is by comparing their

Charton's Size Parameter ( $\delta v$ ).<sup>96</sup> This parameter is derived from the Taft equation that is a modification of the Hammett equation to include field, inductive, resonance effects as well as the steric influence. These defined values are derived from van der Waals radii and are independent of electronic influences. This parameter shows a linear correlation between size of the substituent and the temperature of the melting and clearing temperatures, figure 2-8. A similar trend is witnessed in the di-halogenated DBA series, where the melting temperatures are 36.3, 30.6 and 48.2 °C, and the clearing temperatures are 53.9, 142.1 and 162.9, respectively, for compounds **14a**, **16** and **18**.

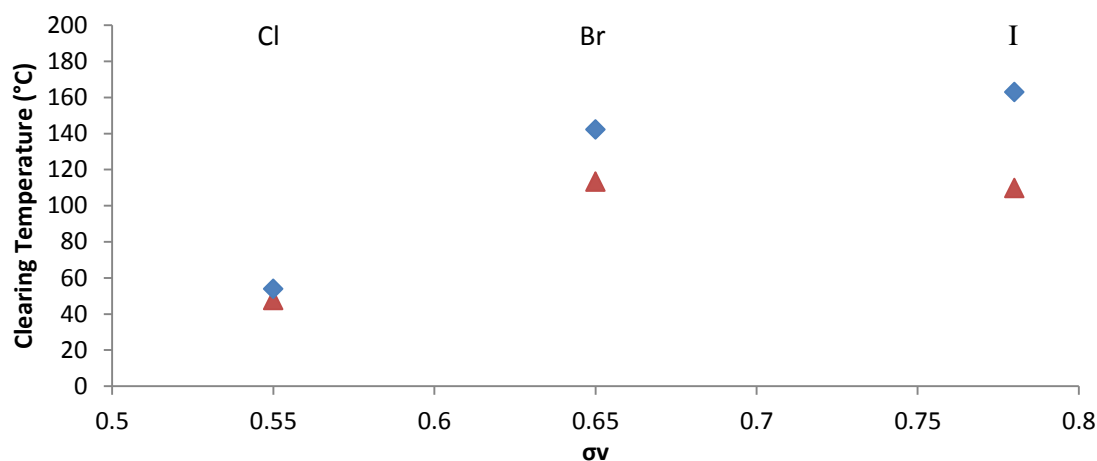


Figure 2-8: Comparison of the clearing temperatures taken on heating of the mono-halogenated, compounds **15**, **13**, **17**, (triangle) and di-halogenated, compounds **16**, **14**, **18** (diamond).

There is clearly a correlation between size and clearing temperature of the dibenzanthracene derivatives **13-18**. These groups show a significant correlation,  $R^2 = 0.64$  (for the monosubstituted series) and 0.84 (for the disubstituted series). This trend may arise from

increased dispersion forces that are seen due to the increased atomic radii of the atoms at the 10 and 13 positions.

Nitro-substituted compound **23** would be expected to have the highest clearing temperature, as it possesses the most electron withdrawing group. This is not what is seen as the transition temperature is 54.6 °C. This result may arise from the combination of two effects. If the Hammett parameters are considered, they assume the molecule can withdraw the electron density, however the nitro group must be in plane with the aromatic core, which is made difficult by the alkoxy side chain ortho to this position. The nitro group may also be forcing the alkoxy side chain out of plane to a degree where it causes destabilization of the liquid crystal phase by preventing effective  $\pi$ -stacking.

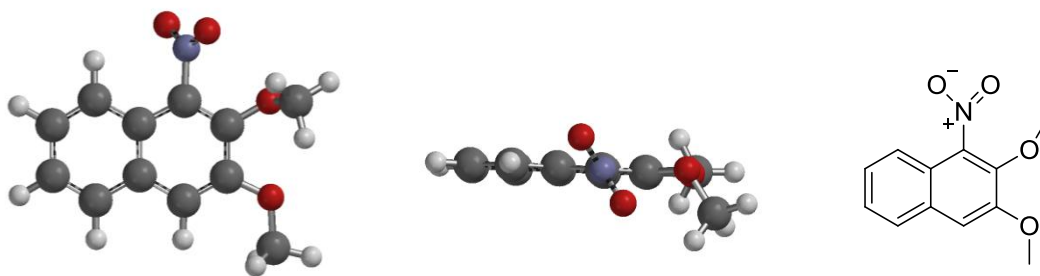


Figure 2-9: Representative moiety of **23** that illustrates lowest energy conformation (106°) of nitro group ortho to an alkoxy side chain. Calculations done using Spartan '06 software with geometry optimization done using B3LYP/6-31G\*\*.

To better understand the behaviour of compounds **1**, **13-20**, **23** and **24** we can compare our results with that of a known series of substituted hexaalkoxytriphenylene compounds **2**, **25a-f**.<sup>95, 97, 98</sup> A study by Boden *et al.* compares the nitrated, **25a**, and halogenated, **25b-d**, series (figure 2-10). The melting temperature from crystal to discotic columnar mesophase drops from 70 °C for **2b** to <25 °C, 39, 37 and 37, for **25a**, **b**, **c** and **d**, respectively. The transition from columnar mesophase to isotropic liquid goes from 100 for **2b** to 136, 116, 98 and 83 °C for **25a**, **b**,

**c** and **d**, respectively. The increase in stabilization of these compounds can be a result of  $\pi$ - $\pi$  electron donor-acceptor interactions between adjacent molecules and may also be attributed to the stabilization caused by an induced dipole-dipole interaction.<sup>99</sup> When compound **2b** is substituted with an amino group (**25e**) the phase is drastically reduced, moreover, when a methyl substituent is introduced (**25f**) the phase disappears completely. The disappearance of the columnar phase is attributed to a sterically overloaded situation.<sup>97</sup>

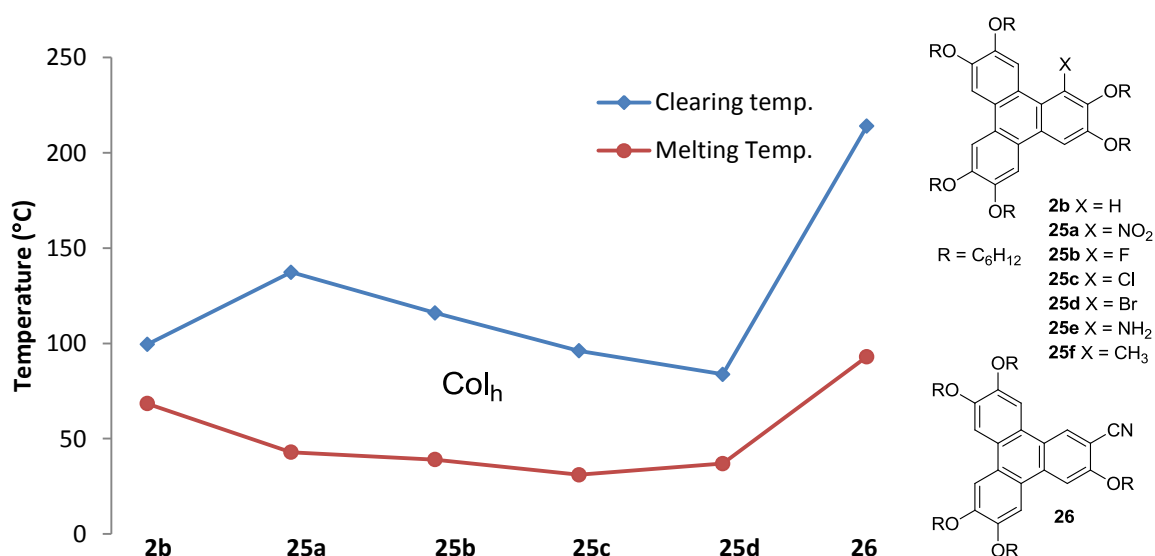


Figure 2-10: Phase behaviour of hexaalkoxytriphenylene (**2**) and the substituted compounds **25a**,<sup>97</sup> **b**,<sup>98</sup> **c**, **d** and **26**.<sup>95</sup>

In a study by Williams *et al.*,<sup>90</sup> there is a striking correlation between the tendency of tetraalkoxydibenzophenazines (compounds **27a-g**) to form columnar phases with respect to the electron withdrawing and donating ability of the functional group attached to the core. Compounds with an electron withdrawing group (**27a-d**) tend to form a columnar hexagonal phase. This series shows a linear correlation when the electron withdrawing abilities ( $\sigma_m$ ) of the

substituents are plotted against the clearing temperatures of the liquid crystal phases (figure 2-11). As the  $\sigma_m$  values increase, so do the clearing temperatures. The compounds that contain an electron donating group (**27e-g**) are non-mesogenic. This may be explained in terms similar to the previous system (**2b**, **25a-d**) where the electron withdrawing nature of the functional groups helps to minimize the repulsive interaction between the aromatic systems, favouring  $\pi$ - $\pi$  stacking,<sup>91, 92</sup> although this situation is separate as the steric situation is no longer applicable. It has also been shown computationally that  $\sigma_m$  values and the strength of the arene-arene stacking correlate well.<sup>100</sup> In this case the discogens may also benefit from dipole-dipole interactions as the molecules orient themselves in an antiferroelectric fashion. An increase in the electron withdrawing ability of the substituent should increase the dipole of the molecule allowing more uniform and stable stacking. This also explains why the XRD data shows a symmetrical hexagonal arrangement from such a low-symmetry compound.<sup>90</sup>

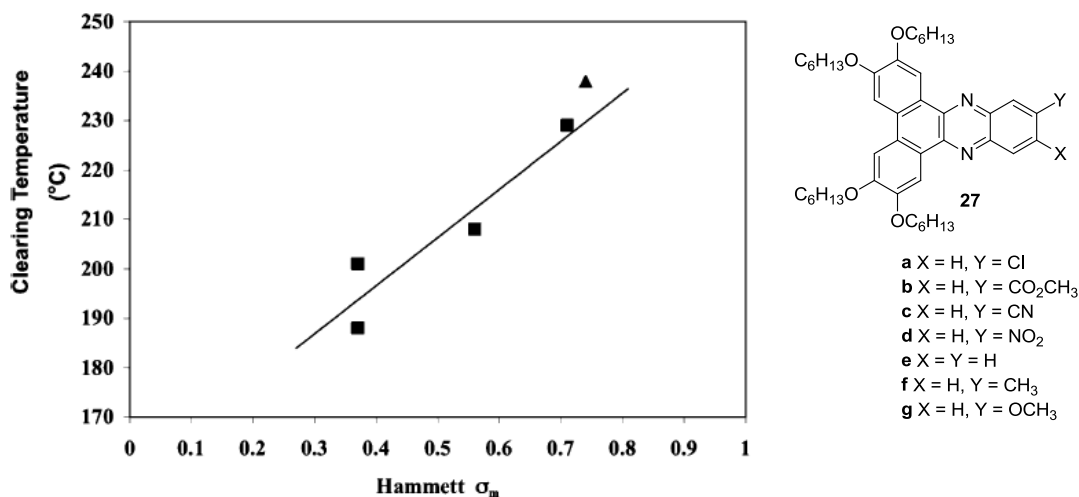


Figure 2-11: Comparison of clearing temperature of compound 17a-d with respect to their Hammett  $\sigma_m$  values.<sup>90</sup>



Based on this trend one would expect that an increase in electron density would reduce the ability to form a liquid crystal phase. This is not the case for compound **3**, a dibenzanthracene core molecule that possesses two methyl substituents at the 10 and 13 positions.

This class of compounds demonstrates a correlation between size of substituent and electron withdrawing ability of the substituents and the clearing temperatures as well as a requirement of a substituent on the core at the 10 and 13 positions. As a result the liquid crystallinity is a product of an interplay between steric and electronic effects.

## 2.6 Summary

A modular synthesis of a novel hexaalkoxydibenzanthracene (**1a-i**) has been reported. Unfortunately, compounds **1a-i** do not exhibit a liquid crystalline phase, despite the structural similarity to previously reported mesogenic compounds. When substituents were introduced into the 10 and 13 position on the aromatic core of this molecule, there is the appearance of a mesophase over a broad temperature range. These results show that small structural variation to the core molecule can greatly affect the mesogenic character of these compounds. The variety of functionalization gives a synthetic handle for further post-functionalization of this compound which describes a class of compounds with highly tuneable properties. The mesogenic range is found to depend on the electronics and size of the substituent.

## Chapter 3 Dibenzo -tetra/pentacene and Tetrabenzopentacene -diones

### 3.1 Introduction

In chapter 2 we showed that electron withdrawing substituents on the aromatic core promote columnar mesophase formation. It is therefore plausible that incorporation of quinone groups into the core would also produce compounds with columnar phases. There is evidence that discotic frameworks with carbonyl groups bonded to the

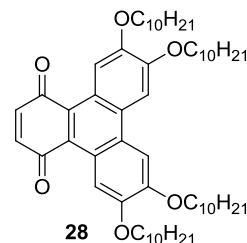


**Figure 3-1: Triphenylene dione derivative.**

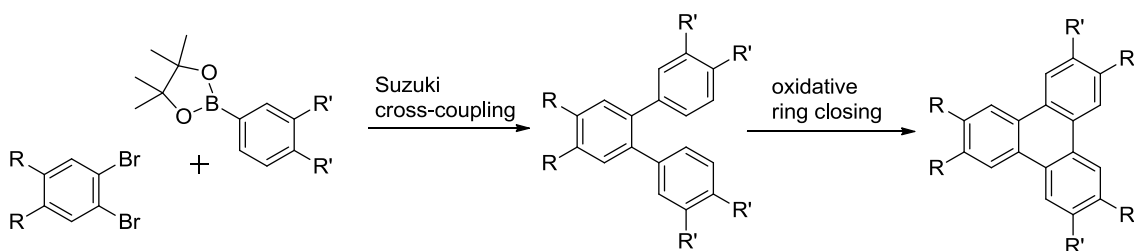
core atom should show a liquid crystal phase. Swager et al. have shown that a triphenylene-dione half-disc mesogen (**28**) demonstrates this intermediate state of matter (figure 3-1).<sup>101</sup> To probe the theory that an electron withdrawing substituent present in the ring should increase the propensity of a discogen to form a liquid crystal, a series of novel polyaromatic hydrocarbons with carbonyl groups in the core system will be synthesized utilizing a synthetic approach similar to that employed for the dibenzanthracenes described in chapter 2. The electron withdrawing substituent should decrease the electron density in the aromatic system which will effectively promote favourable  $\pi$ - $\pi$  stacking of the discogens to create a broad liquid crystal phase at a convenient temperature range.

The presence of the carbonyl groups on the aromatic cores will also provide a synthetic handle that will be a convenient route for further synthetic transformations. The synthetic derivatives of the acene diones can provide important information necessary for an understanding of a structure-property relationship of these mesogens.

### 3.2 Synthesis of dibenzo -tetra/pentacene and tetrabenzopentacene -diones

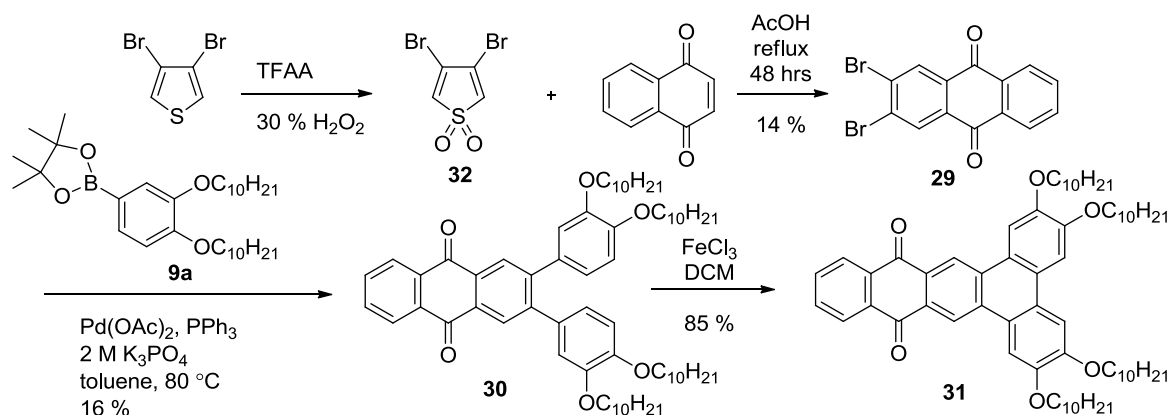
The synthesis of a new class of discotic molecules, compounds **31**, **36** and **46** employed similar methodology to the synthesis of the dibenz[*a,c*]anthracene and its derivatives (**1**, **13-20**, **23**, **24**), as described in chapter 2. This modular synthesis could prove to be a general method for the preparation of a diverse set of polycyclic aromatic hydrocarbons and related compounds. They involve a Suzuki cross-coupling followed by oxidative cyclization reaction (figure 3-1).

**Scheme 3-1: General synthetic scheme demonstrating the suzuki coupling and ring closing reaction.**



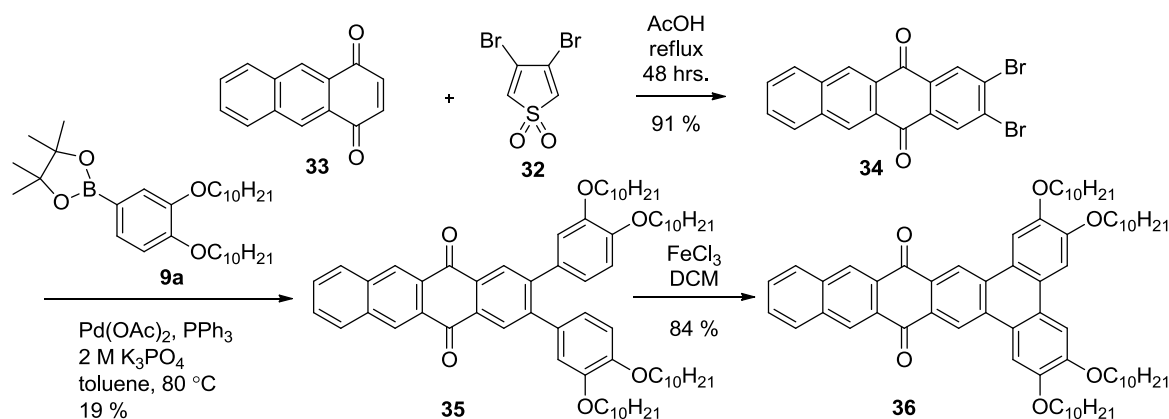
The first step in the modular synthesis of 2,3,6,7-tetrakis(decyloxy)dibenzo[*a,c*]tetracene-10,15-dione (**31**) involved the formation of 3,4-dibromothiophene-1,1-dioxide (**32**) from 3,4-dibromothiophene using a procedure by Lu *et al.*,<sup>102</sup> (scheme 3-2). This reaction used the oxidation of thiophene with 30 % H<sub>2</sub>O<sub>2</sub> and the dropwise addition of trifluoroacetic anhydride at -15 °C. This compound was subjected to a Diels-Alder cycloaddition reaction that was a modified version of Williams *et al.*<sup>103</sup> using 2 equivalents of 1,4-naphthoquinone in glacial acetic acid. This mixture was heated to reflux for 2 days which yielded 2,3-dibromoanthracene-9,10-dione (**29**) in relatively low yield (14 %). The synthesis of the boronate ester, 1-pinacolatoboron-3,4-bis(decyloxy)benzene (**9a**), was previously described in chapter 2 (figure 2-1). Compound **9a** and **29** were combined using a Suzuki-Miyaura cross coupling reaction to give the 2,3-bis[3,4-didecyloxybenzene]anthracene-9,10-dione (**30**) in 14 % yield. This was followed by an FeCl<sub>3</sub> mediated oxidative ring closing reaction that gave the desired product, dibenz[*a,c*]tetracene-6,11-dione (**31**), in 85 % yield.

**Scheme 3-2: Synthesis of dibenzotetracenedione 31.**



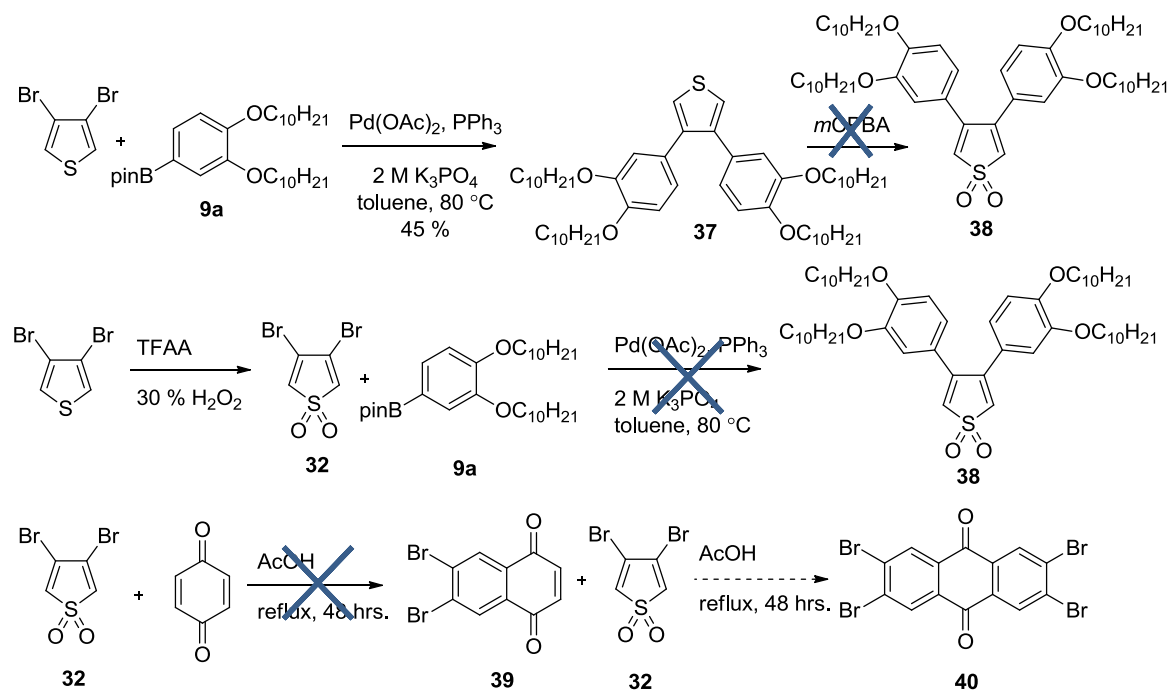
The synthesis of 2,3,6,7-tetrakis(decyloxy)dibenzo[*a,c*]pentacene-10,17-dione (**36**) utilized several of the same steps including the Diels-Alder cycloaddition, the Suzuki-Miyaura cross coupling and the oxidative ring closing reactions. The anthracene-1,4-dione (**33**) was acquired from a reduction of quinizarin from  $\text{NaBH}_4$  in MeOH followed by treatment with concentrated acetic acid and water.<sup>104</sup> Two equivalents of this compound were combined with the 3,4-dibromothiophene-1,1-dioxide (**32**) under reflux conditions in acetic acid for 2 days to give 2,3-dibromotetracene-5,12-dione (**34**) in 91 % yield (scheme 3-3).<sup>103</sup> The dione was combined with 2.1 equivalents of the boronic ester **9a** under cross coupling conditions described previously mentioned and gave the adduct **35** in 19 % yield. Compound **35** was then treated with 6 equivalents of  $\text{FeCl}_3$  to yield compound **36** with a yield of 84 %.

**Scheme 3-3: Synthesis of dibenzopentacenedione 36.**



The synthesis of 2,3,6,7,13,14,17,18-octakis[decyloxy]-tetrabenz[e,*a,c,d,f*]pentacene-5,21-dione (**45**) proved to be more difficult (scheme 3-4). Initially this synthesis was undertaken with an attempt to perform a cross-coupling reaction on the 3,4-dibromothiophene starting material, followed by the oxidation of sulfur atom, then an oxidative ring closing followed by a Diels-Alder reaction to obtain the final product. The C-C bond formation of the thiophene and the boronic ester (**9a**) was a successful reaction to create compound **37**; however once the compound was exposed to the oxidation conditions, we saw a decomposition of the molecule. An initial oxidation of the thiophene to afford **32**, followed by the cross coupling reaction to achieve the new C-C bond to make compound **38** was also unsuccessful. An attempt at an initial Diels-Alder with benzoquinone directly from the 3,4-dibromothiophene (**32**) was performed, although this reaction gave low yield of compound **39** and required a small scale reaction, which was not ideal for the beginning steps of a multi-step synthesis. The sequential Diels-Alder reaction of **32** with **39** to make compound **40** was also unsuccessful.

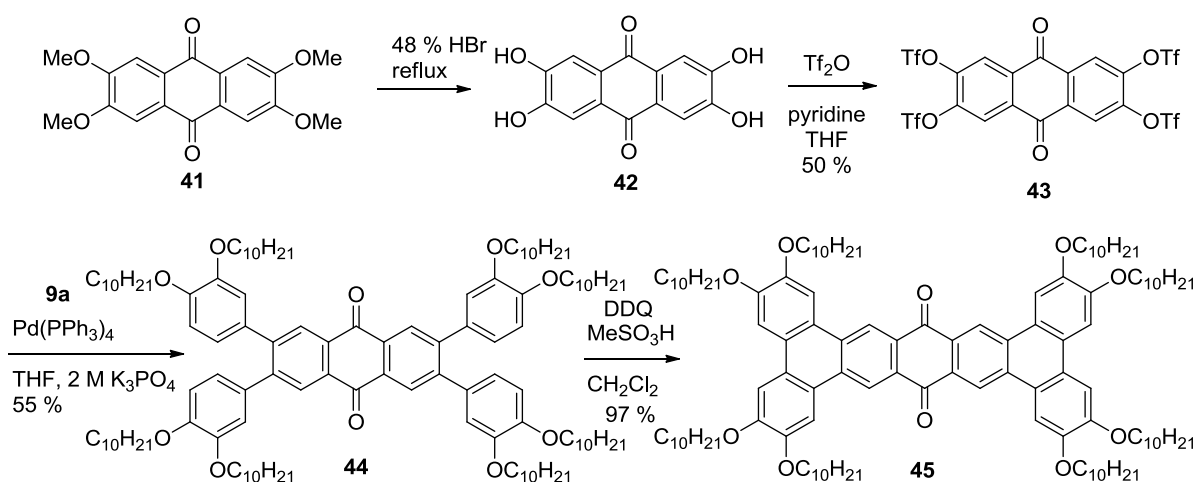
**Scheme 3-4: Synthetic attempts toward the synthesis of tetrabenzopentacene.**



Therefore, a new tactic was employed (scheme 3-5) that would utilize an anthraquinone starting material (**41**) present with four functional groups that are convenient for a cross-coupling reaction and two carbonyl groups for further post-modification of the extended aromatic system. 2,3,7,8-tetramethoxyanthracene-5,10-dione (**41**) was previously prepared in our lab using known procedures.<sup>105, 106</sup> Compound **41** then underwent a demethylation using 48 % HBr at a reflux for 3 days to give 2,3,7,8-tetrahydroxyanthracene-5,10-dione (**42**) in 24 % yield.<sup>107</sup> The next step that was required was the installation of triflate groups at the hydroxyl positions to allow for the cross-coupling reaction with the boronate ester **9a**. This reaction was modified from a procedure from Zöphel et al.<sup>108</sup> Compound **42** was treated with triflic anhydride at  $-78^\circ\text{C}$  in the presence of pyridine and THF. The reaction mixture was then warmed to room temperature and stirred for 3 days. Once purified, this procedure gave pure product, 2,3,7,8-tetrakis(trifluoromethanesulfonate)anthracene-5,10-dione (**43**) in 50 % yield. To compound **43** was added **9a** and palladium tetrakis(triphenylphosphine) in dry THF. This mixture was combined with degassed 2M

$K_3PO_4$ , and the reaction mixture was heated to 60 °C and stirred for 2 days. The compound was extracted and purified via column chromatography to give a 55 % yield of compound **44**. A ring closing was performed on this adduct in a mixture of dichloromethane and methanesulfonic acid at 0 °C in the presence of 2,3-dichloro-5,6-dicyano-1,4-benzoquinone (DDQ) for 30 minutes to give 2,3,6,7,13,14,17,18-octakis[decyloxy]-tetrabenzene[*a,c,d,f*]pentacene-5,21-dione (**45**) with an excellent yield of 97 %, although the product had very low solubility in the solvents used.

**Scheme 3-5: Synthesis of tetrabenzopentacenedione.**



### 3.3 Mesophase Characterization

The initial characterization of these compounds was done using POM to acquire approximate temperatures of transition and to characterize the liquid crystal phases that are formed. Compounds **31**, **36** and **45** all displayed liquid crystal phases that exhibit textures consistent with a columnar phase (figure 3-2).

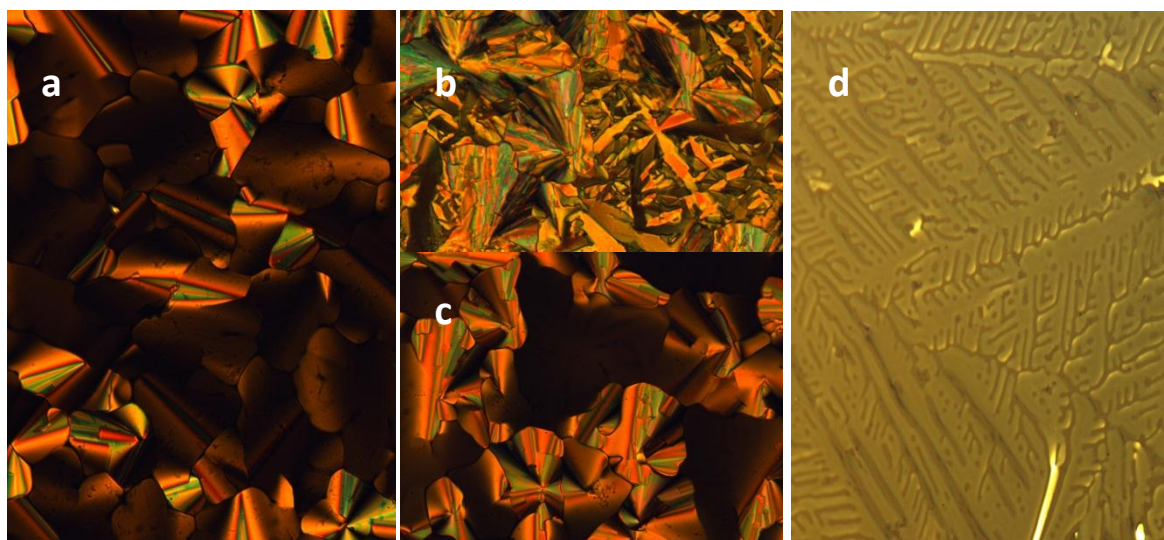


Figure 3-2: Micrographs of compounds **31**, **36** and **45** showing textures typical of a columnar hexagonal phase: a) **31** at 170 °C, b) **36** (cr2) at 165 °C, c) **36** (col) at 185 °C, d) **45** at 250 °C. The micrographs are taken on cooling and were taken at 100x magnification.

The ranges and temperatures of the liquid crystal phases are shown in table 3-1. The range of the triphenylene quinone (**28**)<sup>101</sup> is included for comparison.

Table 3-1: Phase behaviour of compounds **31**, **36** and **45** as determined by DSC on heating at 5 °C·min<sup>-1</sup>.

Compound	Phase Transition						
	Transition Temperature °C (enthalpies of transition J·g <sup>-1</sup> )						
<b>28</b> <sup>101</sup>	Cr	87.7 (36.7)	Col	94.5 (2.0)			I
<b>31</b>	Cr	129.41 (46.35)	Col	186.41 (2.91)			I
<b>36</b>	Cr	170.07 (49.39)	Col	187.37 (1.13)			I
<b>45</b>	Cr 1	117.77 (22.72)	Cr 2	154.44 (9.90)	Col	284.02 (2.70)	I

For a direct comparison of the mesophase behaviour the temperatures of transition of compounds **28**, **31**, **36** and **45** are summarized graphically in figure 3-3.



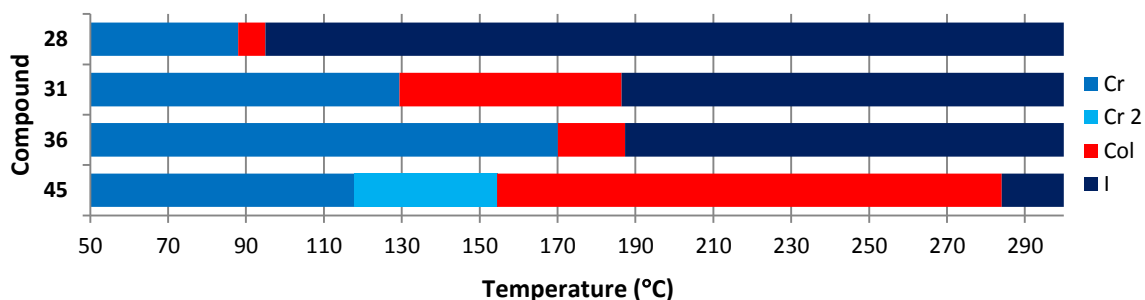


Figure 3-3: Graphical representation of phase behaviour of 28,<sup>101</sup> 31, 36 and 45 on heating.

For a designation of the liquid crystal phase, XRD studies must be completed. However, the textures seen by POM (figure 3-2a, c, d) are characteristic of a columnar phase.

### 3.4 Discussion

Previous results with substituted dibenzanthracenes suggest that electron-deficient PAHs promote stable columnar mesophases because  $\pi$ -stacking is electrostatically favoured. A comparison of compounds **31**, **36**, and **45** provides an opportunity to probe the effects of changing the core size on the mesophase temperature range. We in fact see a liquid crystal phase in all three compounds. The closest comparison to compound **31** found in the literature would be 2,3,6,7-tetraalkoxytriphenylene-9,12-dione (**47**).<sup>109</sup> The main difference is an increase in the length of the core by two benzene rings. As for the mesophase, there is an increase in the breadth of the liquid crystal phase. This trend supports the argument that an increased core size will lead to an increase in the size of liquid crystal phase.<sup>79</sup> This theory, however, is not true for **36**, where the breadth of the mesophase is reduced significantly, even though the core length is increased to a pentacene dione ring system. This compound possesses only 4 aliphatic chains on one side of the molecule, which may affect the stability of the liquid crystal phase. As the length

of the core increases, it may increase the stability of these molecules to pack in the crystal state; as a result an increase the temperature of the transition from crystal to liquid crystal is seen. At the same time, the clearing point is nearly unaffected. If compound **28** had the carbonyl groups removed from the core structure, it would be a 2,3,6,7-tetraalkoxytriphenylene (**46**). Compound **46** does not exhibit mesogenic character.<sup>109</sup> However, if in place of carbonyl groups there is a bromine substitution at the 2 and 3 position (**47**), we again see a liquid crystal phase, from 130 to 141 °C on heating (hexyloxy chains),<sup>109</sup> or for a nitrile substitution at the 2 and 3 position, compound (**48**) exhibits a liquid crystal phase from 164 to 190 °C on heating.<sup>110</sup> This comparison suggests that the mesogenic properties of these materials requires an electron withdrawing group present on the molecule or merely requires the presence of a substituent at these positions.

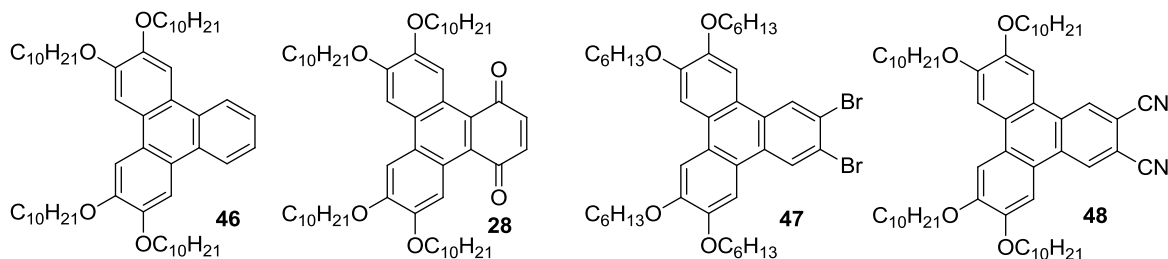


**Figure 3-4: Derivatives of discotic triphenylene molecules.**

As compound **45** is a new class of liquid crystals, there is no literature with which to compare this molecule. To understand the physical and chemical properties that determine the mesogenic characteristics of this compound, a series of derivatives must be prepared. A rough comparison of compound **45** to its dibenzopentacene (**36**) counterpart shows an increased liquid crystal range. The increase in the number of flexible decyloxy side chains from 4 to 8 no doubt gives it a more stable mesophase. This compound may be dependent on the presence of the

dione functional groups to withdraw electron density from the core so that there is increased  $\pi$ - $\pi$  stacking.

### 3.5 Summary

A series of extended conjugated core systems based on acenedione cores (**31**, **36**, **45**) have been prepared. These compounds, as predicted, show mesogenic character, due in part to the electron withdrawing nature of the oxygen on the core system. The extension of the aromatic system did not increase the length of the liquid crystal phase due to reduced number of aliphatic side chains from 6 to 4 and the increased stability of the crystalline phase for the dibenzo- compounds (**31** and **36**). The tetrabenzopentacenedione (**45**) exhibited a relatively large mesophase which was at a higher temperature than the previous reported dibenzanthracene series (**13-20**, **23**, **24**). This may also be explained by the increased stability of these discotic systems in the crystal phase. The discogens also have a convenient synthetic handle for post-synthetic modification for creation of a series of compounds for further investigation of the structure-property relationships.

## Chapter 4 Conclusions and Future Work

A series of hexaalkoxydibenzanthracene derivatives (**13-20**, **23**, **24**) were synthesized using a modular approach. These compounds exhibited a mesophase over broad temperatures, with the largest mesophase being the nitrile substituted compound (**20**). The structure-property relationship that was formed from this class of compounds demonstrates that there is the necessity for a substituent in the 10 or 10 and 13 positions for mesophase formation. The substituents have a general trend of increasing the breadth of the mesophase temperature range based on the electron withdrawing ability. There are, however, notable exceptions to this trend. The nitro substituted compound (**23**) shows a surprisingly narrow liquid crystal range; this is thought to occur due to poor conjugation with the core and distortion of the orthogonal aliphatic side chain out of plane, disrupting the packing arrangement of the columns. The halogen series (**13-18**) also demonstrates a trend that correlates with the size of the substituent rather than the electronics of the atom. This may be due in part to increased dispersion that promotes  $\pi$ -stacking within the columns.

This study has prepared two new classes of columnar liquid crystals and provided insight into the structural features that affect liquid crystal properties. Furthermore, the synthetic approach is versatile, and can be applied to the synthesis of other novel discotic systems. The elongated aromatic systems (**31**, **36**, **45**) all exhibited liquid crystalline phases. These compounds are thought to be mesogenic due to their elongated aromatic core and due to the carbonyl groups withdrawing electron density from the aromatic core. The liquid crystal range is smaller than the DBA molecules due to the decrease in number of aliphatic chains for compounds **31** and **36**, which may result in an increased stability of the crystalline state as shown by the increasing melting point. Compound **45** exhibits a relatively large mesophase; however, this range is elevated and therefore is inconvenient for potential applications.

Modification of **45** will reveal if the electron withdrawing ability of the oxygen is essential to the formation of a liquid crystal phase. This is what is seen in the dibenzanthracene compounds **1a-i**, where the substituent at the 10 and/or 13 positions are necessary for the presence of a mesophase. Post-synthetic modification of compound **31**, **36** and **45** will be facilitated by the dione synthetic handle present in the 5 and 10 positions. This will allow for synthetic transformations, e.g.: reduction to a fully aromatic discotic core, nucleophilic addition at the position of the carbonyl groups. This would provide a method to tune the properties of these novel discotic materials.

The future directions of this research should include the synthesis of compounds that possess 6 aliphatic side chains, figure 4-1 (**50** and **51**) for a more direct comparison with known liquid crystal to achieve a more accurate and revealing structure-property relationship.

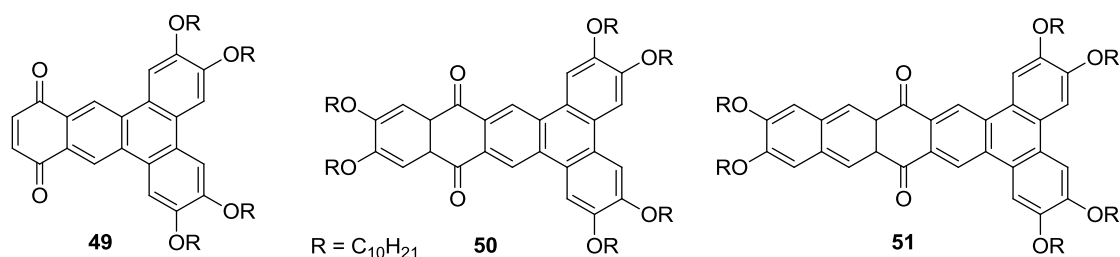


**Figure 4-1: Future target compounds.**

The synthesis of compound **49**, was attempted with no success. A different synthetic route will be required in order to synthesize this molecule. This will also allow a more direct comparison with the DBA series.

Furthermore, the carbonyl groups give a convenient synthetic handle for post-synthetic modification as seen with the dibenzanthracene series (**13-20**, **23**, **24**). A series of these compounds, for example **53-55**, along with the series previously synthesized compounds may elucidate some trends for elongated aromatic discotics.

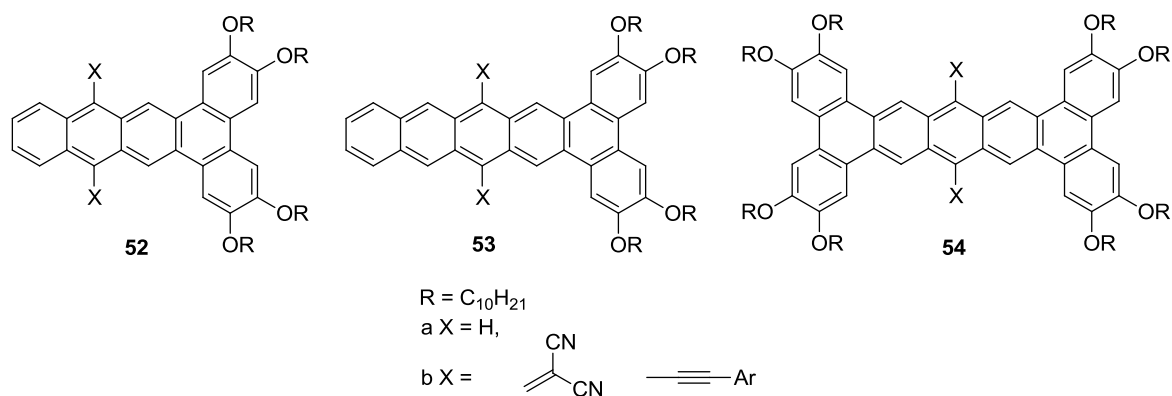


**Figure 4-2: Future target discotic molecules.**

The fully conjugated analogues of compounds **31**, **36** and **45** do not exist in literature; therefore, a reduction of these compounds to their fully aromatic analogues (**52a**, **53a**, **54a**) will give insight into the effects of an electron withdrawing group attached to the core molecule, and potentially exhibit interesting electronic properties suitable for applications in semiconductor technologies. Ultimately, this study will allow us to tune the liquid crystal properties as well as the HOMO-LUMO band gap by modifying the core systems. Control of the electronic properties of these mesogens will enable the design of compounds suitable for applications in semiconducting devices.

## Chapter 5 Experimental

### 5.1 General

Oven or flame-dried glassware was used for all reactions. Melting points were determined using a Barnstead Electrothermal 9100 melting point apparatus (uncorrected) or with a Differential Scanning Calorimeter using a TA Instruments DSC Q200 with a scanning rate of 5 or 10 °C/min.

#### 5.1.1 NMR Spectroscopy

$^1\text{H}$ -NMR and  $^{13}\text{C}$ -NMR were recorded using a Varian 300 MHz ( $^1\text{H}$ ) Unity Inova NMR Spectrometer, using indicated deuterated solvents purchased from CIL Inc. Chemical shifts are reported in  $\delta$  and scale downfield from the peak for tetramethylsilane.

In some cases not all aliphatic  $^{13}\text{C}$  peaks are observed in substituted hexaalkoxydibenzanthracene precursors and products due to overlapping signals.

#### 5.1.2 Mesophase Characterization

Polarized optical microscopy studies were carried out using an Olympus BX-51 polarized optical microscope equipped with a Linkam LTS 350 heating stage and a digital camera. Differential Scanning Calorimetry (DSC) studies were carried out using a TA Instruments DSC Q200 with a scanning rate of 5 °C/min. Variable temperature X-Ray diffraction measurements were carried out by Oliver Calderon and Professor Vance Williams at Simon Fraser University on a Rigaku RAXIS rapid diffractometer using Cu K $\alpha$  radiation ( $\lambda=1.5418\text{\AA}$ ), a graphite monochromator and a Fujifilm Co. Ltd curved image plate (460 mm x 256 mm). Samples were heated to the isotropic liquid phase on a hot plate and loaded by capillary action. Excess material was cleaned off the sides with clean dry tweezers. Capillaries

were then cut to length and mounted in our capillary furnace. Temperature was controlled with an Omega temperature controller connected to the capillary furnace with a K-type thermocouple for feedback. Owing to technical issues, the controller was set to manual mode. Due to thermal equilibration, the temperature often dropped during a run. Only the final temperature is reported. A 0.3 mm collimator was used and all samples were irradiated for 30 minutes. Peaks and their respective angle measurements and d-spacings were determined using the MDL JADE software. Peak type was analyzed by taking the reciprocal d-spacings and dividing them by the highest intensity peak. Only peaks with greater than 1% intensity in the low angle region were reported in this précis. Columnar hexagonal unit cell parameters were determined from the d-spacing using the formula  $a = \frac{2}{\sqrt{3}}d$  which is derived from the sine relationship in right angle triangles formed by inscribing the hexagonal unit cell in a rectangle.

#### **5.1.4 – High Resolution Mass Spectrometry**

High resolution MALDI mass spectra were recorded at the Centre Régional de Spectrométrie de Masse à l'Université de Montréal using an Agilent LC-MSD TOF spectrometer.

#### **5.1.3 Chemicals and Solvents**

All chemicals used were purchased from Sigma-Aldrich and were used as received, with the exception of triflic anhydride and pyridine which were purified by distillation.<sup>111</sup> Ir (III) chloride used to synthesize the catalyst for borylation was purchased from Pressure Chemicals. Anhydrous and oxygen-free solvents were dispensed from a custom-built solvent purification system which used purification columns packed with activated alumina and supported copper

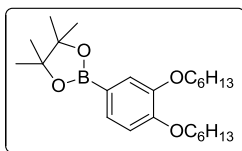


catalyst (Glasscontour, Irvine, CA). The following compounds were prepared according to literature procedures: 1,2,6,7-tetrabromo-2,3-dihydroxynaphthalene,<sup>81</sup> 6,7-dibromo-2,3-dihydroxynaphthalene (**10**),<sup>81</sup> 1,2-bis(hexyloxy)benzene (**8c**),<sup>83</sup> 1,2-bis(octyloxy)benzene (**8b**),<sup>83</sup> 1,2-bis(decyloxy)benzene (**8a**),<sup>83</sup> 2,3-dibromo-6,7-bis(hexyloxy)naphthalene (**11c**),<sup>81</sup> 2,3-dibromo-6,7-bis(octyloxy)naphthalene (**11b**),<sup>81</sup> 2,3-dibromo-6,7-bis(decyloxy)naphthalene (**11a**),<sup>81</sup> [Ir(OMe)COD]<sub>2</sub>,<sup>112</sup> 3,4-dibromothiophene-1,1-dioxide (**32**),<sup>102</sup> anthracene-1,4-dione (**33**),<sup>104</sup> 2,3-dibromoanthracene-5,10-dione (**39**),<sup>103</sup> 2,3,7,8-tetramethoxyanthracene-5,10-dione (**41**),<sup>106</sup> 2,3,7,8-tetrahydroxyanthracene-5,10-dione (**43**).<sup>107</sup>

## 5.2 Synthesis

**General Procedure for borylation of 1,2-bis(alkoxy)benzene (**9**)**<sup>113</sup>: Cyclohexane (50 mL) was degassed with N<sub>2</sub> for 15 minutes. To the solvent 4-4'-di-*tert*-butyl-2,2'-dipyridyl (0.081 g, 0.30 mmol), bis(pinacolato)diboron (1.67 g, 6.58 mmol) and [Ir(OMe)COD]<sub>2</sub> (0.099 g, 0.15 mmol) were added followed by 1,2-bis(alkoxy)benzene (5.98 mmol). The solution was heated to 80°C and left to stir under positive N<sub>2</sub> flow for 2 days. The reaction mixture was concentrated and the crude products were further purified as is using column chromatography using the solvent systems as indicated. NMR data compared to literature values.<sup>30</sup>

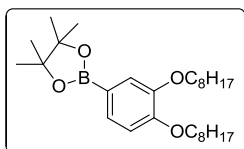
**Synthesis of 1-pinacolatoboron-3,4-bis(hexyloxy)benzene (**9c**)**: 1,2-bis(hexyloxy)benzene (1.67 g,



5.98 mmol) was used. A brown oil was obtained as a crude product. Column chromatography with hex/EtOAc (98:2) was used to purify the crude product to yield a clear colourless liquid (1.26 g, 52 % yield). <sup>1</sup>H

NMR (300 MHz,  $\text{CDCl}_3$ ):  $\delta$  7.39 (d,  $J$  = 7.35 Hz, 1H), 7.29 (s, 1H), 6.88 (d,  $J$  = 7.80 Hz, 1H), 4.05-3.99 (m, 4H), 1.84-1.79 (m, 4H), 1.49-1.45 (m, 4H), 1.37-1.26 (m, 20H), 0.93-0.88 (m, 6H).

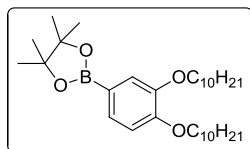
**Synthesis of 1-pinacolatoboron-3,4-bis(octyloxy)benzene (9b):** 1,2-bis(octyloxy)benzene (2.00 g,



5.98 mmol) was used to obtain a brown oil. The crude product was purified using column chromatography with hex/EtOAc (98:2) to yield a clear colourless oil (2.56 g, 93 % yield).  $^1\text{H}$  NMR (300 MHz,  $\text{CDCl}_3$ ):  $\delta$  7.40

(d,  $J$  = 1.5 Hz, 1H), 7.29 (s, 1H), 6.89 (d,  $J$  = 8.4 Hz, 1H), 4.05-3.99 (m, 4H), 1.86-1.78 (m, 4H), 1.47-1.23 (m, 32H), 0.89-0.86 (m, 6H).

**Synthesis of 1-pinacolatoboron-3,4-bis(decyloxy)benzene (9a):** 1,2-bis(decyloxy)benzene (2.34 g,



5.98 mmol) was used to obtain a black oil. The oil was purified using column chromatography with hex/EtOAc (96:4) to give a colourless solid (1.82 g, 59 % yield).  $^1\text{H}$  NMR (300 MHz,  $\text{CDCl}_3$ ):  $\delta$  7.39 (d,  $J$  = 6.6 Hz, 1H),

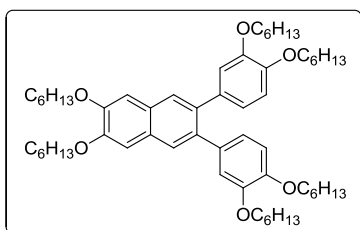
7.29 (s, 1H), 6.88 (d,  $J$  = 7.8 Hz, 1H), 4.05-3.99 (m, 4H), 1.84-1.79 (m, 4H), 1.33-1.24 (m, 40H), 0.90-0.88 (m, 6H).

**General procedure for the synthesis of 1,2-dialkoxy-5,6-bis(3,4-dialkoxybenzene)naphthalene**

**(12):**  $\text{Pd}(\text{OAc})_2$  (5 mol %) and  $\text{PPh}_3$  (10 mol %) were dissolved in 20 mL degassed toluene, followed by the addition of 2,3-dibromo-6,7-bis(decyloxy)naphthalene (1 eq) and 1-pinacolatoboron-3,4-bis(decyloxy)benzene (2.09 eq.). To the reaction mixture 7 mL degassed aq. 2.0 M  $\text{K}_3\text{PO}_4$  (excess) was added. The mixture was heated to 80°C and left to stir for 48 hours. The solution was cooled to room temperature, followed by the addition of 20 mL dichloromethane and washed with  $\text{H}_2\text{O}$  (2x20 mL) and brine (1x20 mL). The organic layer was dried with  $\text{MgSO}_4$  and solvent removed

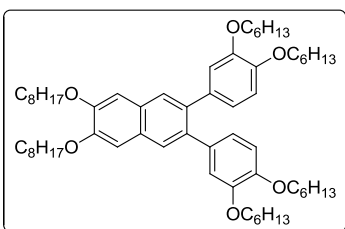
under reduced pressure to give product. The crude product was used in the next step without further purification with the exception of compound **12a**.

**2,3-bis[3,4-dihexyloxybenzene]-6,7-bis(hexyloxy)naphthalene (12i):** Pd(OAc)<sub>2</sub> (0.024 g, 0.112



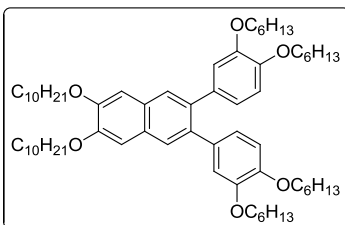
mmol) and PPh<sub>3</sub> (0.058 g, 0.224 mmol), aq. 2.0 M K<sub>3</sub>PO<sub>4</sub> (excess), 2,3-dibromo-6,7-bis(hexyloxy)naphthalene (0.49 g, 1.08 mmol) and 1-boropinacolato-3,4-dihexyloxybenzene (0.96 g, 2.37 mmol) were used to give a dark brown oil (1.07 g, 96%).

**2,3-bis[3,4-dihexyloxyphenyl]-6,7-dioctyloxynaphthalene (12h)** Pd(OAc)<sub>2</sub> (0.011 g, 0.049 mmol)



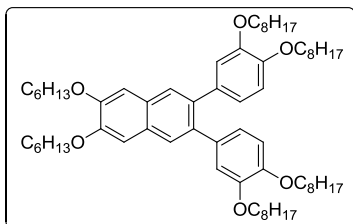
and PPh<sub>3</sub> (0.023 g, 0.098 mmol), aq. 2.0 M K<sub>3</sub>PO<sub>4</sub> (excess), 2,3-dibromo-6,7-bis(octyloxy)naphthalene (0.267 g, 0.490 mmol) and 1-pinacolatoboron-3,4-bis(hexyloxy)benzene (0.419 g, 1.036 mmol) were used to give a light brown solid. (0.20 g, 43.5 % yield).

**2,3-bis[3,4-dihexyloxyphenyl]-6,7-didecyloxynaphthalene (12g):** Pd(OAc)<sub>2</sub> (0.017 g, 0.079 mmol)



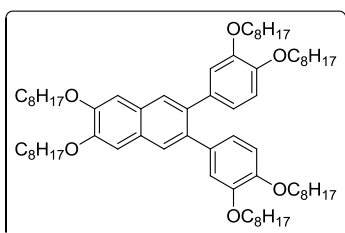
and PPh<sub>3</sub> (0.041 g, 0.158 mmol), aq. 2.0 M K<sub>3</sub>PO<sub>4</sub> (excess), 2,3-dibromo-6,7-bis(decyloxy)naphthalene (0.474 g, 0.79 mmol) and 1-pinacolatoboron-3,4-bis(hexyloxy)benzene (0.675 g, 1.67 mmol) were used to give a light brown solid. (0.75 g, 96 % yield).

**2,3-bis[3,4-dioctyloxyphenyl]-6,7-dihexyloxynaphthalene (12f):** Pd(OAc)<sub>2</sub> (0.005 g, 0.021 mmol)



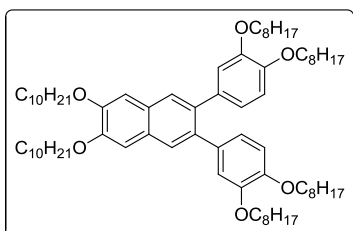
and PPh<sub>3</sub> (0.011 g, 0.041 mmol), aq. 2.0 M K<sub>3</sub>PO<sub>4</sub> (excess), 2,3-dibromo-6,7- bis(hexyloxy)naphthalene (0.201 g, 0.414 mmol) and 1-pinacolatoboron-3,4-bis(octyloxy)benzene (0.400 g, 0.869 mmol) were used to give a light brown solid. (0.22 g, 54 % yield).

**2,3-bis[3,4-dioctyloxyphenyl]-6,7-dioctyloxynaphthalene (12e):** : Pd(OAc)<sub>2</sub> (0.012 g, 0.052



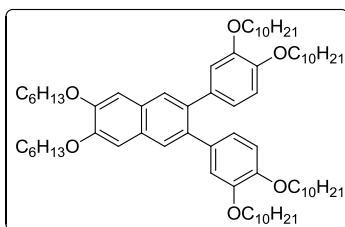
mmol) and PPh<sub>3</sub> (0.027 g, 0.104 mmol), aq. 2.0 M K<sub>3</sub>PO<sub>4</sub> (excess), 2,3-dibromo-6,7- bis(octyloxy)naphthalene (0.56g, 1.039 mmol) and 1-pinacolatoboron-3,4-bis(octyloxy)benzene (1.00 g, 2.172 mmol) were used to give a light brown solid. (0.574 g, 53 %).

**2,3-bis[3,4-dioctyloxyphenyl]-6,7-didecyloxynaphthalene (12d):** Pd(OAc)<sub>2</sub> (0.012 g, 0.052 mmol)



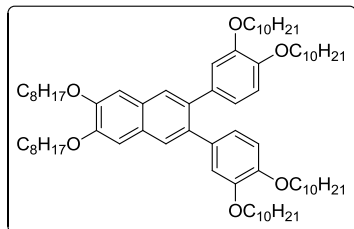
and PPh<sub>3</sub> (0.027 g, 0.104 mmol), aq. 2.0 M K<sub>3</sub>PO<sub>4</sub> (excess) 2,3-dibromo-6,7- bis(decyloxy)naphthalene (0.62 g, 2.172 mmol) and 1-pinacolatoboron-3,4-bis(octyloxy)benzene (1.00 g, 2.172 mmol) were used to give a brown solid (0.648 g, 56 %).

**2,3-bis[3,4-didecyloxyphenyl]-6,7-dihexyloxynaphthalene (12c):** Pd(OAc)<sub>2</sub> (0.043 g, 0.192 mmol)



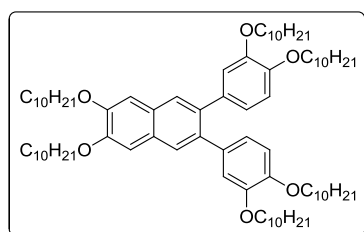
and PPh<sub>3</sub> (0.100 g, 0.383 mmol), aq. 2.0 M K<sub>3</sub>PO<sub>4</sub> (excess) 2,3-dibromo-6,7- bis(hexyloxy)naphthalene (0.90 g, 1.85 mmol) and 1-pinacolatoboron-3,4-bis(decyloxy)benzene (2.05 g, 3.97 mmol) were used to give a brown solid (0.90 g, 44 %).

**2,3-bis[3,4-didecyloxyphenyl]-6,7-dioctyloxynaphthalene (12b):** Pd(OAc)<sub>2</sub> (0.017 g, 0.074 mmol)



and PPh<sub>3</sub> (0.039 g, 0.148 mmol), aq. 2.0 M K<sub>3</sub>PO<sub>4</sub> (excess), 2,3-dibromo-6,7-bis(octyloxy)naphthalene (0.80 g, 1.475 mmol) and 1-pinacolatoboron-3,4-bis(decyloxy)benzene (1.59 g, 3.08 mmol) was added to give a white solid (0.60 g, 35 % yield).

**2,3-bis[3,4-didecyloxyphenyl]-6,7-didecyloxynaphthalene (12a):** Pd(OAc)<sub>2</sub> (0.037 g, 0.167 mmol)



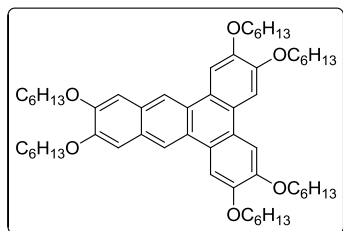
and PPh<sub>3</sub> (0.088 g, 0.334 mmol), aq. 2.0 M K<sub>3</sub>PO<sub>4</sub> (excess), 2,3-dibromo-6,7-bis(decyloxy)naphthalene (2.00g, 3.34 mmol) and 1-pinacolatoboron-3,4-bis(decyloxy)benzene (3.61 g, 6.98 mmol). was added to give a white solid (3.01 g, 74 %). <sup>1</sup>H-NMR

(300 MHz, CDCl<sub>3</sub>): δ 7.68 (s, 2H), 7.14 (s, 2H), 6.79 (s, 4H), 6.66 (s, 2H), 4.12 (t, *J* = 6.6 Hz, 4H), 3.96 (t, *J* = 6.6 Hz, 4H), 3.70 (t, *J* = 6.6 Hz, 4H), 1.93-1.89 (m, 4H), 1.83-1.79 (m, 4H), 1.70-1.65 (m, 4H), 1.46-1.28 (m, 84H), 0.91-0.87 (m, 18H). <sup>13</sup>C NMR (300 MHz, CDCl<sub>3</sub>): δ 150.00, 148.60, 148.01, 137.23, 135.11, 128.69, 127.69, 122.29, 116.52, 113.63, 107.83, 69.55, 69.35, 69.14, 32.20, 32.18, 29.98, 29.92, 29.90, 29.88, 29.85, 29.77, 29.72, 29.71, 29.66, 29.63, 29.62, 29.42, 29.38, 26.35, 26.31, 22.95, 14.35. HRMS (MALDI) calc'd for C<sub>82</sub>H<sub>136</sub>O<sub>6</sub>+H *m/z* 1217.0337, found 1217.0331.

**General Procedure for the synthesis of 2,3,6,7,11,12-hexaalkoxydibenze[*a,c*]anthracenes (1):**

2,3-bis[3,4-dialkoxypheyl]-6,7-dialkoxynaphthalene (1 eq, 0.20 mmol.) was dissolved in 20 mL dry CH<sub>2</sub>Cl<sub>2</sub>. FeCl<sub>3</sub> (6 eq., 1.20 mmol) was added to the solution and stirred for 1 hour. The solution was poured into MeOH (100 mL) and the resulting precipitate was collected by suction filtration. The crude product was purified by a short silica column eluting with CH<sub>2</sub>Cl<sub>2</sub> and the solvent was removed via rotary evaporator, followed by recrystallization in acetone.

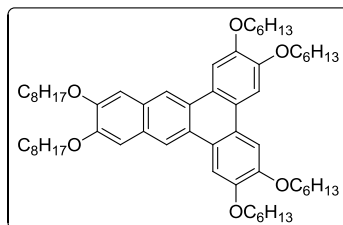
**2,3,6,7,11,12-hexakis(hexyloxy)dibenz[a,c]anthracene (1i):** 2,3-bis[3,4-dihexyloxybenzene]-6,7-



bis(hexyloxy)naphthalene (0.214 g, 0.243 mmol) and FeCl<sub>3</sub> (0.241 g, 1.48 mmol) were used. Yielded a light brown solid (0.136 g, 64 %). M.P. 89.11 °C. <sup>1</sup>H NMR (300 MHz, CDCl<sub>3</sub>): δ 8.70 (s, 2H), 8.11 (s, 2H), 7.81 (s, 2H), 7.33 (s, 2H), 4.31-4.18 (m, 12H), 2.00-1.93 (m,

12H), 1.61-1.55 (m, 12H), 1.47-1.39 (m, 24H), 0.98-0.92 (18H). <sup>13</sup>C NMR (300 MHz, CDCl<sub>3</sub>): δ 150.08, 149.50, 149.28, 128.31, 126.71, 124.28, 124.14, 119.57, 107.93, 107.70, 107.02, 70.02, 69.63, 69.07, 31.93, 31.87, 29.68, 29.65, 29.33, 26.11, 26.08, 22.92, 22.89, 14.32, 14.30. HRMS (MALDI) calc'd for C<sub>58</sub>H<sub>86</sub>O<sub>6</sub>+H *m/z* 878.6424, found 878.6419.

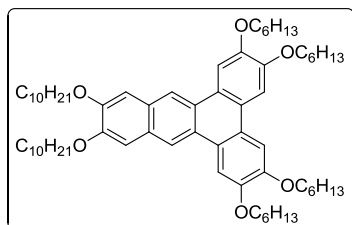
**2,3,6,7-tetrakis(hexyloxy)-11,12-bis(octyloxy)dibenz[a,c]anthracene (1h):** 2,3-bis[3,4-



dihexyloxyphenyl]-6,7-dioctyloxynaphthalene (0.20 g, 0.214 mmol) and FeCl<sub>3</sub> (0.212g, 1.304 mmol) were used to obtain a light brown solid (0.19 g, 95 % yield). M.P. 87.24 °C. <sup>1</sup>H NMR (300 MHz, CDCl<sub>3</sub>): δ 8.71 (s, 2H), 8.12 (s, 2H), 7.81 (s, 2H), 7.33 (s, 2H),

4.32-4.18 (m, 12H), 2.00-1.93 (m, 12H), 1.62-1.55 (m, 12H), 1.43-1.32 (m, 32H), 0.98-0.91 (m, 18H). <sup>13</sup>C NMR (300 MHz, CDCl<sub>3</sub>): δ 149.41, 148.83, 148.60, 127.63, 126.02, 123.60, 123.47, 118.86, 107.26, 107.05, 106.36, 69.34, 68.96, 68.39, 31.39, 31.23, 28.95, 28.84, 28.67, 25.68, 25.38, 25.01, 22.20, 13.65, 13.59. HRMS (MALDI) calc'd for C<sub>62</sub>H<sub>94</sub>O<sub>6</sub>+H *m/z* 934.7050, found 934.7033.

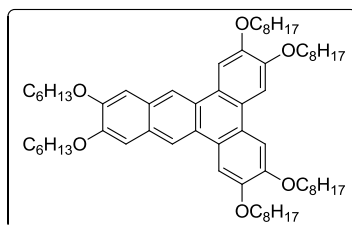
**2,3,6,7-tetrakis(hexyloxy)-11,12-bis(decyloxy)dibenz[a,c]anthracene (1g):** 2,3-bis[3,4-



dihexyloxyphenyl]-6,7-didecyloxynaphthalene (0.75 g, 0.75 mmol) and FeCl<sub>3</sub> (0.737 g, 4.53 mmol) were used to obtain a light brown product (0.70 g, 94 % yield). M.P. 83.18 °C. <sup>1</sup>H NMR (300 MHz, CDCl<sub>3</sub>): δ 8.70 (s, 2H), 8.11 (s, 2H), 7.80 (s, 2H), 7.32 (s, 2H),

4.31-4.17 (m, 12H), 1.97-1.92 (m, 12H), 1.61-1.56 (m, 12H), 1.42-1.38 (m, 40H), 0.97-0.91 (m, 18H). <sup>13</sup>C NMR (300 Mhz, CDCl<sub>3</sub>): δ 150.10, 149.52, 149.29, 128.32, 126.71, 124.29, 124.16, 119.56, 107.97, 107.72, 107.05, 70.03, 69.64, 69.08, 32.16, 31.93, 31.16, 29.90, 29.84, 29.71, 29.67, 29.65, 29.61, 29.38, 26.38, 26.10, 26.08, 25.00, 22.93, 22.91, 22.90, 14.35, 14.31, 14.29. HRMS (MALDI) calc'd for C<sub>66</sub>H<sub>102</sub>O<sub>6</sub>+H *m/z* 990.7676, found 990.7685.

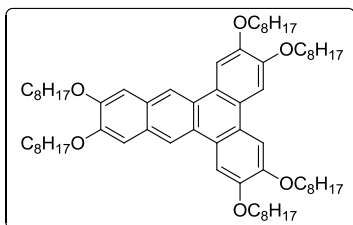
**2,3,6,7-tetrakis(octyloxy)-11,12-bis(hexyloxy)dibenz[a,c]anthracene (1f):** 2,3-bis[3,4-



dioctyloxyphenyl]-6,7-dihexyloxynaphthalene (0.20 g, 0.201 mmol) and FeCl<sub>3</sub> (0.19 g, 1.23 mmol) to give a light brown solid (0.15 g, 75 % yield). M.P. 86.12 °C. <sup>1</sup>H (300 MHz, CDCl<sub>3</sub>): δ 8.68 (s, 2H), 8.10 (s, 2H), 7.80 (s, 2H), 7.32 (s, 2H), 4.31-4.18 (m, 12H),

2.00-1.93 (m, 12H), 1.61-1.57 (m, 12H), 1.43-1.33 (m, 40H), 0.97-0.89 (m, 18H). <sup>13</sup>C NMR (300 MHz, CDCl<sub>3</sub>): δ 150.11, 149.55, 149.31, 128.33, 126.72, 124.32, 124.19, 119.55, 108.02, 107.83, 107.08, 70.06, 69.69, 69.08, 32.11, 31.88, 29.74, 29.58, 29.36, 26.45, 26.44, 26.06, 22.94, 22.88, 14.35, 14.27. HRMS (MALDI) calc'd for C<sub>66</sub>H<sub>102</sub>O<sub>6</sub>+H *m/z* 990.7685, found 990.7676.

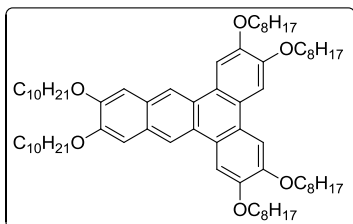
**2,3,6,7,11,12-hexakis(octyloxy)dibenz[a,c]anthracene (1e):** 2,3-bis[3,4-dioctyloxyphenyl]-6,7-



dioctyloxynaphthalene (0.574 g, 0.547 mmol) and FeCl<sub>3</sub> (0.541 g, 3.340 mmol) were used to give a light brown solid (0.521 g, 90.9 % yield). M.P. 74 °C. <sup>1</sup>H (300 MHz, CDCl<sub>3</sub>): δ 8.69 (s, 2H), 8.11 (s, 2H), 7.80 (s, 2H), 7.32 (s, 2H), 4.30-4.18 (m, 12H), 1.97-1.92 (m,

12H), 1.60-1.57 (m, 12H), 1.42-1.32 (m, 48H), 0.92-0.88 (m, 18H). <sup>13</sup>C NMR (300 MHz, CDCl<sub>3</sub>): δ 150.10, 149.52, 149.30, 128.32, 126.71, 142.30, 124.17, 119.56, 107.98, 107.77, 107.05, 70.05, 69.67, 69.09, 32.16, 32.10, 29.90, 29.84, 29.73, 29.71, 29.61, 29.58, 29.34, 26.44, 26.39, 25.01, 25.00, 22.93, 14.35. HRMS (MALDI) calc'd for C<sub>70</sub>H<sub>110</sub>O<sub>6</sub>+H *m/z* 1046.8302, found 1046.8297.

**2,3,6,7-tetrakis(octyloxy)-11,12-bis(decyloxy)dibenz[a,c]anthracene (1d):** 2,3-bis[3,4-

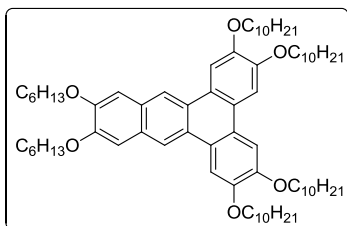


dioctyloxyphenyl]-6,7-didecyloxynaphthalene (0.648 g, 0.586 mmol) and FeCl<sub>3</sub> (0.580 g, 3.57 mmol) were used to get a pale brown solid (0.208 g, 32 % yield). M.P. 73.51 °C. <sup>1</sup>H NMR (300 MHz, CDCl<sub>3</sub>): δ 8.69 (s, 2H), 8.11 (s, 2H), 7.80 (s, 2H), 7.32 (s, 2H),

4.30-4.17 (m, 12H), 1.99-1.92 (m, 12H), 1.54-1.58 (m, 12H), 1.42-1.29 (m, 56H), 0.92-0.87 (m, 18H). <sup>13</sup>C NMR (300 MHz, CDCl<sub>3</sub>): δ 150.10, 149.53, 149.30, 128.33, 126.72, 124.30, 124.17, 119.57, 107.98, 107.77, 107.06, 70.05, 69.68, 69.09, 32.17, 32.11, 29.91, 29.85, 29.73, 29.72, 29.61, 29.58, 29.39, 26.44, 26.39, 25.00, 22.94, 14.36. HRMS (MALDI) calc'd for C<sub>74</sub>H<sub>118</sub>Br<sub>2</sub>O<sub>6</sub>+H *m/z* 1102.8928, found 1102.8924.



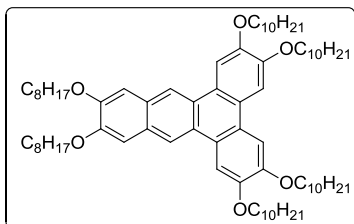
**2,3,6,7-tetrakis(decyloxy)-11,12-bis(hexyloxy)dibenz[a,c]anthracene (1c):** 2,3-bis[3,4-



didecyloxyphenyl]-6,7-dihexyloxynaphthalene (0.90 g, 0.91 mmol) and FeCl<sub>3</sub> (0.88 g, 5.44 mmol) were used to obtain a light brown solid (0.85 g, 85 % yield). M.P. 63.22 °C. <sup>1</sup>H NMR (300 MHz, CDCl<sub>3</sub>): δ 8.69 (s, 2H), 8.10 (s, 2H), 7.80 (s, 2H), 7.32 (s, 2H), 4.30-

4.18 (m, 12H), 1.99-1.92 (m, 12H), 1.63-1.55 (m, 12H), 1.45-1.29 (m, 56H), 0.97-0.87 (m, 18H). <sup>13</sup>C NMR (300 MHz, CDCl<sub>3</sub>): δ 150.12, 149.55, 149.32, 128.33, 126.72, 124.32, 124.19, 119.56, 108.04, 107.84, 107.09, 70.07, 69.69, 69.08, 32.16, 31.87, 29.93, 29.86, 29.78, 29.76, 29.61, 29.35, 26.44, 26.05, 22.93, 22.87, 14.33, 14.27. HRMS (MALDI) calc'd for C<sub>74</sub>H<sub>118</sub>O<sub>6</sub>+H *m/z* 1102.8928, found 1102.8923.

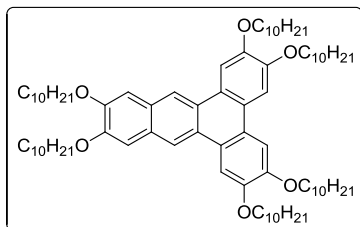
**2,3,6,7-tetrakis(decyloxy)-11,12-bis(octyloxy)dibenz[a,c]anthracene (1b):** 2,3-bis[3,4-



didecyloxyphenyl]-6,7-dioctyloxynaphthalene (0.06 g, 0.052 mmol) and FeCl<sub>3</sub> (0.051 g, 0.315 mmol) were used to give a light brown solid (0.033 g, 55 % yield). M.P. 64.16 °C. <sup>1</sup>H NMR (300 MHz, CDCl<sub>3</sub>): δ 8.70 (s, 2H), 8.11 (s, 2H), 7.80 (s, 2H), 7.32 (s, 2H),

4.28-4.20 (m, 12H), 1.97-1.94 (m, 12H), 1.59-1.55 (m, 12H), 1.36-1.25 (m, 64H), 0.90-0.86 (m, 18H). <sup>13</sup>C NMR (300 MHz, CDCl<sub>3</sub>): δ 150.11, 149.54, 149.30, 128.33, 126.72, 124.31, 124.18, 119.57, 107.99, 107.77, 107.10, 70.04, 69.68, 69.08, 32.13, 32.02, 29.91, 29.4, 29.73, 29.71, 29.61, 29.51, 29.40, 26.44, 26.40, 24.98, 22.93, 14.30. HRMS (MALDI) calc'd for C<sub>78</sub>H<sub>126</sub>O<sub>6</sub>+H *m/z* 1158.9554, found 1158.9549.

**2,3,6,7,11,12-hexakis(decyloxy)dibenz[a,c]anthracene (1a):** 2,3-bis[3,4-didecyloxyphenyl]-6,7-

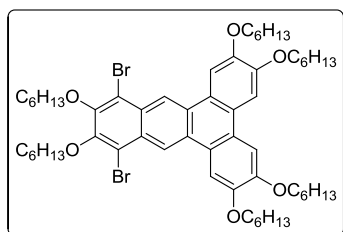


didecyloxynaphthalene (1.214g, 1.00 mmol) was dissolved in 20 mL dry  $\text{CH}_2\text{Cl}_2$ .  $\text{FeCl}_3$  (0.97 g, 6.00 mmol) was added to the solution and stirred for 1 hour. Yielded a light yellow solid (1.11 g, 91 %). M.P. 59.50 °C.  $^1\text{H}$  NMR (300 MHz,  $\text{CDCl}_3$ ):  $\delta$  8.69 (s,

2H), 8.10 (s, 2H), 7.80 (s, 2H), 7.32 (s, 2H), 4.28-4.20 (m, 12H), 1.97-1.95 (m, 12H), 1.59-1.55 (m, 12H), 1.43-1.28 (m, 72H), 0.91-0.87 (m, 18H).  $^{13}\text{C}$  NMR (300 MHz,  $\text{CDCl}_3$ ):  $\delta$  150.08, 149.50, 149.28, 128.31, 126.71, 124.29, 124.16, 119.55, 107.96, 107.74, 107.04, 70.03, 69.65, 69.07, 32.17, 29.94, 29.91, 29.87, 29.85, 29.79, 29.77, 29.72, 29.63, 29.39, 26.45, 26.39, 22.94, 14.35. HRMS (MALDI) calc'd for  $\text{C}_{82}\text{H}_{134}\text{O}_6 + \text{H}$   $m/z$  1215.0180, found 1215.0175.

**General Procedure for dibromination of dibenzanthracene (14):** The precursor, compounds **1a-i**, (1 eq.) was dissolved in 50 mL chloroform.  $\text{Br}_2$  (2.3 equivalents) was added dropwise to the solution and the mixture was left to stir for 1 hour. The reaction was washed with sodium thiosulfate, water then brine. The organic layer was dried with  $\text{MgSO}_4$ , filtered then dried. The crude product was purified using column chromatography, Hexanes/dichloromethane (50:50). The product was then recrystallized in acetone to yield a light brown solid.

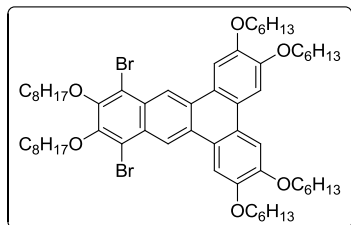
**10,13-dibromo-2,3,6,7,11,12-hexakis(hexyloxy)dibenz[a,c]anthracene (14i):** 2,3,6,7,11,12-



hexakis(hexyloxy)dibenz[a,c]anthracene (0.067 g, 0.076 mmol) and  $\text{Br}_2$  (0.028 g, 0.175 mmol) were used to yield a white solid (92 %)  $^1\text{H}$  (300 MHz,  $\text{CDCl}_3$ ):  $\delta$  9.19 (s, 2H), 8.13 (s, 2H), 7.77 (s, 2H), 4.33-4.17 (m, 12H), 2.01-1.91 (m, 12H), 1.65-1.55 (m, 12H), 1.43-1.39 (m, 24H), 0.97-0.95 (m, 18H).  $^{13}\text{C}$  NMR (300 MHz,  $\text{CDCl}_3$ ):  $\delta$  150.42, 149.99, 149.39, 128.99,

129.09, 124.93, 123.34, 121.22, 116.17, 108.34, 107.59, 74.80, 69.90, 69.74, 31.96, 31.93, 30.55, 29.64, 29.61, 26.12, 26.08, 26.04, 22.93, 22.91, 22.90, 14.31, 14.28. HRMS (MALDI) calc'd for  $C_{58}H_{84}Br_2O_6+H$   $m/z$  1034.4635, found 1034.4647.

**10,13-dibromo-2,3,6,7-tetrakis(hexyloxy)-11,12-bis(octyloxy)dibenz[a,c]anthracene (14h):**

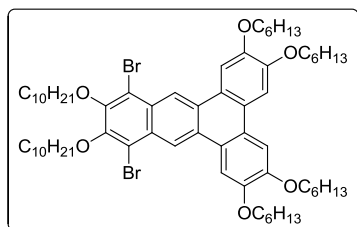


2,3,6,7-tetrakis(hexyloxy)-11,12-

bis(octyloxy)dibenz[a,c]anthracene (0.100 g, 0.106 mmol) and  $Br_2$  (0.0374 g, 0.234 mmol) were used to obtain a light brown solid (0.082 g, 70 % yield).  $^1H$  (300 MHz,  $CDCl_3$ ):  $\delta$  9.22 (s, 2H), 8.15 (s,

2H), 7.78 (s, 2H), 4.33-4.17 (m, 12H), 2.01-1.91 (m, 12H), 1.62-1.55 (m, 12H), 1.44-1.33 (m, 32H), 0.97-0.91 (m, 18H).  $^{13}C$  NMR (300 MHz,  $CDCl_3$ ): 150.44, 150.00, 149.41, 129.01, 128.12, 124.95, 123.36, 121.26, 116.19, 108.41, 107.61, 74.81, 69.91, 69.77, 32.11, 31.95, 31.92, 30.59, 29.74, 29.62, 29.59, 29.57, 26.39, 26.11, 26.08, 22.92, 22.90, 14.35, 14.31, 14.28. HRMS (MALDI) calc'd for  $C_{62}H_{92}Br_2O_6+H$   $m/z$  1090.5261, found 1090.5220.

**10,13-dibromo-2,3,6,7-tetrakis(hexyloxy)-11,12-bis(decyloxy)dibenz[a,c]anthracene (14g):**



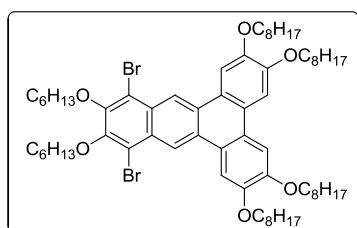
2,3,6,7-tetrakis(hexyloxy)-11,12-

bis(decyloxy)dibenz[a,c]anthracene (0.07 g, 0.0705 mmol) and  $Br_2$  (0.0248 g, 0.150 mmol) were used to obtain a light brown solid (0.071 g, 88 % yield).  $^1H$  NMR (300 MHz,  $CDCl_3$ ):  $\delta$  9.24 (s,

2H), 8.18 (s, 2H), 7.80 (s, 2H), 4.34-4.17 (m, 12H), 2.01-1.91 (m, 12H), 1.65-1.57 (m, 12H), 1.47-1.25 (m, 40H), 0.97-0.87 (m, 18H).  $^{13}C$  (300 MHz,  $CDCl_3$ ):  $\delta$  150.49, 150.03, 149.46, 129.04, 128.15, 124.99, 123.40, 121.28, 116.19, 108.48, 107.65, 74.82, 69.93, 69.81, 32.15, 31.95, 31.91, 30.58,

29.90, 29.85, 29.77, 29.59, 26.38, 26.10, 26.07, 22.96, 22.91, 22.89, 14.34, 14.30, 14.27. HRMS (MALDI) calc'd for  $C_{66}H_{100}Br_2O_6+H$   $m/z$  1146.5887, found 1146.5841.

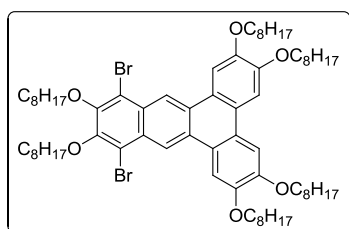
**10,13-dibromo-2,3,6,7-tetrakis(octyloxy)-11,12-bis(hexyloxy)dibenz[a,c]anthracene (14f):**



2,3,6,7-tetrakis(octyloxy)-11,12-bis(hexyloxy)dibenz[a,c]anthracene (0.05 g, 0.05 mmol) and  $Br_2$  (0.018 g, 0.11 mmol) were used to obtain a light brown solid (0.03 g, 52 %).  $^1H$  NMR (300 MHz,  $CDCl_3$ ):  $\delta$  9.21 (s, 2H), 8.15 (s,

2H), 7.77 (s, 2H), 4.30 (t,  $J$  = 7.5 Hz, 4H), 4.25 (t,  $J$  = 6.6 Hz, 4H), 4.19 (t,  $J$  = 6.6 Hz, 4H), 2.01-1.91 (m, 12H), 1.61-1.55 (m, 12H), 1.41-1.29 (m, 42H), 0.97-0.86 (m, 18H).  $^{13}C$  (300 MHz,  $CDCl_3$ ):  $\delta$  150.42, 149.98, 149.39, 128.99, 128.09, 124.94, 123.35, 121.25, 116.18, 108.40, 107.62, 74.81, 69.90, 69.76, 32.16, 31.95, 31.81, 30.54, 29.93, 29.86, 29.79, 29.68, 29.62, 26.45, 26.43, 26.03, 25.50, 22.93, 22.90, 14.34, 14.31.

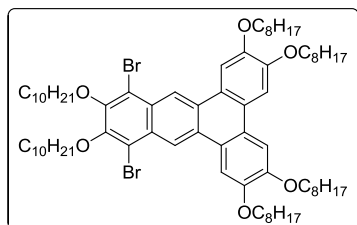
**10,13-dibromo-2,3,6,7,11,12-hexakis(octyloxy)dibenz[a,c]anthracene (14e):**



2,3,6,7,11,12-hexakis(octyloxy)dibenz[a,c]anthracene (0.100 g, 0.095 mmol) and  $Br_2$  (0.035, 0.219 mmol) were used to obtain a white solid (0.11 g, 96 % yield).  $^1H$  NMR (300 MHz,  $CDCl_3$ ):  $\delta$  9.12 (s, 2H), 8.07 (s, 2H), 7.72 (s, 2H), 4.31-4.18 (m, 12H), 2.01-1.92 (m, 12H), 1.65-

1.57 (m, 12H), 1.43-1.33 (m, 48H), 0.94-0.89 (m, 18H).  $^{13}C$  (300 MHz,  $CDCl_3$ ):  $\delta$  149.51, 149.14, 148.49, 128.09, 127.20, 124.05, 122.45, 120.36, 115.38, 107.37, 106.64, 74.011, 69.04, 68.86, 31.35, 29.86, 29.01, 28.94, 28.90, 28.85, 25.70, 25.68, 25.66, 22.17, 13.58. HRMS (MALDI) calc'd for  $C_{70}H_{108}Br_2O_6+H$   $m/z$  1202.6513, found 1202.6544.

**10,13-dibromo-2,3,6,7-tetrakis(octyloxy)-11,12-bis(decyloxy)dibenz[a,c]anthracene (14d):**

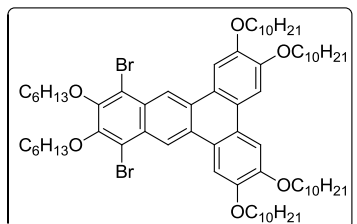


2,3,6,7-tetrakis(octyloxy)-11,12-

bis(decyloxy)dibenz[a,c]anthracene (0.100 g, 0.091 mmol) and  $\text{Br}_2$  (0.033 g, 0.208 mmol) were used to obtain a white solid (0.097 g, 85 %).  $^1\text{H}$  NMR (300 MHz,  $\text{CDCl}_3$ ):  $\delta$  9.16 (s, 2H), 8.10 (s,

2H), 7.75 (s, 2H), 4.32-4.17 (m, 12H), 2.01-1.92 (m, 12H), 1.62-1.57 (m, 12H), 1.43-1.30 (m, 56H), 0.93-0.88 (m, 18H).  $^{13}\text{C}$  NMR (300 MHz,  $\text{CDCl}_3$ ):  $\delta$  150.31, 149.93, 149.26, 128.90, 128.00, 124.84, 123.25, 121.15, 116.17, 108.17, 107.44, 74.79, 69.84, 69.66, 32.18, 32.13, 32.12, 30.63, 29.95, 29.90, 29.82, 29.79, 29.77, 29.71, 29.67, 29.63, 29.14, 26.48, 26.46, 26.43, 22.96, 14.36. HRMS (MALDI) calc'd for  $\text{C}_{74}\text{H}_{116}\text{Br}_2\text{O}_6 + \text{H}$   $m/z$  1258.7139, found 1258.7079.

**10,13-dibromo-2,3,6,7-tetrakis(decyloxy)-11,12-bis(hexyloxy)dibenz[a,c]anthracene (14c):**

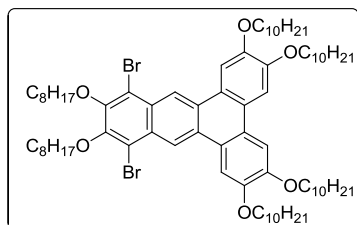


2,3,6,7-tetrakis(decyloxy)-11,12-

bis(hexyloxy)dibenz[a,c]anthracene (0.100 g, 0.091 mmol) and  $\text{Br}_2$  (0.033 g, 0.209 mmol) were used to obtain a light brown solid (0.101 g, 88 % yield).  $^1\text{H}$  NMR (300 MHz,  $\text{CDCl}_3$ ): 9.24 (s, 2H), 8.17

(s, 2H), 7.79 (s, 2H), 4.33-4.17 (m, 12H), 2.01-1.92 (m, 12H), 1.64-1.59 (m, 12H), 1.44-1.29 (m, 56H), 0.93-0.87 (m, 18H).  $^{13}\text{C}$  NMR (300 MHz,  $\text{CDCl}_3$ ): 150.46, 150.01, 149.43, 129.03, 128.13, 124.98, 123.38, 121.28, 116.19, 108.48, 107.68, 74.83, 69.94, 69.80, 32.17, 31.95, 30.55, 29.96, 29.94, 29.87, 29.79, 29.69, 29.62, 26.46, 26.43, 26.04, 22.94, 22.91, 14.35, 14.32. HRMS (MALDI) calc'd for  $\text{C}_{74}\text{H}_{116}\text{Br}_2\text{O}_6 + \text{H}$   $m/z$  1258.7134, found 1258.7156.

**10,13-dibromo-2,3,6,7-tetrakis(decyloxy)-11,12-bis(octyloxy)dibenz[a,c]anthracene (14b):**

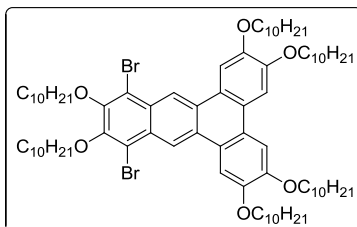


2,3,6,7-tetrakis(decyloxy)-11,12-

bis(octyloxy)dibenz[a,c]anthracene (0.010 g, 0.0086 mmol) and  $\text{Br}_2$  (0.0032 g, 0.0198 mmol) were used to obtain a white solid (0.0107 g, 94 % yield).  $^1\text{H}$  (300 MHz,  $\text{CDCl}_3$ ):  $\delta$  9.24 (s, 2H), 8.18 (s,

2H), 7.79 (s, 2H), 4.33-4.17 (m, 12H), 2.01-1.91 (m, 12H), 1.60-1.55 (m, 12H), 1.43-1.25 (m, 64H), 0.91-0.86 (m, 18H).  $^{13}\text{C}$  NMR (300 MHz,  $\text{CDCl}_3$ ):  $\delta$  150.48, 150.03, 149.44, 129.03, 128.15, 124.99, 123.38, 121.29, 116.19, 108.51, 107.68, 74.83, 69.93, 69.81, 32.16, 32.10, 30.57, 29.93, 29.86, 29.77, 29.72, 29.61, 29.55, 26.43, 26.38, 25.70, 22.92, 14.34. HRMS (MALDI) calc'd for  $\text{C}_{78}\text{H}_{124}\text{Br}_2\text{O}_6+\text{H}$   $m/z$  1314.7765, found 1314.7744.

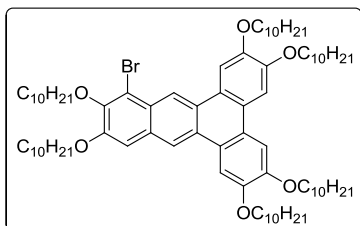
**10,13-dibromo-2,3,6,7,11,12-hexakis(decyloxy)dibenz[a,c]anthracene (14a):** 2,3,6,7,11,12-



hexakis(decyloxy)dibenz[a,c]anthracene (0.300 g, 0.247 mmol) and  $\text{Br}_2$  (0.029 mL, 0.567 mmol) give a light brown solid. (0.319 g, 94 %),  $^1\text{H}$  NMR (300 MHz,  $\text{CDCl}_3$ ):  $\delta$  9.25 (s, 2H), 8.18 (s, 2H), 7.79 (s, 2H), 4.32 (t,  $J$  = 6.60 4H), 4.43 (t,  $J$  = 6.30), 4.18 (t,  $J$  =

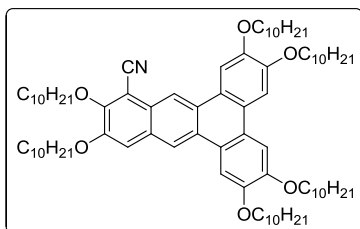
6.30, 4H), 2.00-1.91 (m, 12H), 1.60-1.54 (m, 12H), 1.38-1.26 (m, 72H), 0.90-0.86 (m, 18H).  $^{13}\text{C}$  NMR (300 MHz,  $\text{CDCl}_3$ ):  $\delta$  150.47, 150.02, 149.43, 129.04, 128.14, 124.98, 123.39, 121.29, 116.20, 108.34, 107.67, 74.83, 69.94, 69.80, 32.17, 30.59, 29.95, 29.93, 29.91, 29.87, 29.78, 29.62, 29.60, 26.43, 26.39, 25.00, 22.94, 14.34. HRMS (MALDI) calc'd for  $\text{C}_{82}\text{H}_{132}\text{Br}_2\text{O}_6+\text{H}$   $m/z$  1370.8391, found 1370.8385.

**Synthesis of 10-bromo-2,3,6,7,11,12-hexakis(decyloxy)dibenz[a,c]anthracene (13):**



2,3,6,7,11,12-hexakis(decyloxy)dibenz[a,c]anthracene, (0.250 g, 0.206 mmol) was dissolved in 50 mL  $\text{CHCl}_3$ . Bromine (0.035 g, 0.216 mmol) was added dropwise to the solution and left to stir for 1 hour. The organic layer was washed with sodium thiosulfate, water then brine. The organic layer was dried with  $\text{MgSO}_4$ , filtered and the solvent was removed under reduced pressure. A column was performed on the crude product, Hexanes/DCM (50:50), followed by recrystallization in acetone to yield a pale yellow/brown solid (0.243 g, 91 %).  $^1\text{H-NMR}$  (300 MHz,  $\text{CDCl}_3$ , 30 mM):  $\delta$  9.15 (s, 1H), 8.65 (s, 1H), 8.17 (s, 1H), 8.07 (s, 1H), 7.78 (s, 2H), 7.30 (s, 1H), 4.31-4.22 (m, 8H), 4.18-4.16 (m, 4H), 1.98-1.91 (m, 12H), 1.60-1.56 (m, 12H), 1.42-1.29 (m, 84H), 0.91-0.87 (m, 18H).  $^{13}\text{C-NMR}$  (300 MHz,  $\text{CDCl}_3$ ):  $\delta$  152.29, 149.98, 149.87, 149.36, 149.26, 147.17, 129.89, 128.14, 127.36, 126.51, 124.73, 124.30, 124.16, 123.48, 120.69, 119.96, 116.28, 108.15, 107.96, 107.81, 107.70, 106.84, 73.94, 69.99, 69.92, 69.69, 68.93, 32.18, 30.63, 29.96, 29.92, 29.89, 29.81, 29.74, 29.64, 29.53, 26.53, 26.46, 22.95, 14.36. HRMS (MALDI) calc'd for  $\text{C}_{82}\text{H}_{133}\text{BrO}_6 + \text{H}$   $m/z$  1292.9286, found 1292.9280.

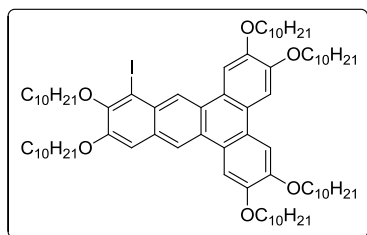
**Synthesis of 10-cyano-2,3,6,7,11,12-hexakis(decyloxy)dibenz[a,c]anthracene (19):** 10-bromo-



2,3,6,7,11,12-hexakis(decyloxy)dibenz[a,c]anthracene (0.10 g, 0.077 mmol) was dissolved in dry DMF (5 mL).  $\text{CuCN}$  (9.0 mg, 0.10 mmol) was added to the solution. The flask was fitted with a condenser and heated to reflux for 18 hours while kept under a  $\text{N}_2$  atmosphere. The solution was cooled to room temperature, followed by the addition of 20 mL of water. Ethylenediamine (1 mL) was added to the solution and shaken. The mixture was extracted with DCM (3 x 25 mL), washed with water followed by 1 M HCl. The organic layer was

dried with  $\text{MgSO}_4$ , filtered and the solvent was removed under reduced pressure. A brown solid crude product was obtained. Column chromatography was performed hexanes/dichloromethane (50:50), followed by recrystallization in acetone to yield a bright yellow solid (0.042 g, 48 % yield with spillage).  $^1\text{H-NMR}$  (300 MHz,  $\text{CDCl}_3$ ) :  $\delta$  8.73 (s, 1H), 8.37 (s, 1H), 7.94 (s, 1H), 7.80 (s, 1H), 7.63 (s, 1H), 7.62 (s, 1H), 7.28 (s, 1H), 4.34 (t,  $J$  = 6.6 Hz, 2H), 4.30-4.22 (m, 8H), 4.17 (t,  $J$  = 6.3 Hz, 2H), 1.96-1.91 (m, 12H), 1.56-1.52 (m, 12H), 1.43-1.26 (m, 72H), 0.93-0.89 (m, 18H).  $^{13}\text{C-NMR}$  (300 MHz,  $\text{CDCl}_3$ ):  $\delta$  154.90, 150.62, 150.08, 150.00, 149.44, 149.14, 128.38, 128.35, 128.13, 125.76, 124.57, 124.37, 123.40, 123.04, 120.10, 117.59, 116.11, 112.17, 107.66, 107.52, 107.45, 107.28, 101.80, 75.36, 69.89, 69.72, 69.58, 69.10, 32.21, 32.20, 30.61, 30.01, 29.99, 29.93, 29.89, 29.80, 29.76, 29.68, 29.65, 29.48, 26.52, 26.19, 22.97, 14.37. HRMS (MALDI) calc'd for  $\text{C}_{83}\text{H}_{133}\text{NO}_6 + \text{H}$   $m/z$  1240.0133, found 1240.0127.

**Synthesis of 10-iodo-2,3,6,7,11,12-hexakis(decyloxy)dibenz[a,c]anthracene (17):** 10-bromo-



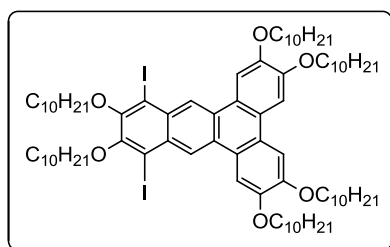
2,3,6,7,11,12-hexakis(decyloxy)dibenz[a,c]anthracene (0.247 g, 0.191 mmol) was added to 25 mL dry THF. The solution was placed in a solution of  $\text{CH}_3\text{CN}/\text{CO}_{2(s)}$  and cooled to  $-42^\circ\text{C}$ . To the cooled solution was added  $n\text{-BuLi}$  (0.11 mL, 2.10 M, 1.2 eq.)

where it was stirred to 30 minutes while maintaining  $-42^\circ\text{C}$ . Iodine (0.097 g, 0.382 mmol) was added to solution, then it was allowed to warm to room temperature. The reaction mixture was then treated with saturated sodium thiosulfate (50 mL). The organic layer was removed and further washed with brine (1x50 mL) and  $\text{H}_2\text{O}$  (1x50 mL). It was dried with  $\text{MgSO}_4$  and solvent was removed under reduced pressure. Column chromatography was performed with Hexanes/DCM (70:30). The product was recrystallized in acetone to yield a white solid (0.130 g, 51 %).  $^1\text{H-NMR}$  (300 MHz,  $\text{CDCl}_3$ ) :  $\delta$  9.12 (s, 1H), 8.65 (s, 1H) 8.21 (s, 1H), 8.10 (s, 1H), 7.80 (s, 2H),



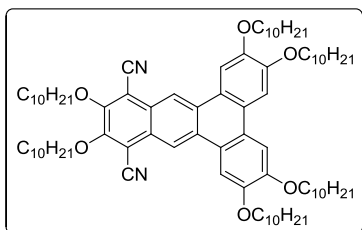
7.34 (s, 1H), 4.32-4.15 (m, 12H), 1.95-1.93 (m, 12H), 1.60-1.54 (m, 12H), 1.42-1.29 (m, 72H), 0.91-0.86 (m, 18H). (Aromatic signals absent due to overlapping peaks.)  $^{13}\text{C}$ -NMR (300 MHz,  $\text{CDCl}_3$ ):  $\delta$  151.50, 150.28, 149.99, 149.85, 149.38, 149.29, 129.98, 128.71, 128.08, 127.73, 125.97, 124.74, 124.25, 124.09, 123.44, 120.02, 108.08, 108.03, 107.91, 107.77, 96.18, 73.75, 70.05, 69.94, 69.72, 69.63, 68.89, 53.63, 32.16, 30.65, 29.94, 29.91, 29.86, 29.78, 29.73, 29.62, 29.54, 26.53, 26.48, 26.44, 25.01, 22.93, 14.34. HRMS (MALDI) calc'd for  $\text{C}_{82}\text{H}_{133}\text{IO}_6 + \text{H}$   $m/z$  1340.9147, found 1340.9210.

**Synthesis of 10,13-diiodo-2,3,6,7,11,12-hexakis(decyloxy)dibenz[a,c]anthracene (18):**



2,3,6,7,11,12-hexakis(decyloxy)dibenz[a,c]anthracene (0.200 g, 0.164 mmol) was dissolved in 20 mL AcOH, 0.75 mL conc.  $\text{H}_2\text{SO}_4$  and 2.0 mL  $\text{H}_2\text{O}$ .  $\text{I}_2$  (0.083 g, 0.329 mmol) and  $\text{H}_5\text{IO}_6$  (0.041 g, 0.180 mmol) was added to the solution. The solution was heated solution to  $80^\circ\text{C}$  and left to stir for 24 hours. The solution was cooled to room temperature then poured over ice water, extracted with DCM (2 x 50 mL). The organic layer was then washed with saturated sodium thiosulfate (1 x 50 mL) and then aqueous  $\text{NaHCO}_3$  (3 x 100 mL). It was dried with  $\text{Mg}_2\text{SO}_4$ , filtered and solvent was removed under reduced pressure to give a deep red solid as crude product. Column chromatography was performed in hexanes/DCM (60:40  $\rightarrow$  40:60) to yield a light brown solid (0.050 g, 23 %)  $^1\text{H}$ -NMR (300 MHz,  $\text{CDCl}_3$ ):  $\delta$  9.08 (s, 2H), 7.78 (s, 2H), 7.60 (s, 2H), 4.28-4.20 (m, 12H), 1.96-1.91 (m, 12H), 1.54-1.51 (m, 12H), 1.43-1.25 (m, 72H), 0.91-0.88 (m, 18H).  $^{13}\text{C}$ -NMR (300 MHz,  $\text{CDCl}_3$ ):  $\delta$  187.28, 153.46, 151.26, 150.51, 129.56, 129.11, 128.82, 123.09, 110.81, 108.97, 104.51, 69.59, 69.39, 69.03, 32.17, 29.92, 29.85, 29.82, 29.74, 29.62, 29.59, 29.46, 29.26, 26.44, 26.40, 26.21, 22.93, 14.35.

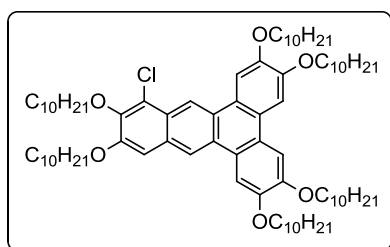
**Synthesis of 10,13-dicyano-2,3,6,7,11,12-hexakis(decyloxy)dibenz[a,c]anthracene (20):** 10,13-



dibromo-2,3,6,7,11,12-hexakis(decyloxy)dibenz[a,c]anthracene (0.42 g, 0.306 mmol) was dissolved in 10 mL dry DMF. CuCN (69 mg, 0.76 mmol) was added to the solution. The reaction mixture was heated to reflux and stirred for 24 hours under a N<sub>2</sub>

atmosphere. The solution was then cooled to room temperature; 10 mL of ethylenediamine was added, followed by 20 mL H<sub>2</sub>O. It was then extracted with DCM (3x20 mL). The organic layer was washed with 1 M HCl (3x50 mL), H<sub>2</sub>O (50 mL) and brine (50 mL). Organic layer was dried with MgSO<sub>4</sub>, filtered and concentrated under reduced pressure. Column chromatography was performed with hexanes/dichloromethane (60:40), followed by recrystallization in acetone to yield a bright orange solid (0.04 g, 10 %). <sup>1</sup>H-NMR (300 MHz, CDCl<sub>3</sub>): δ 8.63 (s, 2H), 7.71 (s, 2H), 7.58 (s, 2H), 4.44 (t, *J* = 6.9 Hz, 4H), 4.21 (m, 8H), 1.96 (m, 12H), 1.61 (m, 12H), 1.29 (m, 72H), 0.89 (m, 18H). <sup>13</sup>C-NMR (300 MHz, CDCl<sub>3</sub>): δ 155.71, 150.55, 149.14, 129.72, 126.17, 124.72, 122.01, 118.29, 114.95, 107.02, 106.72, 106.50, 76.31, 69.50, 69.30, 32.19, 30.57, 30.04, 30.00, 29.97, 29.96, 29.94, 29.78, 29.75, 29.72, 29.66, 29.64, 26.50, 26.18, 22.94, 14.35. HRMS (MALDI) calc'd for C<sub>83</sub>H<sub>133</sub>NO<sub>6</sub>+H *m/z* 1265.0085, found 1265.0080.

**Synthesis of 10-chloro-2,3,6,7,11,12-hexakis(decyloxy)dibenz[a,c]anthracene (15):** A 30 mL

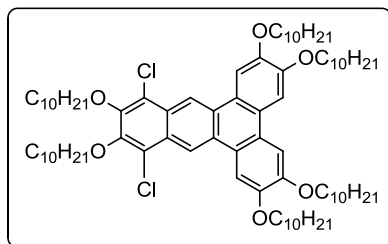


pressure tube with Teflon cap was charged with 2,3,6,7,11,12-hexakis(decyloxy)dibenz[a,c]anthracene (0.415 g, 0.341 mmol), N-chlorosuccinimide (0.055 g, 0.410 mmol), and a stir bar. 20 mL of dichloromethane was added and the tube was

sealed and heated to 100 °C for 36 hours. The mixture was removed from heat, cooled to room

temperature, where the solvent was removed under reduced pressure. Column chromatography was performed in hexanes/dichloromethane (60:40), followed by recrystallization in acetone to yield pale yellow solid (0.175 g, 41 %)  $^1\text{H-NMR}$  (300 MHz,  $\text{CDCl}_3$ ):  $\delta$  8.98 (s, 1H), 8.60 (s, 1H), 7.98 (s, 1H), 7.81 (s, 1H), 7.74 (s, 1H), 7.73 (s, 1H), 7.29 (s, 1H), 4.26-4.18 (m, 12H), 1.96-1.91 (m, 12H), 1.58-1.54 (m, 12H), 1.30-1.24 (m, 72H), 0.89-0.86 (m, 18H).  $^{13}\text{C-NMR}$  (300 MHz,  $\text{CDCl}_3$ ):  $\delta$  150.96, 150.19, 149.88, 149.39, 149.16, 146.99, 128.46, 128.28, 127.19, 126.11, 125.90, 124.95, 124.56, 123.81, 123.07, 118.51, 114.44, 108.10, 107.67, 107.52, 107.26, 104.91, 69.91, 69.79, 69.49, 69.16, 68.20, 32.16, 29.93, 29.89, 29.86, 29.84, 29.77, 29.73, 29.69, 29.61, 29.55, 29.31, 26.42, 26.35, 25.83, 25.00, 22.93, 14.34. HRMS (MALDI) calc'd for  $\text{C}_{82}\text{H}_{133}\text{ClO}_6 + \text{H}$   $m/z$  1248.9791, found 1248.9785.

**Synthesis of 10,13-dichloro-2,3,6,7,11,12-hexakis(decyloxy)dibenz[a,c]anthracene (16):** A 30 mL

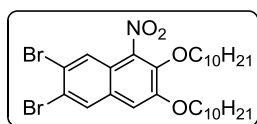


pressure tube with A 30 mL pressure tube with Teflon cap was charged with 2,3,6,7,11,12-hexakis(decyloxy)dibenz[a,c]anthracene (0.415 g, 0.341 mmol) N-chlorosuccinimide (0.110 g, 0.820 mmol) and a stir

bar. 20 mL of dichloromethane was added and the tube was sealed and heated to 100 °C for 36 hours. Mixture was removed from heat, cooled to room temperature, where the solvent was removed under reduced pressure. Column chromatography was performed in hexanes/dichloromethane (60:40), followed by recrystallization in acetone to yield pale yellow solid (0.10 g, 23 %).  $^1\text{H-NMR}$  (300 MHz,  $\text{CDCl}_3$ ):  $\delta$  8.61 (s, 2H), 7.79 (s, 2H), 7.61 (s, 2H), 4.24-4.21 (m, 4H), 4.16 (t,  $J$  = 6.3 Hz, 8H), 1.96-1.87 (m, 12H), 1.57-1.50 (m, 12H), 1.33-1.25 (m, 72H), 0.89-0.86 (m, 18H).  $^{13}\text{C-NMR}$  (300 MHz,  $\text{CDCl}_3$ ):  $\delta$  150.95, 149.60, 147.46, 127.61, 126.56, 125.85, 123.60, 122.79, 113.90, 107.74, 105.14, 69.85, 69.54, 69.29, 32.15, 29.91, 29.87, 29.84, 29.82,

29.74, 29.69, 29.66, 29.60, 29.47, 29.23, 26.36, 26.33, 25.01, 22.91, 14.33. HRMS (MALDI) calc'd for  $C_{82}H_{132}Cl_2O_6+H$   $m/z$  1282.9401, found 1282.9395.

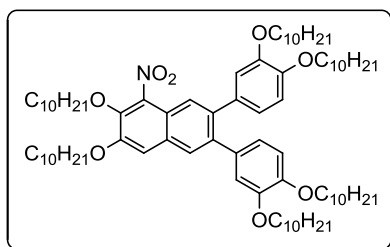
**Synthesis of 2,3-dibromo-5-nitro-6,7-bis(decyloxy)naphthalene (21):** of nitric acid (50 mL) was



cooled to 0 °C in an ice bath and 20 drops of concentrated sulfuric acid was added. 2,3-dibromo-6,7-bis(decyloxy)naphthalene (2.00 g, 3.34 mmol) was slowly added to the acidic mixture. Solution was stirred

vigorously overnight while allowing the mixture to warm to room temperature overnight (12 hours). The solution was neutralized with saturated  $NaHCO_3$  (50 mL). The product was then extracted with 50 mL EtOAc, followed by a washing with  $NaHCO_3$  (1 x 50 mL), brine (50 mL) and water (50 mL). The organic layer was dried with  $MgSO_4$ , filtered and concentrated under reduced pressure. Column chromatography was performed with hexanes/EtOAc (90:10), followed by a recrystallization in EtOH to give a white solid (1.18 g, 55 %).  $^1H$ -NMR (300 MHz,  $CDCl_3$ ):  $\delta$  8.01 (s, 1H), 7.87 (s, 1H), 7.10 (s, 1H), 4.21 (t,  $J$  = 6.6 Hz, 2H), 4.10 (t,  $J$  = 6.3 Hz, 2H), 1.92-1.87 (m, 2H), 1.79-1.75 (m, 2H), 1.29-1.25 (m, 28H), 0.90-0.86 (m, 6H).  $^{13}C$ -NMR (300 MHz,  $CDCl_3$ ):  $\delta$  152.50, 142.58, 140.90, 130.98, 129.95, 125.64, 123.14, 122.51, 120.22, 108.81, 75.69, 69.61, 32.12, 30.19, 29.81, 29.78, 29.61, 29.55, 29.22, 26.36, 25.92, 22.91, 14.32.

**2,3-bis[3,4-didecyloxyphenyl]-6,7-didecyloxy-5-nitronaphthalene (22):** A flask was charged with

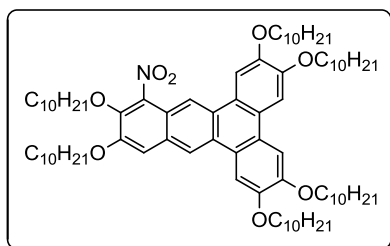


2,3-dibromo-5-nitro-6,7-bis(decyloxy)naphthalene (1.00 g, 1.55 mmol), 1-pinacolatoboron-3,4-bis(decyloxy)benzene (1.67 g, 3.24 mmol),  $Pd(OAc)_2$  (0.035 g, 0.16 mmol) and triphenylphosphine (0.081 g, 0.31 mmol). 15 mL of degassed

toluene was added to reagent mixture, followed by 7 mL of 2 M  $K_3PO_4$ . The flask was fitted with a

condenser, heated to 80 °C and left to stir for 48 hours under a N<sub>2</sub> atmosphere. The reaction was cooled to room temperature, 20 mL of dichloromethane was added, where the organic layer was separated and washed with water then brine. The organic layer was dried with MgSO<sub>4</sub>, filtered and removed solvent under reduced pressure. Column chromatography was performed in hexanes/dichloromethane (60:40) and recrystallized in acetone to yield a yellow solid (1.15 g, 59 %). <sup>1</sup>H-NMR (300 MHz, CDCl<sub>3</sub>): δ 7.74 (s, 1H), 7.60 (s, 1H), 7.27 (s, 1H), 6.79 (s, 4H), 6.63 (s, 1H), 6.59 (s, 1H), 4.23 (t, *J* = 6.6, 2H), 4.14 (t, *J* = 6.7, 2H), 3.97 (t, *J* = 6.6, 4H), 3.70-3.67 (m, 4H), 1.91-1.79 (m, 12H), 1.68-1.64 (m, 4H), 1.49-1.45 (m, 8H), 1.30-1.27 (m, 72H), 0.91-0.87 (m, 18H). <sup>13</sup>C-NMR (300 MHz, CDCl<sub>3</sub>): δ 151.51, 149.72, 148.68, 148.52, 142.10, 141.42, 138.97, 139.66, 133.92, 133.84, 129.60, 127.87, 122.36, 122.22, 122.06, 119.60, 116.29, 113.65, 113.58, 109.88, 75.53, 69.50, 32.15, 30.26, 29.94, 29.88, 29.84, 29.72, 29.67, 29.63, 29.59, 29.37, 26.42, 26.31, 26.26, 26.01, 22.92, 14.32. (Aromatic signal absent due to overlapping peaks.) HRMS (MALDI) calc'd for C<sub>82</sub>H<sub>135</sub>NO<sub>8</sub>+H *m/z* 1262.0188, found 1262.0182.

**Synthesis of 10-nitro-2,3,6,7,11,12-hexakis(decyloxy)dibenz[a,c]anthracene (23):** 2,3-bis[3,4-



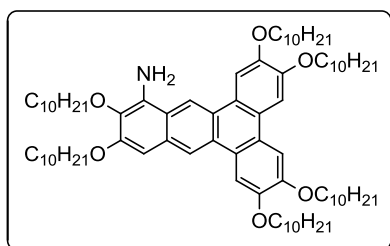
didecyloxyphenyl]-6,7-didecyloxy-5-nitronaphthalene (0.500 g, 0.396 mmol) was added to 20 mL dry dichloromethane.

FeCl<sub>3</sub> (0.385 g, 2.38 mmol) was added to the solution, placed under a N<sub>2</sub> atmosphere and left to stir for 1 hour. The

mixture was poured into MeOH (150 mL) and placed in freezer for 1 hour. The crude product was collected by suction filtration and washed with cold MeOH. A short flash column chromatography was done in dichloromethane to remove the excess FeCl<sub>3</sub> followed by a recrystallization in acetone to yield a yellow solid (0.453 g, 91 %). <sup>1</sup>H-NMR (300 MHz, CDCl<sub>3</sub>): δ

8.48 (s, 1H), 8.37 (s, 1H), 7.91 (s, 1H), 7.74 (s, 1H), 7.63 (s, 1H), 7.61 (s, 1H), 7.25 (s, 1H), 4.27-4.14 (m, 12H), 1.99-1.95 (m, 10H), 1.86-1.81 (m, 2H), 1.59-1.54 (m, 12H), 1.30-1.25 (m, 72H), 0.91-0.86 (m, 18H).  $^{13}\text{C}$ -NMR (300 MHz,  $\text{CDCl}_3$ ):  $\delta$  150.78, 150.09, 149.99, 149.36, 149.13, 141.64, 141.60, 128.50, 128.30, 128.07, 124.68, 124.32, 123.29, 122.87, 119.85, 118.29, 114.11, 109.38, 107.60, 107.48, 107.41, 107.15, 75.57, 69.90, 69.63, 69.57, 69.49, 69.25, 32.22, 32.21, 32.19, 30.37, 30.01, 29.95, 29.93, 29.91, 29.88, 29.83, 29.79, 29.76, 29.68, 29.65, 29.51, 26.55, 26.51, 26.10, 22.97, 14.37. HRMS (MALDI) calc'd for  $\text{C}_{82}\text{H}_{133}\text{NO}_8 + \text{H}$   $m/z$  1260.0031, found 1260.0026.

**Synthesis of 10-amino-2,3,6,7,11,12-hexakis(decyloxy)dibenz[a,c]anthracene (24):** 10-nitro-

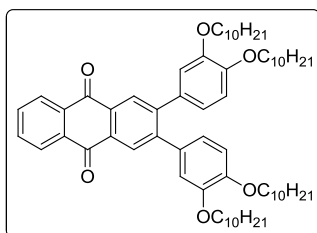


2,3,6,7,11,12-hexakis(decyloxy)dibenz[a,c]anthracene (0.453 g, 0.359 mmol) and  $\text{NiCl}_2 \cdot 6\text{H}_2\text{O}$  (0.426 g, 1.795 mmol) were dissolved in 20 mL dry THF and 7 mL dry MeOH to form an orange/green solution.  $\text{NaBH}_4$  (0.14 g, 3.59 mmol) was

added in small portions to the solutions, where the mixture turned black. The solution was stirred for an additional 45 minutes after the addition of base. The crude mixture was filtered and washed with dichloromethane. It was dissolved in 50 mL dichloromethane. The organic layer was washed with water (50 mL) and brine (50 mL). The organic layer was dried with  $\text{MgSO}_4$ , filtered and solvent was removed under reduced pressure. Column chromatography was performed in hexanes/dichloromethane (60:40  $\rightarrow$  40:60), followed by a recrystallization in acetone to give a light brown solid (0.108 g, 62 %).  $^1\text{H}$ -NMR (300 MHz,  $\text{CDCl}_3$ ):  $\delta$  8.72 (s, 1H), 8.66 (s, 1H), 8.11 (s, 1H), 8.08 (s, 1H), 7.78 (s, 2H), 6.91 (s, 1H), 4.48 (bs, 2H), 4.29-4.21 (m, 8H), 4.17 (t,  $J = 6.6$  Hz, 2H), 4.11 (t,  $J = 6.6$  Hz, 2H), 1.99-1.85 (m, 12H), 1.59-1.55 (m, 12H), 1.49-1.21 (m, 72H), 0.89 (t,  $J = 6.6$  Hz, 18H).  $^{13}\text{C}$ -NMR (300 MHz,  $\text{CDCl}_3$ ):  $\delta$  152.58, 149.69, 149.59, 149.29, 149.26, 134.51, 133.68, 129.95, 127.71, 125.51, 124.46, 124.44, 124.23, 124.03, 120.23, 120.00, 114.51,

108.07, 107.92, 107.85, 107.80, 98.20, 73.43, 69.99, 69.62, 68.39, 32.18, 30.81, 29.95, 29.88, 29.80, 29.72, 29.64, 29.62, 26.58, 26.51, 26.46, 26.44, 22.95, 14.36. HRMS (MALDI) calc'd for  $C_{82}H_{135}NO_6+H$   $m/z$  1230.0289, found 1230.0284.

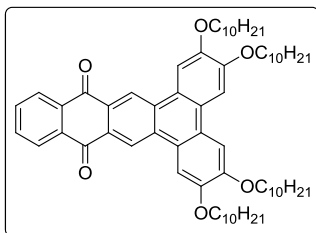
**Synthesis of 2,3-bis[3,4-bis(decyloxy)phenyl]anthracene-5,10-dione (30):** To a solution of



degassed toluene (12 mL) was added 2,3-dibromoanthracene-5,10-dione (0.168 g, 0.459 mmol), and 1-pinacolatoboron-3,4-bis(decyloxy)benzene (0.498 g, 0.964 mmol). To the mixture  $Pd(OAc)_2$  (0.0052 g, 0.023 mmol) and  $PPh_3$  (0.0120 g, 0.0459 mmol)

were added. The organic mixture was combined with 5 mL of 2M aqueous  $K_3PO_4$ . The solution was heated solution to 80 °C and left it to stir for 3 days where is was cooled to room temperature and extracted with dichloromethane. The organic layer was removed and washed with water and brine. The organic extracts were dried with  $MgSO_4$ , filtered and the solvent was removed under reduced pressure. Column chromatography was performed in hexanes/EtOAc (95:5) to give the pure product (0.095 g, 16 %).  $^1H$ -NMR (300 MHz,  $CDCl_3$ ):  $\delta$  8.36-8.33 (m, 2H), 8.34 (s, 2H), 7.84-7.81 (m, 2H), 6.83-6.82 (m, 4H), 6.68 (s, 2H), 3.98 (t,  $J$  = 6.9 Hz, 4H), 3.72 (t,  $J$  = 6.6 Hz, 4H), 1.83-1.79 (m, 4H), 1.69-1.65 (m, 4H), 1.47-1.25 (m, 56H), 0.89-0.86 (m, 12H).  $^{13}C$ -NMR (300 MHz,  $CDCl_3$ ):  $\delta$  183.30, 149.12, 148.87, 146.41, 134.24, 134.00, 132.66, 132.08, 129.56, 127.42, 122.38, 115.66, 113.48, 69.44, 32.15, 29.93, 29.88, 29.85, 29.83, 29.71, 29.65, 29.63, 29.59, 29.53, 29.35, 26.29, 26.24, 22.92, 14.33. HRMS (MALDI) calc'd for  $C_{66}H_{96}O_6+H$   $m/z$  984.7201, found 984.7207.

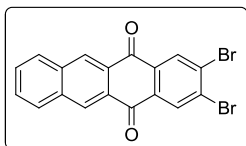
**Synthesis of 2,3,6,7-tetrakis(decyloxy)dibenzo[*a,c*]tetracene-10,15-dione (31):** 2,3-bis[3,4-



bis(decyloxy)phenyl]anthracene-5,10-dione (0.025 g, 0.025 mmol) was dissolved in 25 mL dry dichloromethane. The reaction was allowed to stir for 30 minutes under a nitrogen atmosphere. The reaction mixture was poured into 100 mL MeOH and placed in

freezer. The resulting precipitate was collected by filtration and recrystallized in hexanes to get a burgundy solid (0.021 g, 85 %). <sup>1</sup>H-NMR (300 MHz, CDCl<sub>3</sub>): δ 9.33 (s, 2H), 8.41-8.39 (m, 2H), 8.12 (s, 2H), 7.83-7.81 (m, 2H), 7.78 (s, 2H), 4.31-4.23 (m, 8H), 1.98-1.94 (m, 8H), 1.61-1.54 (m, 8H), 1.32-1.27 (m, 48H), 0.89-0.87 (m, 12H). <sup>13</sup>C-NMR (300 MHz, CDCl<sub>3</sub>): δ 183.45, 151.25, 149.84, 134.63, 134.20, 132.88, 129.79, 127.51, 125.88, 123.31, 107.63, 106.67, 69.78, 69.67, 32.17, 29.92, 29.85, 29.76, 29.62, 26.40, 22.92, 18.66, 14.32. (Aromatic signal absent due to overlapping peaks.) HRMS (MALDI) calc'd for C<sub>66</sub>H<sub>94</sub>O<sub>6</sub>+H *m/z* 982.7050, found 982.7027.

**Synthesis of 2,3-dibromotetracene-5-12-dione (34):** Adopted from the procedure of Williams *et*



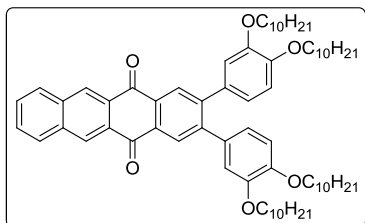
*al.*<sup>103</sup> Anthracene-1,4-dione (0.500 g, 2.40 mmol, 2 eq.) and 3,4-dibromothiophene-1,1-dioxide (0.329 g, 1.20 mmol, 1 eq.) were added to 125 mL concentrated AcOH. The 250 mL round bottom flask was fitted

with a reflux condenser and heated (~ 120 °C) with a heating mantle and stirred for 2 days. After the 2 days reaction time the mixture was cooled to room temperature and poured into 400 mL deionized H<sub>2</sub>O. The precipitate was filtered using vacuum suction filtration. The crude product was washed with MeOH to give a yellow filtrate and a green solid. Let product air dry overnight to give a dark green solid (0.452 g, 91 %). <sup>1</sup>H-NMR (300 MHz, CDCl<sub>3</sub>): δ 8.82 (s, 2H), 8.57 (s, 2H),



8.09-8.05 (m, 2H), 7.9-7.5 (m, 2H).  $^{13}\text{C}$ -NMR (300 MHz,  $\text{CDCl}_3$ ):  $\delta$  181.54, 135.47, 133.96, 132.95, 132.45, 130.47, 130.28, 130.13, 129.42. The product was used without further purification.

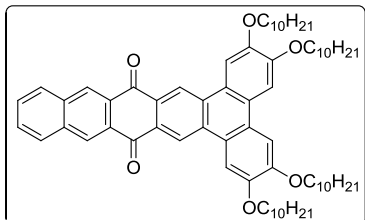
**Synthesis of 2,3-bis[3,4-bis(decyloxy)phenyl]tetracene-5,12-dione (35):** A solution of 2,3-



dibromotetracene-5,12-dione (0.150 g, 0.361 mmol), 1-pinacolatoboron-3,4-bis(decyloxy)benzene (0.391 g, 0.757 mmol),  $\text{Pd}(\text{OAc})_2$  (0.004 g, 0.018 mmol) and  $\text{PPh}_3$  (0.009 g, 0.036 mmol) was combined in 4 mL toluene and degassed with  $\text{N}_2$  for

25 minutes. A 2M solution of  $\text{K}_3\text{PO}_4$  was degassed with  $\text{N}_2$  for 25 minutes. The solutions were combined, stirred vigorously and heated at 80 °C for 2 days. The mixture went from yellow to black within minutes. The solution was cooled to room temperature. 20 mL  $\text{CH}_2\text{Cl}_2$  was added to solution. The organic layer was washed with  $\text{H}_2\text{O}$  (2 x 20 mL), brine (1 x 20 mL), then it was dried with  $\text{MgSO}_4$ , filtered and the solvent was removed under reduced pressure. The black solid was purified using column chromatography with Hexanes/EtOAc (95:5) to yield a bright yellow solid (0.072 g, 19 %).  $^1\text{H}$ -NMR (300 MHz,  $\text{CDCl}_3$ ):  $\delta$  8.86 (s, 2H), 8.40 (s, 2H), 8.11-8.08 (m, 2H), 7.70-7.67 (m, 2H), 6.87-6.80 (m, 4H), 6.69 (s, 2H), 3.98 (t,  $J$  = 6.6 Hz, 4H), 3.73 (t,  $J$  = 6.6 Hz, 4H), 1.82 (t,  $J$  = 6.9 Hz, 4H), 1.68 (t,  $J$  = 6.3 Hz, 4H), 1.50-1.28 (m, 56H), 0.88-0.86 (m, 12H).  $^{13}\text{C}$ -NMR (300 MHz,  $\text{CDCl}_3$ ):  $\delta$  183.11, 149.13, 148.88, 146.49, 135.40, 133.08, 132.72, 130.35, 130.30, 129.80, 129.71, 129.64, 122.42, 115.72, 113.51, 69.42, 32.16, 29.94, 29.88, 29.86, 29.84, 29.72, 29.66, 26.64, 29.60, 29.55, 29.36, 26.30, 26.26, 22.92, 14.33. HRMS (MALDI) calc'd for  $\text{C}_{70}\text{H}_{98}\text{O}_6 + \text{H}$   $m/z$  1035.7436, found 1035.7445.

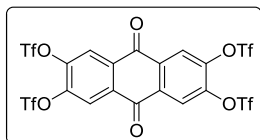
**Synthesis of 2,3,6,7-tetrakis(decyloxy)dibenzo[*a,c*]pentacene-10,17-dione (36):** Dissolved 2,3-



bis[3,4-bis(decyloxy)phenyl]tetracene-5,12-dione (0.070 g, 0.068 mmol) in 25 mL dry CH<sub>2</sub>Cl<sub>2</sub>. FeCl<sub>3</sub> (0.066 g, 0.406 mmol) to solution. Stirred at room temperature for 30 mins. The reaction mixture was poured into 100 mL MeOH and placed in freezer.

The orange precipitate was collected by filtration and recrystallized in CHCl<sub>3</sub> to yield orange crystals (0.059 g, 84 %). <sup>1</sup>H-NMR (300 MHz, CDCl<sub>3</sub>, 50 °C): δ 9.29 (s, 2H), 8.81 (s, 2H), 8.09 (s, 4H), 7.67 (s, 4H), 4.31 (t, *J* = 5.1 Hz, 4H), 4.21 (s, 4H), 2.02-1.95 (m, 8H), 1.65-1.60 (m, 8H), 1.49-1.28 (m, 48H), 0.91 (s, 12H). <sup>13</sup>C-NMR (300 MHz, CDCl<sub>3</sub>, 50 °C): δ 182.98, 151.37, 149.95, 135.40, 132.90, 130.87, 130.65, 130.25, 129.45, 129.28, 125.90, 123.38, 123.32, 108.16, 107.02, 69.86, 32.12, 32.10, 29.87, 29.80, 29.76, 29.72, 29.66, 29.56, 29.53, 26.40, 22.83, 14.17. HRMS (MALDI) calc'd for C<sub>70</sub>H<sub>96</sub>O<sub>6</sub>+H *m/z* 1032.7207, found 1032.7173.

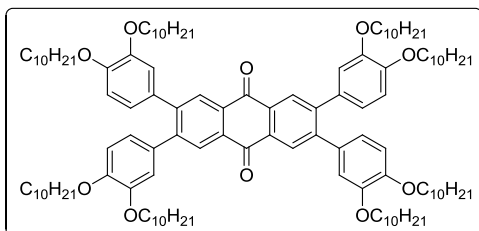
**Synthesis of 2,3,7,8-tetrakis(trifluoromethanesulfonyloxy)anthracene-5,10-dione (43):** A



modified procedure from Zöphel *et al.*<sup>108</sup> 2,3,7,8-tetrahydroxyanthracene-5,10-dione (0.13 g, 0.514 mmol) was placed under an N<sub>2</sub> atmosphere. Freshly distilled pyridine was transferred via

cannula to reaction flask with vigorous stirring. The solution was cooled to -78 °C. Tf<sub>2</sub>O (triflic anhydride, 0.87 g, 3.086 mmol) was added. The mixture was then warmed to room temperature overnight and then stirred for 2 days. Solvent was then removed *in vacuo*. Column chromatography was performed in hexanes/EtOAc (90:10) to give pure white crystals (0.204 g, 50 %). <sup>1</sup>H-NMR (300 MHz, CDCl<sub>3</sub>): δ 8.43 (s, 4H). <sup>13</sup>C-NMR (300 MHz, CDCl<sub>3</sub>): δ 177.56, 145.18, 133.70, 123.52, 118.75 (q, *J*<sub>C-F</sub> = 321 Hz).

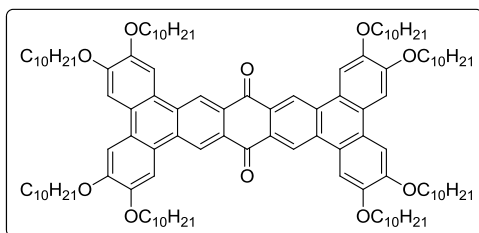
**Synthesis of 2,3,7,8-tetrakis[3,4-didecyloxyphenyl]-anthracene-5,10-dione (44):** 2,3,7,8-



tetratriflateanthracene-5,10-dione (0.228 g, 0.285 mmol) and 1-pinacolatoboron-3,4-bis(decyloxy)benzene (0.618 g, 0.618 mmol) were added to 8 mL toluene and degassed with N<sub>2</sub> for 15

minutes. Added Pd(PPh<sub>3</sub>)<sub>4</sub> (0.029 g, 0.033 mmol) the organic mixture. After 4 mL of 2M K<sub>3</sub>PO<sub>4</sub> was degassed for 15 minutes, it was added to the toluene mixture. The combined mixture was heated to 80 °C and stirred for 6 days. The mixture was cooled to room temperature and extracted with dichloromethane (40 mL) and washed organic layer with water (40 mL). Performed column chromatography on the crude product with hexanes/dichloromethane (60:40 → 0:100). Didecyloxybenzene eluted first followed by pure red solid product (0.276 g, 55 %). <sup>1</sup>H-NMR (300 MHz, CDCl<sub>3</sub>): δ 8.36 (s, 4H), 6.84 (d, *J* = 2.1 Hz, 4H), 6.83 (s, 4H), 6.69 (d, *J* = 2.1 Hz, 4H), 3.99 (t, *J* = 6.6 Hz, 8H), 3.73 (t, *J* = 6.6 Hz, 8H), 1.85-1.79 (m, 8H), 1.71-1.64 (m, 8H), 1.51-1.46 (m, 16H), 1.32-1.27 (m, 96H), 0.90-0.87 (m, 24H). <sup>13</sup>C-NMR (300 MHz, CDCl<sub>3</sub>): δ 183.22, 149.11, 148.88, 146.32, 132.74, 132.35, 129.55, 122.40, 115.71, 113.53, 69.45, 32.15, 31.12, 29.93, 29.84, 29.70, 29.62, 29.58, 29.53, 29.35, 26.28, 26.24, 22.91, 18.65, 14.32. HRMS (MALDI) calc'd for C<sub>118</sub>H<sub>184</sub>O<sub>10</sub>+H *m/z* 1762.3962, found 1762.3939.

**Synthesis of 2,3,6,7,13,14,17,18-octakis[decyloxy]-tetrabenze[*a,c,d,f*]pentacene-5,21-dione (45):** Modified procedure taken from literature.<sup>114</sup> To



a solution of 4.5 mL of dry dichloromethane and 0.5 mL methanesulfonic acid at 0 °C was added 2,3,7,8-tetrakis[3,4-didecyloxyphenyl]-anthracene-5,10-dione

(0.0715 g, 0.0406 mmol), which was then treated with DDQ (0.0193 g, 0.0852 mmol). The progress of the reaction was monitored by TLC and was complete after 10 minutes. The reaction was then quenched with  $\text{NaHCO}_3$  (20 mL) and extracted with dichloromethane (50 mL, due to solubility issues). The organic layer was dried with  $\text{MgSO}_4$ , filtered and solvent removed *in vacuo*. Product was recrystallized in chloroform to yield a dark red solid (0.0695 g, 97 %).  $^1\text{H}$ -NMR (300 MHz, 60 °C,  $\text{CDCl}_3$ ): 9.22 (s, 4H), 8.10 (s, 4H), 7.61 (s, 4H), 4.35 (t,  $J$  = 6.3 Hz, 8H), 4.14-4.12 (m, 8H), 2.10-1.93 (m, 16H), 1.68-1.51 (m, 16H), 1.51-1.35 (m, 96H), 0.93-0.90 (m, 24H).  $^{13}\text{C}$ -NMR could not be performed due to low solubility. HRMS (MALDI) calc'd for  $\text{C}_{118}\text{H}_{180}\text{O}_{10}+\text{H}$   $m/z$  1758.3649, found 1758.3630.

## References

1. Brown, G. H.; Wolken, J. J., *Liquid crystals and biological structures*. Academic Press: New York, 1979; p xi, 187 p.
2. Jones, W.; Rao, C. N. R., *Supramolecular organization and materials design*. Cambridge University Press: Cambridge ; New York, 2002; p ix, 446 p.
3. Whitesides, G. M.; Grzybowski, B., Self-assembly at all scales. *Science* **2002**, 295, 2418-2421.
4. Ringsdorf, H.; Schlarb, B.; Venzmer, J., Molecular Architecture and Function of Polymeric Oriented Systems - Models for the Study of Organization, Surface Recognition, and Dynamics of Biomembranes. *Angew. Chem. Int. Ed.* **1988**, 27, 113-158.
5. Goodby, J. W.; Saez, I. M.; Cowling, S. J.; Gasowska, J. S.; MacDonald, R. A.; Sia, S.; Watson, P.; Toyne, K. J.; Hird, M.; Lewis, R. A.; Lee, S. E.; Vaschenko, V., Molecular complexity and the control of self-organising processes. *Liq. Cryst.* **2009**, 36, 567-605.
6. Percec, V.; Glodde, M.; Bera, T. K.; Miura, Y.; Shiyanovskaya, I.; Singer, K. D.; Balagurusamy, V. S. K.; Heiney, P. A.; Schnell, I.; Rapp, A.; Spiess, H. W.; Hudson, S. D.; Duan, H., Self-organization of supramolecular helical dendrimers into complex electronic materials. *Nature* **2002**, 419, 384-387.
7. Kumar, S., *Chemistry of discotic liquid crystals : from monomers to polymers*. CRC Press: Boca Raton, 2011.
8. Reinitzer, F., Beiträge zur Kenntniss des Cholesterins. *Monatshefte für Chemie / Chemical Monthly* **1888**, 9, 421-441.
9. Lehmann, O., Über fließende Krystalle. *Z. Phys. Chem.* **1889**, 4, 462-472.
10. Sluckin, T. J.; Dunmur, D.; Stegemeyer, H., *Crystals that flow : classic papers from the history of liquid crystals*. Taylor & Francis: London ; New York, 2004; p xxii, 738 p.

11. Vorlander, D., The influence of the molecular figure on the crystallised-fluid state. *Ber. Dtsch. Chem. Ges.* **1907**, *40*, 1970-1972.
12. Friberg, S., Lyotropic Liquid-Crystals - Preface. *Adv. Chem. Ser.* **1976**, R7-R7.
13. Petrov, A. G., Liquid crystal physics and the physics of living matter. *Mol. Cryst. Liq. Crys. A* **1999**, *332*, 3087-3094.
14. Collings, P. J.; Hird, M., *Introduction to liquid crystals chemistry and physics*. Taylor & Francis: London ; Bristol, PA, 1997; p xi, 298 p.
15. Isihara, A., Theory of Anisotropic Colloidal Solutions. *J. Chem. Phys.* **1951**, *19*, 1142-1147.
16. Alben, R., Phase-Transitions in a Fluid of Biaxial Particles. *Phys. Rev. Lett.* **1973**, *30*, 778-781.
17. Straley, J. P., Ordered Phases of a Liquid of Biaxial Particles. *Phys. Rev. A* **1974**, *10*, 1881-1887.
18. Runnels, L. K.; Colvin, C., *Liquid Crystals*. Gordon and Breach: New York, 1972; Vol. 3.
19. Chandrasekhar, S.; Sadashiva, B. K.; Suresh, K. A., Liquid-Crystals of Disc-Like Molecules. *Pramana* **1977**, *9*, 471-480.
20. Billard, J.; Dubois, J. C.; Huutinh, N.; Zann, A., Mesophase of Disc-Like Molecules. *Nouv. J. Chim.* **1978**, *2*, 535-540.
21. Levelut, A. M., Structure of a Disk-Like Mesophase. *J. Phys. Lett.* **1979**, *40*, L81-L84.
22. Xiao, S. X.; Myers, M.; Miao, Q.; Sanaur, S.; Pang, K. L.; Steigerwald, M. L.; Nuckolls, C., Molecular wires from contorted aromatic compounds. *Angew. Chem. Int. Ed.* **2005**, *44*, 7390-7394.
23. Schmidt-Mende, L.; Fechtenkotter, A.; Mullen, K.; Moons, E.; Friend, R. H.; MacKenzie, J. D., Self-organized discotic liquid crystals for high-efficiency organic photovoltaics. *Science* **2001**, *293*, 1119-1122.

24. Nelson, J., Solar energy - Solar cells by self-assembly? *Science* **2001**, 293, 1059-1060.
25. Kumar, S., Playing with discs. *Liq. Cryst.* **2009**, 36, 607-638.
26. Chandrasekhar, S., Discotic Liquid-Crystals - a Brief Review. *Liq. Cryst.* **1993**, 14, 3-14.
27. Bisoyi, H. K.; Kumar, S., Discotic nematic liquid crystals: science and technology. *Chem. Soc. Rev.* **2010**, 39, 264-285.
28. Praefcke, K., *Physical Properties of Liquid Crystals: Nematics*. INSPEC: London, U.K., 2001.
29. Sakashita, H.; Nishitani, A.; Sumiya, Y.; Terauchi, H.; Ohta, K.; Yamamoto, I., X-Ray-Diffraction Study on Discotic Lamellar Phase in Bis(1,3-Di(P-N-Alkoxyphenyl)Propane-1,3-Dionato)Copper(II). *Mol. Cryst. Liq. Cryst.* **1988**, 163, 211-219.
30. Steinke, N.; Frey, W.; Baro, A.; Laschat, S.; Drees, C.; Nimtz, M.; Hagele, C.; Giesselmann, F., Columnar and smectic liquid crystals based on crown ethers. *Chem.-Eur. J.* **2006**, 12, 1026-1035.
31. Destrade, C.; Foucher, P.; Gasparoux, H.; Tinh, N. H.; Levelut, A. M.; Malthete, J., Disc-Like Mesogen Polymorphism. *Mol. Cryst. Liq. Cryst.* **1984**, 106, 121-146.
32. Hatsusaka, K.; Ohta, K.; Yamamoto, I.; Shirai, H., Discotic liquid crystals of transition metal complexes, Part 30: spontaneous uniform homeotropic alignment of octakis(dialkoxyphenoxy)phthalocyaninatocopper(II) complexes. *J. Mater. Chem.* **2001**, 11, 423-433.
33. Voisin, E.; Foster, E. J.; Rakotomalala, M.; Williams, V. E., Effects of Symmetry on the Stability of Columnar Liquid Crystals. *Chem. Mater.* **2009**, 21, 3251-3261.
34. Dean, J. A., *Analytical chemistry handbook*. McGraw-Hill: New York, 1995.
35. West, A. R., *Basic solid state chemistry*. 2nd ed.; John Wiley & Sons: New York, 1999; p xvi, 480 p.

36. Chandrasekhar, S.; Sadashiva, B. K.; Suresh, K. A., Liquid crystals of disc-like molecules (Reprinted from Pramana, vol 9). *Mol. Cryst. Liq. Cryst.* **2003**, *397*, 595-605.
37. Goozner, R. E.; Labes, M. M., Solute-Solvent Interactions in Discotic Mesophases. *Mol. Cryst. Liq. Cryst.* **1979**, *56*, 75-81.
38. Frank, F. C.; Chandrasekhar, S., Evidence of a Tilted Columnar Structure for Mesomorphic Phases of Benzene-Hexa-N-Alkanoates. *J. Phys.-Paris* **1980**, *41*, 1285-1288.
39. Usol'tseva, N.; Praefcke, K.; Smirnova, A.; Blunk, D., Comparative lyotropy study of homologous hexaesters of hexahydroxy-benzene and -cyclohexane (scyllitol) in linear and cyclic hydrocarbons: microsegregation and mesophase formation of discotics [1]. *Liq. Cryst.* **1999**, *26*, 1723-1734.
40. Lillya, C. P.; Thakur, R., Tetrahydroxy-Para-Benzoquinone Tetraesters, the Simplest Discotics. *Mol. Cryst. Liq. Cryst.* **1989**, *170*, 179-&.
41. Chang, J. Y.; Baik, J. H.; Lee, C. B.; Han, M. J.; Hong, S. K., Liquid crystals obtained from disclike mesogenic diacetylenes and their polymerization. *J. Am. Chem. Soc.* **1997**, *119*, 3197-3198.
42. Destrade, C.; Mondon, M., C.; Malthete, J., Hexasubstituted Triphenylenes: A New Mesomorphic Order. *J. Phys. Colloques* **1979**, *40*, C3-17-C3-21.
43. Paraschiv, I.; Delforterie, P.; Giesbers, M.; Posthumus, M. A.; Marcelis, A. T. M.; Zuilhof, H.; Sudholter, E. J. R., Asymmetry in liquid crystalline hexaalkoxytriphenylene discotics. *Liq. Cryst.* **2005**, *32*, 977-983.
44. Keinan, E.; Kumar, S.; Moshenberg, R.; Ghirlando, R.; Wachtel, E. J., Trisubstituted Decacyclene Derivatives - Bridging the Gap between the Carbonaceous Mesophase and Discotic Liquid-Crystals. *Adv. Mater.* **1991**, *3*, 251-254.



45. Saji, T.; Aoyagui, S., Electrochemical Formation of Decacyclene Tetranegative Ion. *J. Electroanal. Chem.* **1979**, *102*, 139-141.
46. Sano, T.; Fujii, H.; Nishio, Y.; Hamada, Y.; Takahashi, H.; Shibata, K., Organic electroluminescent devices doped with condensed polycyclic aromatic compounds. *Synth. Met.* **1997**, *91*, 27-30.
47. van de Craats, A. M.; Warman, J. M.; Fechtenkotter, A.; Brand, J. D.; Harbison, M. A.; Mullen, K., Record charge carrier mobility in a room-temperature discotic liquid-crystalline derivative of hexabenzocoronene. *Adv. Mater.* **1999**, *11*, 1469-1472.
48. Van der Pol, J. F.; Neeleman, E.; Zwikker, J. W.; Nolte, R. J. M.; Drenth, W.; Aerts, J.; Visser, R.; Picken, S. J., Homologous series of liquid-crystalline metal free and copper octa-n-alkoxyphthalocyanines. *Liq. Cryst.* **2006**, *33*, 1378-1387.
49. Sleven, J.; Cardinaels, T.; Binnemans, K.; Nelis, D.; Mullens, J.; Hinz-Hubner, D.; Meyer, G., Mesophase behaviour and thermal stability of octa-alkoxy substituted phthalocyaninatocobalt(II) complexes. *Liq. Cryst.* **2003**, *30*, 143-148.
50. Laschat, S.; Baro, A.; Steinke, N.; Giesselmann, F.; Hagele, C.; Scalia, G.; Judele, R.; Kapatsina, E.; Sauer, S.; Schreivogel, A.; Tosoni, M., Discotic liquid crystals: From tailor-made synthesis to plastic electronics. *Angew. Chem. Int. Ed.* **2007**, *46*, 4832-4887.
51. Bahadur, B. e., *Liquid Crystals: Applications and Uses*. World Scientific: Singapore, 1990; Vol. 1-3.
52. Schadt, M.; Helfrich, W., Voltage-Dependent Optical Activity of a Twisted Nematic Liquid Crystal. *Appl. Phys. Lett.* **1971**, *18*, 127-&.
53. Mori, H.; Itoh, Y.; Nishiura, Y.; Nakamura, T.; Shinagawa, Y., Performance of a novel optical compensation film based on negative birefringence of discotic compound for

- wide-viewing-angle twisted-nematic liquid-crystal displays. *Jpn. J. Appl. Phys.* **1997**, *36*, 143-147.
54. Mori, H., The Wide View (WV) Film for Enhancing the Field of View of LCDs. *J. Disp. Technol.* **2005**, *1*, 179-186.
  55. Boden, N.; Bushby, R. J.; Clements, J.; Movaghar, B., Device applications of charge transport in discotic liquid crystals. *J. Mater. Chem.* **1999**, *9*, 2081-2086.
  56. Scott, J. C., Optoelectronics - Upwardly-Mobile Organics. *Nature* **1994**, *371*, 102-102.
  57. Becher, J.; Schaumburg, K.; North Atlantic Treaty Organization. Scientific Affairs Division., *Molecular engineering for advanced materials*. Kluwer Academic Publishers: Dordrecht ; Boston, 1995; p 376.
  58. Cheung, D. L.; Troisi, A., Modelling charge transport in organic semiconductors: from quantum dynamics to soft matter. *Phys. Chem. Chem. Phys.* **2008**, *10*, 5941-5952.
  59. Hanack, M.; Lang, M., Conducting Stacked Metallophthalocyanines and Related-Compounds. *Adv. Mater.* **1994**, *6*, 819-833.
  60. Bushby, R. J.; Lozman, O. R., Photoconducting liquid crystals. *Curr. Opin. Solid St. M.* **2002**, *6*, 569-578.
  61. Vaughan, G. B. M.; Heiney, P. A.; Mccauley, J. P.; Smith, A. B., Conductivity and Structure of a Liquid-Crystalline Organic Conductor. *Phys. Rev. B* **1992**, *46*, 2787-2791.
  62. Markovitsi, D., Energy transport in columnar mesophases. *Mol. Cryst. Liq. Cryst.* **2003**, *397*, 389-398.
  63. Ohta, K.; Hatsusaka, K.; Sugibayashi, M.; Ariyoshi, M.; Ban, K.; Maeda, F.; Naito, R.; Nishizawa, K.; van de Craats, A. M.; Warman, J. M., Discotic liquid crystalline semiconductors. *Mol. Cryst. Liq. Cryst.* **2003**, *397*, 325-345.
  64. vanNostrum, C. F., Self-assembled wires and channels. *Adv. Mater.* **1996**, *8*, 1027-1030.

65. Bleyl, I.; Erdelen, C.; Schmidt, H. W.; Haarer, D., One-dimensional hopping transport in a columnar discotic liquid-crystalline glass. *Philos. Mag. B* **1999**, *79*, 463-475.
66. Eichhorn, H., Mesomorphic phthalocyanines, tetraazaporphyrins, porphyrins and triphenylenes as charge-transporting materials. *J. Porphyrins Phthalocyanines* **2000**, *4*, 88-102.
67. Brabec, C. J., *Organic photovoltaics : concepts and realization*. Springer: New York, 2003; p xii, 297 p.
68. de Freitas, J. N.; Nogueira, A. F.; De Paoli, M. A., New insights into dye-sensitized solar cells with polymer electrolytes. *J. Mater. Chem.* **2009**, *19*, 5279-5294.
69. Tang, C. W., 2-Layer Organic Photovoltaic Cell. *Appl. Phys. Lett.* **1986**, *48*, 183-185.
70. Percec, V.; Glodde, M.; Bera, T. K.; Miura, Y.; Shiyanovskaya, I.; Singer, K. D.; Balagurusamy, V. S. K.; Heiney, P. A.; Schnell, I.; Rapp, A.; Spiess, H. W.; Hudson, S. D.; Duan, H., Self-organization of supramolecular helical dendrimers into complex electronic materials (vol 419, pg 384, 2002). *Nature* **2002**, *419*, 862-862.
71. Wang, Z. H.; Li, C.; Scherr, E. M.; Macdiarmid, A. G.; Epstein, A. J., 3 Dimensionality of Metallic States in Conducting Polymers - Polyaniline. *Phys. Rev. Lett.* **1991**, *66*, 1745-1748.
72. Bacher, A.; Bleyl, I.; Erdelen, C. H., Low molecular weight and polymeric triphenylenes as hole transport materials inorganic two-layer LEDs. *Adv. Mater.* **1997**, *9*, 1031-&.
73. Stapff, I. H.; Stumpfen, V.; Wendorff, J. H.; Spohn, D. B.; Mobius, D., Preliminary communication - Multilayer light emitting diodes based on columnar discotics. *Liq. Cryst.* **1997**, *23*, 613-617.
74. Freudenmann, R.; Behnisch, B.; Hanack, M., Synthesis of conjugated-bridged triphenylenes and application in OLEDs. *J. Mater. Chem.* **2001**, *11*, 1618-1624.

75. Boden, N.; Borner, R. C.; Bushby, R. J.; Cammidge, A. N.; Jesudason, M. V., The Synthesis of Triphenylene-Based Discotic Mesogens - New and Improved Routes. *Liq. Cryst.* **1993**, *15*, 851-858.
76. Christ, T.; Glusen, B.; Greiner, A.; Kettner, A.; Sander, R.; Stumpflen, V.; Tsukruk, V.; Wendorff, J. H., Columnar discotics for light emitting diodes. *Adv. Mater.* **1997**, *9*, 48-52.
77. Adam, D.; Schuhmacher, P.; Simmerer, J.; Haussling, L.; Siemensmeyer, K.; Etzbach, K. H.; Ringsdorf, H.; Haarer, D., Fast Photoconduction in the Highly Ordered Columnar Phase of a Discotic Liquid-Crystal. *Nature* **1994**, *371*, 141-143.
78. Paraschiv, I.; Giesbers, M.; van Lagen, B.; Grozema, F. C.; Abellon, R. D.; Siebbeles, L. D. A.; Marcelis, A. T. M.; Zuilhof, H.; Sudholter, E. J. R., H-bond-stabilized triphenylene-based columnar discotic liquid crystals. *Chem. Mater.* **2006**, *18*, 968-974.
79. Lau, K.; Foster, J.; Williams, V., Synthesis of a hexaalkoxybenzo[b]triphenylene mesogen. *Chem. Commun.* **2003**, 2172-2173.
80. van de Craats, A. M.; Warman, J. M., The core-size effect on the mobility of charge in discotic liquid crystalline materials. *Adv. Mater.* **2001**, *13*, 130-133.
81. Lynett, P. T.; Maly, K. E., Synthesis of Substituted Trinaphthylenes via Aryne Cyclotrimerization. *Org. Lett.* **2009**, *11*, 3726-3729.
82. Ong, C. W.; Liao, S. C.; Chang, T. H.; Hsu, H. F., In situ synthesis of hexakis(alkoxy)diquinoxalino[2,3-a : 2',3'-c]phenazines: Mesogenic phase transition of the electron-deficient discotic compounds. *J. Org. Chem.* **2004**, *69*, 3181-3185.
83. Mohr, B.; Wegner, G.; Ohta, K., Synthesis of Triphenylene-Based Porphyrinato Metal(II) Complexes Which Display Discotic Columnar Mesomorphism. *J. Chem. Soc. Chem. Comm.* **1995**, 995-996.

84. Cammidge, A. N.; Chambrier, I.; Cook, M. J.; Garland, A. D.; Heeney, M. J.; Welford, K., Octaalkyl- and Octaalkoxy-2,3-naphthalocyanines. *J. Porphyrins Phthalocyanines* **1997**, *1*, 77-86.
85. Kalyani, D.; Dick, A. R.; Anani, W. Q.; Sanford, M. S., A simple catalytic method for the regioselective halogenation of arenes. *Org. Lett.* **2006**, *8*, 2523-2526.
86. Martin, R. B., Comparisons of indefinite self-association models. *Chem. Rev.* **1996**, *96*, 3043-3064.
87. Maly, K. E.; Maris, T.; Gagnon, E.; Wuest, J. D., Inclusion compounds of hexakis(4-cyanophenyl)benzene: Open networks maintained by C-H center dot center dot center dot N interactions. *Cryst. Growth. Des.* **2006**, *6*, 461-466.
88. Kumar, S.; Manickam, M.; Balagurusamy, V. S. K.; Schonherr, H., Electrophilic aromatic substitution in triphenylene discotics: Synthesis of alkoxy-nitrotriphenylenes. *Liq. Cryst.* **1999**, *26*, 1455-1466.
89. Ong, C. W.; Hwang, J. Y.; Tzeng, M. C.; Liao, S. C.; Hsu, H. F.; Chang, T. H., Dibenzo[a,c]phenazine with six-long alkoxy chains to probe optimization of mesogenic behavior. *J. Mater. Chem.* **2007**, *17*, 1785-1790.
90. Foster, E. J.; Jones, R. B.; Lavigueur, C.; Williams, V. E., Structural factors controlling the self-assembly of columnar liquid crystals. *J. Am. Chem. Soc.* **2006**, *128*, 8569-8574.
91. Cozzi, F.; Ponzini, F.; Annunziata, R.; Cinquini, M.; Siegel, J. S., Polar Interactions between Stacked Pi-Systems in Fluorinated 1,8-Diarylnaphthalenes - Importance of Quadrupole-Moments in Molecular Recognition. *Angew. Chem. Int. Ed.* **1995**, *34*, 1019-1020.
92. Cozzi, F.; Cinquini, M.; Annunziata, R.; Siegel, J. S., Dominance of Polar/Pi over Charge-Transfer Effects in Stacked Phenyl Interactions. *J. Am. Chem. Soc.* **1993**, *115*, 5330-5331.

93. Hammett, L. P., The effect of structure upon the reactions of organic compounds benzene derivatives. *J. Am. Chem. Soc.* **1937**, *59*, 96-103.
94. Boden, N.; Bushby, R. J.; Cammidge, A. N.; Headdock, G., Novel discotic liquid crystals created by electrophilic aromatic substitution. *J. Mater. Chem.* **1995**, *5*, 2275-2281.
95. Boden, N.; Bushby, R. J.; Lu, Z. B.; Cammidge, A. N., Cyano substituted triphenylene-based discotic mesogens. *Liq. Cryst.* **1999**, *26*, 495-499.
96. Charton, M., Nature of Ortho Effect .2. Composition of Taft Steric Parameters. *J. Am. Chem. Soc.* **1969**, *91*, 615-&.
97. Praefcke, K.; Eckert, A.; Blunk, D., Core-halogenated, helical-chiral triphenylene-based columnar liquid crystals. *Liq. Cryst.* **1997**, *22*, 113-119.
98. Boden, N.; Bushby, R. J.; Cammidge, A. N.; Duckworth, S.; Headdock, G., alpha-Halogenation of triphenylene-based discotic liquid crystals: Towards a chiral nucleus. *J. Mater. Chem.* **1997**, *7*, 601-605.
99. Praefcke, K.; Holbrey, J. D., Inclusions between large flat organic molecules; The induction of columns and mesophases. *J. Inclusion Phenom. Mol. Recognit. Chem.* **1996**, *24*, 19-41.
100. Williams, V. E.; Lemieux, R. P.; Thatcher, G. R. J., Substituent effects on the stability of arene-arene complexes: An AM1 study of the conformational equilibria of cis-1,3-diphenylcyclohexanes. *J. Org. Chem.* **1996**, *61*, 1927-1933.
101. Paraskos, A. J.; Nishiyama, Y.; Swager, T. M., Synthesis and characterization of triphenylene-dione half-disc mesogens. *Mol. Cryst. Liq. Cryst.* **2004**, *411*, 1405-1417.
102. Lu, Y. C.; Lemal, D. M.; Jasinski, J. P., Bond alternation in azulenes. *J. Am. Chem. Soc.* **2000**, *122*, 2440-2445.
103. Bailey, D.; Williams, V. E., An efficient synthesis of substituted anthraquinones and naphthoquinones. *Tetrahedron Lett.* **2004**, *45*, 2511-2513.

104. Molina, O. M. T.; Honghao, S.; Taliansky, C. S.; Carnero, M. A.; Blanco, R. F.; Moneo, O. M. V. Quinone antitumor compounds, particularly 1,4-anthraquinones and their derivatives, process for their preparation, and their uses. WO2007026041A2, 2007.
105. Muller, A.; Raltschewa, M.; Papp, M., The dimerisation of the isoegenolmethylethers (Heart phenole I). *Ber. Dtsch. Chem. Ges.* **1942**, 75, 692-703.
106. Pozzo, J. L.; Desvergne, J. P.; Clavier, G. M.; Bouas-Laurent, H.; Jones, P. G.; Perlstein, J., The unusual molecular organization of 2,3-bis(n-hexyloxy) anthracene in the crystal. A hint to the origin of the gelifying properties of 2,3-bis(n-alkyloxy)anthracenes? *J. Chem. Soc. Perk. T. 2* **2001**, 824-826.
107. Balaban, T. S.; Eichhofer, A.; Krische, M. J.; Lehn, J. M., Hierarchic supramolecular interactions within assemblies in solution and in the crystal of 2,3,6,7-tetrasubstituted 5,5'-(anthracene-9,10-diyl)bis[pyrimidin-2-amines]. *Helv. Chim. Acta* **2006**, 89, 333-351.
108. Zophel, L.; Enkelmann, V.; Rieger, R.; Mullen, K., Saddle Shaped Hexaaryl[a,c,fg,j,l,op]tetracenes from 4,5,9,10-Tetrafunctionalized Pyrenes. *Org. Lett.* **2011**, 13, 4506-4509.
109. Cammidge, A. N.; Gopee, H., Structural factors controlling the transition between columnar-hexagonal and helical mesophase in triphenylene liquid crystals. *J. Mater. Chem.* **2001**, 11, 2773-2783.
110. Ichihara, M.; Suzuki, H.; Mohr, B.; Ohta, K., Different disk structures in the hexagonal columnar mesophases of 2,3-dicyano-6,7,10,11-tetraalkoxy-1,4-diazatriphenylenes and 2,3-dicyano-6,7,10,11-tetraalkoxytriphenylenes. *Liq. Cryst.* **2007**, 34, 401-410.
111. Leonard, J.; Lygo, B.; Procter, G., *Advanced practical organic chemistry*. 2nd ed.; Nelson Thornes: Cheltenham, 2001; p xiii, 298 p.

112. Herde, J. L.; Lambert, J. C.; Senoff, C. V.; Cushing, M. A., Cyclooctene and 1,5-Cyclooctadiene Complexes of Fridium(I). In *Inorg. Synth.*, John Wiley & Sons, Inc.: 2007; pp 18-20.
113. Mkhalid, I. A. I.; Barnard, J. H.; Marder, T. B.; Murphy, J. M.; Hartwig, J. F., C-H Activation for the Construction of C-B Bonds. *Chem. Rev.* **2010**, *110*, 890-931.
114. Zhai, L. Y.; Shukla, R.; Rathore, R., Oxidative C-C Bond Formation (Scholl Reaction) with DDQ as an Efficient and Easily Recyclable Oxidant. *Org. Lett.* **2009**, *11*, 3474-3477.